The Pennsylvania State University

The Graduate School

College of Engineering

DEVELOPMENT AND OPTIMIZATION OF ACTIVATED CARBON AIR CATHODE TOWARDS SCALE UP APPLICATIONS OF MICROBIAL FUEL CELLS

A Dissertation in

Environmental Engineering

by

Wulin Yang

Submitted in Partial Fulfillment
of the Requirements
for the Degree of

Doctor of Philosophy

August 2016

The dissertation of Wulin Yang was reviewed and approved* by the following:

Bruce E. Logan
Evan Pugh and Kappe Professor of Environmental Engineering
Dissertation Advisor
Chair of Committee

Michael A. Hickner
Associate Professor of Materials Science and Engineering

John M. Regan
Professor of Environmental Engineering

Manish Kumar
Assistant Professor of Chemical Engineering

William D. Burgos
Professor of Environmental Engineering
Chair of Graduate Program

*Signatures are on file in the Graduate School

ABSTRACT

Microbial fuel cells (MFCs) are emerging technologies that produce bio-electricity from inorganic and organic wastes. Air cathodes used in MFCs need to have high catalytic activity for oxygen reduction, but they must also be easy to manufacture, inexpensive, and watertight. Several different approaches were used here to improve air cathode performance, and reduce water leakage. A low cost poly(vinylidene fluoride-co-hexafluoropropylene) (PVDF-HFP) phase inversion coating was developed as a cathode diffusion layer (DL) to improve power. A maximum power density of 1430 ± 90 mW m^{-2} was achieved at a PVDF-HFP loading of 7.1 mg cm^{-2} (4:1 polymer:carbon black), with activated carbon as the oxygen reduction cathode catalyst. This power density was 31% higher than that obtained with a more conventional platinum (Pt) catalyst on a carbon cloth (Pt/C) cathode with a poly(tetrafluoroethylene) (PTFE) diffusion layer (1090 ± 30 mW m^{-2}). The improved performance was due in part to the larger oxygen mass transfer coefficient of 3×10^{-3} cm s^{-1} for the PVDF-HFP coated cathode, compared to 1.7×10^{-3} cm s^{-1} for the carbon cloth/PTFE-based cathode. The diffusion layer was resistant to electrolyte leakage up to water column heights of 41 ± 0.5 cm (7.1 mg cm^{-2} loading of 4:1 polymer:carbon black) to 70 ± 5 cm (14.3 mg cm^{-2} loading of 4:1 polymer:carbon black). This new type of PVDF-HFP/carbon black diffusion layer could reduce the cost of manufacturing cathodes for MFCs.

A simple one-step, phase inversion process was used to construct an inexpensive cathode using a poly(vinylidene fluoride) (PVDF) binder and an activated carbon catalyst. The phase inversion process enabled cathode preparation at room temperatures, without the need for additional heat treatment, and it produced for the first time a cathode that did not require a separate diffusion layer to prevent water leakage. MFCs using this new type of cathode produced a maximum power density of 1470 ± 50 mW m^{-2} with acetate as a substrate (28 mL reactor), and 230 ± 10 mW m^{-2} with domestic wastewater (130 mL reactor). These power densities were similar to those obtained using

cathodes made using more expensive materials or more complex procedures, such as cathodes with a polytetrafluoroethylene (PTFE) binder and a poly(dimethylsiloxane) (PDMS) diffusion layer, or a Pt catalyst. Even though the PVDF cathodes did not have a diffusion layer, they withstood up to 1.22 ± 0.04 m of water head (~12 kPa) without leakage, compared to 0.18 ± 0.02 m for cathodes made using PTFE binder and PDMS diffusion layer. The cost of PVDF and activated carbon ($3 m^{-2}) was less than that of the stainless steel mesh current collector ($12 m^{-2}). PVDF-based AC cathodes therefore are inexpensive, have excellent performance in terms of power and water leakage, and they can be easily manufactured using a single phase inversion process at room temperature.

Applications of MFCs will require cathodes that are highly resistant to water leakage. This can be accomplished by using a better diffusion layer even with cathodes relatively resistant to water leakage, but the materials must be inexpensive. To improve the resistance of the cathode to leakage, a hydrophobic PVDF membrane synthesized using a simple phase inversion process was examined as an additional low cost ($0.9/$m^2$), carbon black free DL that could prevent water leakage at high pressure heads compared to a more expensive PTFE/carbon black DL ($11/$m^2$). The power density produced with a PVDF (20% ,w/v) DL membrane of 1400 ± 7 mW/m^2 was similar to that obtained using a wipe DL [cloth coated with poly(dimethylsiloxane)]. Water head tolerance reached 1.9 m (~19 kPa) with no mesh supporter, and 2.1 m (~21 kPa, maximum testing pressure) with a mesh supporter, compared to 0.2 ± 0.05 m for the wipe DL. The elimination of carbon black from the DL greatly simplified the fabrication procedure and further reduced overall cathode costs.

While the PVDF membrane was shown to be a useful DL, a method was needed to integrate the DL into the cathode structure. A hot pressing method was used to bind the PVDF DL onto the air side of the activated carbon cathode, and additional catalyst layers were added to improve performance. Cathodes pressed at 60 °C produced a 16% higher maximum power density of 1630

± 10 mW m^{-2} than non-pressed controls (1400 ± 7 mW m^{-2}). Cathode performance was further increased to 1850 ± 90 mW m^{-2} by catalyst stacking, through the addition of an extra catalyst layer (CL), which better utilized the available surface area of the stainless steel mesh (SS) current collector. The use of one stainless steel current collector and two catalyst layers (SS/2CLs) produced more positive cathode potentials compared to other designs (SS/CL or 2SS/2CL). Low materials costs and high power production for MFCs using these cathodes could enable more cost effective power production using MFCs.

To improve oxygen reduction kinetics of the cathode catalyst, an iron-nitrogen-carbon co-catalyst was incorporated into activated carbon (Fe-N-C/AC), resulting in a nearly four electron transfer, compared to a two-electron transfer for plain activated carbon (AC). With acetate as the fuel in 200 mM phosphate buffer solution, the maximum power density was 4.7 ± 0.2 W m^{-2}, which is higher than any previous report for an air-cathode MFC. With domestic wastewater as a fuel, MFCs with the Fe-N-C/AC cathode produced up to 0.8 ± 0.03 W m^{-2}, which was twice that obtained with a platinum-catalyzed cathode. The use of this Fe-N-C/AC catalyst can therefore substantially increase power production, and enable broader applications of MFCs for renewable electricity generation using waste materials.

Long-term operation of MFCs can result in substantial degradation of AC air-cathode performance. In order to examine a possible role in fouling from natural organic matter in water, cathodes were exposed to high concentrations of humic acids. Cathodes treated with 100 mg L^{-1} of humic acids did not exhibit any significant change in performance. Exposure to 1000 mg L^{-1} of humic acids, which increased the mass of the cathodes by ~5% (14 ± 2 mg of organic matter per cathode), decreased the maximum power density of the MFCs by 14% (from 1310 ± 30 mW m^{-2} to 1130 ± 30 mW m^{-2}). Total cathode resistance increased by 30% (from 57 Ω to 74 Ω) for cathodes treated with 1000 mg L^{-1} of humic acids, primarily due to an increase in the diffusion resistance (from 32 Ω to 50 Ω), based on resistance components measured using electrochemical impendance

spectroscopy. The adsorption of the humic acids decreased the total surface area by 12% (from 520 $m^2\ g^{-1}$ to 460 $m^2\ g^{-1}$), suggesting that the main impact of the adsorption of organic matter was due to pore blockage. Minimization of external mass transfer resistances using a rotating disk electrode reduced the impact of organic matter adsorption to only a 5% reduction in current, indicating about half the impact of the humics was associated with external mass transfer resistance and the remainder was due to internal resistances. Rinsing the cathodes with deionized water did not restore cathode performance. These results demonstrated that humic acids could contribute to cathode fouling, but the extent of power reduction was relatively small in comparison to the large mass of humics adsorbed. Other factors, such as microbially produced biopolymers, or precipitation of inorganic chemicals in the water, are therefore likely more important contributors to long term fouling of MFC cathodes.

TABLE OF CONTENTS

LIST OF FIGURES

LIST OF TABLES

ACKNOWLEDGEMENTS

I would first like to thank my advisor, Prof. Bruce Logan, for the past four years at Penn State. His passion and persistence in science have constantly encouraged me during my graduate study. In my first year, Dr. Logan spent enormous efforts guiding me on research and never lost his patience when my experiment was not going well. Dr. Logan would seek every chance to train my English writing and presenting skills that help build my confidence and become a qualified researcher. Without his constant support, I would never be able to accomplish my PhD study. All the knowledge and merit that Dr. Logan passed on me, has made me today and will continue benefiting my future life.

I would also like to thank Dr. John Regan, Dr. Michael Hickner, Dr. Manish Kumar and Dr. William Burgos for their support and serving as my committee members. In particular, I sincerely thank Dr. Michael Hickner for advising me on polymer chemistry.

I want to thank all my lab mates for their help on my research and life. The Logan lab is always a collaborative and pleasant family to stay with. I will surely miss our Friday basketball game at Orchard Park.

Finally, I would like to thank my parents for their constant support and love at every stage of my life. Completing this degree would never be possible without their love and encouragement. I especially want to thank my wife, Shuxing Deng, for her persistent support. I become brave enough to face the toughness of life because of her unconditional love, encouragement and understanding.

Chapter 1

General Introduction

The world is experiencing an ever increasing energy demand due to rapid growth of the global population. There are currently over seven billion people on earth with a projection of between 9.6 billion and 12.3 billion people in 2100 *(1)*. Fossil fuels such as coal, natural gas, and oil are continuously supporting the global economic growth and account for over 80% of total energy consumption *(2)*. Oil remains the world's dominant fuel of ~ 30% of the total energy consumption, but demand for oil is expected to exceed oil production ten or twenty years from now *(2, 3)*. This primary energy consumption will encounter another increase by 41% between 2012 and 2035, raising an urgent need for an energy infrastructure change *(4)*.

In the US, the annual total energy consumption is ~ 100 quadrillion BTU or 3.3×10^{12} W and accounts for about one fourth of global annual energy consumption *(5)*. Approximately 18% of the energy (600 GW) is generated as electricity in the power plants and 4% of this electricity (~ 24 GW) is used solely to move and treat drinking and wastewater, based on the Electric Power Research Institute (EPRI) report published in 2002 *(6)*. In a typical domestic wastewater treatment plant employing the activated sludge process, the energy needed to treat 1 m^3 of wastewater is ~ 0.6 kWh *(7)*. To alleviate energy consumption in wastewater treatment, recent research has focused on recovering energy or materials from waste streams during the treatment process *(8)*.

Microbial electrochemical technologies (METs) are sustainable platforms to produce valuable products such as electricity from waste streams via different electrochemical reactions catalyzed by microorganisms *(8)*. The microbial fuel cell (MFC) is one of the most widely applied MET as it can be used to convert organic and inorganic substrates to electrical power *(9-13)*. Exoelectrogenic

bacteria on the anode are able to oxidize organics present in wastewater and release electrons, which flow through an external circuit to the cathode where typically oxygen reduction occurs *(9)*. The bio-electricity generated from MFCs could be used as additional power source to achieve sustainable wastewater treatment *(9)*.

To date, there are no commercial applications of MFCs in wastewater treatment plants and there are only limited studies on scaling up MFCs *(14, 15)*. The main limiting factors for commercialization are the high cathode cost and the absence of fabrication method for cathode scale up *(16)*. Another issue is the low power generation from MFCs, mainly due to poor cathode performance. Cathode fouling has also lowered power production over time and shortened the cathode lifetime *(17)*.

1.1 Objectives

My PhD dissertation mainly focuses on developing new fabrication methods to scale up cathode, optimizing cathode performance and understanding cathode fouling mechanisms. There are six objectives:

Objective 1: Apply a hydrophobic phase inversion coating as a new diffusion layer to lower cathode cost and enhance cathode performance.

Objective 2: Integrate catalyst layer with the diffusion layer via a new single-step cathode fabrication method using poly (vinylidene fluoride) (PVDF) to simplify cathode manufacture and lower cathode cost.

Objective 3: Improve cathode water integrity by using a hydrophobic PVDF membrane as a highly waterproof diffusion layer for cathode scale up.

Objective 4: Stabilize the PVDF membrane via hot pressing and increase effective catalyst loading by using AC catalyst on both sides of the current collector.

Objective 5: Improve the oxygen reduction reaction activity of activated carbon catalyst through immobilizing a metal-nitrogen-carbon co-catalyst.

Objective 6: Examine the effect of humic adsorption by activated carbon catalyst on cathode performance.

1.2 Dissertation Scope and Outline

In the research reported here, I described advances in cathode fabrication and optimization and I investigated fouling mechanisms. Following this introduction chapter, Chapter 2 is a literature review of cathode development, and the following chapters address the six stated objectives of this dissertation.

In Chapter 3, I developed a new poly (vinylidene fluoride-co-hexafluoropropylene) (PVDF-HFP) phase inversion coating as cathode diffusion layer. Cathodes with this new phase inversion coating had a larger oxygen mass transfer coefficient of 3×10^{-3} cm s^{-1}, than a conventional platinum/carbon cloth cathode of 1.7×10^{-3} cm s^{-1}. The maximum power density of the cathode with this new phase inversion coating was 31% higher than that obtained with the platinum/carbon cloth cathode. The phase inversion coating was found to be very porous and highly oxygen permeable to produce high power. The results of this work was summarized in a paper by Yang, W.; Zhang, F.; He, W.; Liu, J.; Hickner, M. A.; Logan, B. E., titled "Poly (vinylidene fluoride-co-hexafluoropropylene) phase inversion coating as a diffusion layer to enhance the cathode performance in microbial fuel cells", and it was published in *Journal of Power Sources*. Dr. Zhang Fang, Weihua He and Dr. Jia Liu helped with cathode characterization. Dr. Michael Hickner gave useful suggestions on polymers. I conducted all the experiments, including cathode preparation and MFC tests, and wrote the first manuscript draft. All the co-authors contributed in the preparation of the final manuscript.

In Chapter 4, I developed a single step fabrication method to manufacture activated carbon air cathode using poly(vinylidene fluoride) (PVDF) binder via phase inversion process. It was the first time that the cathode catalyst layer and diffusion layer were fabricated in a single step, which greatly simplified the manufacturing process. The fabricated phase inversion cathode produced a power density similar to a previous activated carbon cathode that used a polytetrafluoroethylene (PTFE) binder and a poly(dimethylsiloxane) (PDMS) diffusion layer, but it had a much higher water pressure resistance of 12 kPa compared to 1.8 kPa *(18, 19)*. The polymer needed was low, with only 8.8 mg cm^{-2}, for an overall cathode cost for materials of \$15 m^{-2}. The results of this work was summarized in a paper by Yang, W.; He, W.; Zhang, F.; Hickner, M. A.; Logan, B. E., titled "Single step fabrication using a phase inversion method of poly (vinylidene fluoride) (PVDF) activated carbon air cathodes for microbial fuel cells", and it was published in *Environmental Science and Technology Letters*. Weihua He and Dr. Fang Zhang helped maintain reactor operation. Dr. Michael Hickner offered useful suggestions on polymers. I conducted all the experiments and wrote the first draft of manuscript. All co-authors assisted in the preparation of the final manuscript.

In Chapter 5, I developed a hydrophobic poly (vinylidene fluoride) (PVDF) membrane as the first carbon free diffusion layer for activated carbon air cathode. The synthesized PVDF membrane showed a porous structure with pore size of ~ 100 nm and good oxygen permeability. Cathodes with this membrane diffusion layer were able to resist a high water pressure of ~ 21 kPa. The results of this work was summarized in a paper by Yang, W.; Kim, K.-Y.; Logan, B. E., titled "Development of carbon free diffusion layer for activated carbon air cathode of microbial fuel cells", and it was published in *Bioresource Technology*. Dr Kyoung-Yeol Kim helped maintain reactor operation. I conducted all the experiments, analyzed the data and prepared the first draft of manuscript. All co-authors contributed in the preparation of the final manuscript.

In Chapter 6, I optimized the performance of activated carbon air cathode using poly (vinylidene fluoride) (PVDF) membrane diffusion layer. The PVDF membrane was hot pressed

onto cathode catalyst layer at 60 °C to prevent water retention between the membrane and catalyst layer. The maximum power density was boosted from 1400 ± 7 mW m^{-2} for a non-pressed cathode to 1630 ± 10 mW m^{-2} for a hot pressed cathode. The cathode performance was further improved by adding additional catalyst layer to utilize more surface area of the stainless steel mesh current collector. The results of this work was summarized in a paper by Yang, W.; Logan, B. E., titled "Engineering a Membrane Based Air Cathode for Microbial Fuel Cells via Hot Pressing and Multi-Catalyst Layer Stacking", and it was published in *Environmental Science: Water Research and Engineering*. I conducted all the experiments, analyzed the data, and wrote the first draft of manuscript. All co-authors contributed to the preparation of the final manuscript.

In Chapter 7, I increased the oxygen reduction reaction (ORR) activity of activated carbon catalyst in the air cathode by immobilizing iron-nitrogen-carbon co-catalyst on activated carbon surface. The modified activated carbon catalyst (Fe-N-C/AC) showed a quasi-four electron transfer compared to a two electron transfer of conventional activated carbon. Cathode with the modified Fe-N-C/AC catalyst achieved a maximum power density of 4.7 ± 0.2 W m^{-2}, which is the highest among all reported air-cathode MFCs to date. This modification process was simple and used inexpensive raw materials (iron chloride and phenanthroline). The results of this work was summarized in a paper by Yang, W.; Logan, B. E., titled "Immobilization of Fe-N-C Co-catalyst on Activated Carbon with Enhanced Cathode Performance in Microbial Fuel Cells", and it was published in *ChemSusChem*. I conducted all the experiment and wrote the first draft of manuscript. All co-authors contributed to the preparation of the final manuscript.

In Chapter 8, I examined the effect of humic acid adsorption to activated carbon on the oxygen reduction activity and cathode performance. Activated carbon, after adsorbing humic acids, showed only 5% drop in current generation during the linear sweep voltammetry test. The drop in the current generation was mainly due to pore blocking as the total surface area of activated carbon decreased from 520 m^2 g^{-1} to 460 m^2 g^{-1} after adsorption. Cathodes after exposing to 1000 mg L^{-1}

humic solution showed a 14% decrease in power production. These results demonstrated that humics could contribute to cathode fouling, but the influence on power production was relatively small. The results was this work was summarized in a paper by Yang, W.; Watson, V. J.; Logan, B. E., titled "Extensive Humic Acid Adsorption to Activated Carbon Air Cathode Producing Small Reduction in Catalytic Activity", and it has been submitted for publication. Dr. Valerie Watson helped with the rotating disk electrode operation for the electrochemical characterization of activated carbon. I conducted all the experiment and wrote the first draft of the manuscript. All co-authors contributed to the preparation of the final manuscript.

1.3 Additional Research Publications

The following list includes research that I contributed to as a co-investigator, but it is not included in this dissertation.

1. Kim, K.-Y; **Yang, W.**; Evans P.J.; Logan B.E.; Continuous Treatment of High Strength Wastewaters Using Air-Cathode Microbial Fuel Cells. (in review)
2. He, W.; Wallack M. J.; Kim, K.-Y.; Zhang, X.; **Yang, W.**; Zhu, X.; Feng, Y.; Logan, B. E., The effect of flow modes and electrode combinations on the performance of a multiple module microbial fuel cell installed at wastewater treatment plant. (in review)
3. Kim, K.-Y.; **Yang, W.**; Ye, Y.; LaBarge, N.; Logan, B. E., Performance of anaerobic fluidized membrane bioreactors using effluents of microbial fuel cells treating domestic wastewater. *Bioresour. Technol.* **2016**, 208, 58-63.
4. Zhang, X.; He, W.; **Yang, W.**; Liu, J.; Wang, Q.; Liang, P.; Huang, X.; Logan, B. E., Diffusion layer characteristics for increasing the performance of activated carbon air cathodes in microbial fuel cells. *Environ.l Sci.: Water Res. Technol.* **2016**, 2, 266-273.

5. Tian, Y.; He, W.; Zhu, X.; **Yang, W**.; Ren, N.; Logan, B. E., Energy efficient electrocoagulation using an air-breathing cathode to remove nutrients from wastewater. *Chem. Eng. J*. 2016, 292, 308-314.
6. Kim, K.-Y.; **Yang, W.**; Logan, B. E., Impact of electrode configurations on retention time and domestic wastewater treatment efficiency using microbial fuel cells. *Water Res.* **2015**, 80, 41-46.
7. Zhang, F.; LaBarge, N.; **Yang, W.**; Liu, J.; Logan B.E., Enhancing the performance of low-grade thermal energy recovery in a thermally regenerative ammonia-based battery (TRAB) using elevated temperatures. *ChemSusChem* **2015**, 8, 1043-1048.
8. Zhang, F.; Liu, J.; **Yang, W.**; Logan, B.E., A thermally regenerative ammonia-based battery for efficient harvesting of low-grade thermal energy as electrical power. *Energy Env. Sci.* **2015**, 8(1), 343-349.
9. Zhu, X.; **Yang, W.**; Hatzell, M.; Logan, B. E., Energy recovery from solutions with different salinities based on swelling and shrinking of hydrogels. *Environ. Sci. Technol.* **2014**, 48, 7175-7163.
10. Liu, J.; Zhang, F.; He, W.; **Yang, W.**; Feng, Y.; Logan, B. E., A microbial fluidized electrode electrolysis cell (MFEEC) for enhanced hydrogen production. *J. Power Sources* **2014**, 271, 530-533.
11. Zhang, F.; Liu, J.; Ivanov, I.; Hatzell, M. C.; **Yang, W.**; Ahn, Y.; Logan, B. E., Reference and counter electrode positions affect electrochemical characterization of bioanodes in different bioelectrochemical systems. *Biotechnol. Bioeng.* **2014**, 111, (10).

1.4 Literature cited

1. Gerland, P.; Raftery, A. E.; Ševčíková, H.; Li, N.; Gu, D.; Spoorenberg, T.; Alkema, L.; Fosdick, B. K.; Chunn, J.; Lalic, N., World population stabilization unlikely this century. *Science* **2014,** *346*, (6206), 234-237.
2. BP Statistical Review of World Energy. **2015**.
3. Rifkin, J., *The Hydrogen Economy*. Tarcher/Putnam: New York, 2002.
4. Marques, L. M.; Fuinhas, J. A.; Marques, A. C., On the Global Energy Consumption and Economic Growth Nexus: a Long Time Span Analysis. *Int Energ J.* **2015,** *15*, (4).
5. International Energy Statistics *U.S. Energy Information Administration* **2012**.
6. Tidwell, V. C.; Moreland, B.; Zemlick, K., Geographic Footprint of Electricity Use for Water Services in the Western US. *Environ. Sci. Technol.* **2014,** *48*, (15), 8897-8904.
7. McCarty, P. L.; Bae, J.; Kim, J., Domestic wastewater treatment as a net energy producer–can this be achieved? *Environ. Sci. Technol.* **2011,** *45*, (17), 7100-7106.
8. Logan, B. E.; Rabaey, K., Conversion of wastes into bioelectricity and chemicals by using microbial electrochemical technologies. *Science* **2012,** *337*, (6095), 686-690.
9. Logan, B. E., *Microbial fuel cells*. John Wiley & Sons, Inc.: Hoboken, NJ, 2008; p 300.
10. Niessen, J.; Schröder, U.; Scholz, F., Exploiting complex carbohydrates for microbial electricity generation- a bacterial fuel cell operating on starch. *Electrochem. Commun.* **2004,** *6*, 955-958.
11. Allen, R. M.; Bennetto, H. P., Microbial fuel cells: Electricity production from carbohydrates. *Appl. Biochem. Biotechnol.* **1993,** *39*, (2), 27-40.
12. Bond, D. R.; Holmes, D. E.; Tender, L. M.; Lovley, D. R., Electrode-reducing microorganisms that harvest energy from marine sediments. *Science* **2002,** *295*, (5554), 483-485.

13. Lovley, D. R., Bug juice: harvesting electricity with microorganisms. *Nat. Rev. Microbiol.* **2006,** *4*, 497-508.

14. He, W.; Zhang, X.; Liu, J.; Zhu, X.; Feng, Y.; Logan, B. E., Microbial fuel cells with an integrated spacer and separate anode and cathode modules. *Environ. Sci.: Water Res. Technol.* **2016,** *2*, (1), 186-195.

15. Dong, Y.; Qu, Y.; He, W.; Du, Y.; Liu, J.; Han, X.; Feng, Y., A 90-liter stackable baffled microbial fuel cell for brewery wastewater treatment based on energy self-sufficient mode. *Biores. Technol.* **2015,** *195*, 66-72.

16. Rozendal, R. A.; Hamelers, H. V. M.; Rabaey, K.; Keller, J.; Buisman, C. J. N., Towards practical implementation of bioelectrochemical wastewater treatment. *Trends Biotechnol.* **2008,** *26*, (8), 450-459.

17. Zhang, F.; Pant, D.; Logan, B. E., Long-term performance of activated carbon air cathodes with different diffusion layer porosities in microbial fuel cells. *Biosens. Bioelectron* **2011,** *30,* (1), 49-55.

18. Wei, B.; Tokash, J. C.; Chen, G.; Hickner, M. A.; Logan, B. E., Development and evaluation of carbon and binder loading in low-cost activated carbon cathodes for air-cathode microbial fuel cells. *RSC Adv* **2012,** *2*, (33), 12751-12758.

19. Yang, W.; He, W.; Zhang, F.; Hickner, M. A.; Logan, B. E., Single step fabrication using a phase inversion method of poly (vinylidene fluoride)(PVDF) activated carbon air cathodes for microbial fuel cells. *Environ. Sci. Technol. Lett.* **2014,** *1*, 416-420.

Chapter 2

Literature review

In order to harvest energy from wastewater treatment, microbial fuel cells (MFCs) (Figure 2-1) are being developed as a sustainable technology that can be used to convert organic and inorganic substrates to electrical power *(1-5)*. Exoelectrogenic bacteria on the anode oxidize different substrates to release electrons, which flow through an external circuit to the cathode where typically oxygen reduction occurs. Oxygen is the most common electron acceptor in MFCs due to its abundance in the air *(6-9)*. The use of air cathodes in MFCs also eliminates the need for wastewater aeration which further reduces the cost of wastewater treatment. For scaled up MFC applications, hundreds to thousands of square meters of cathodes are needed and it remains a challenge to fabricate cathodes at a high capacity *(10)*. Substantial progress has been achieved in developing low cost air cathodes as well as improving power production. This chapter is a review of recent cathode development and optimization. Some cathode fouling issues are also discussed that arise during longer term operation of MFCs.

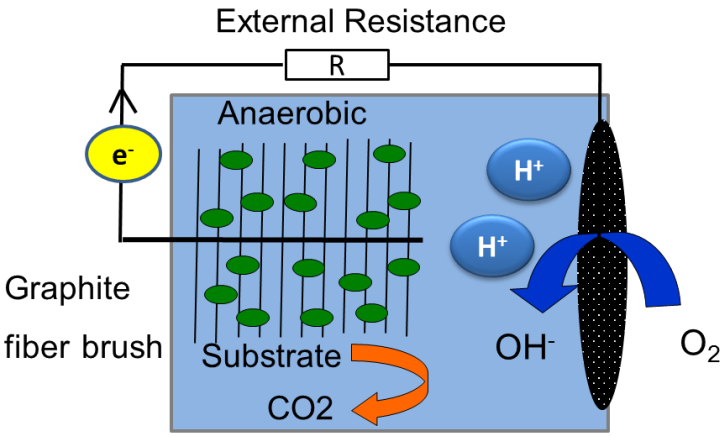

Figure 2-1. Scheme of a single chamber MFC with graphite brush anode and an air cathode.

2.1 Air cathode

2.1.1 Cathode structure

An air cathode is usually made with a catalyst layer (CL), a current collector (CC), and a diffusion layer (DL) facing the air side (Figure 2-2). The CL is the main functioning part of air cathode where the oxygen reduction reaction takes place. The CC plays double roles of conducting current and also mechanically supporting the cathode. The DL is used to enable oxygen diffusion into the cathode while preventing water or electrolyte leaking out of the reactor. There are two cathode configurations that are currently adopted in MFC studies *(11, 12)*. The first configuration has the CL in between the CC and DL, with the CC facing the solution side (Figure 2-2A). The second configuration places the CL close to the solution side, with the CC in the middle (Figure 2-2B). The main difference is the location of CL, depending on fabrication methods, but there was no study that demonstrated which configuration performed better in catalyzing the oxygen reduction reaction. Both configurations put the DL towards the air side to prevent water leakage, and the DL must be oxygen permeable to allow oxygen transport to the catalyst.

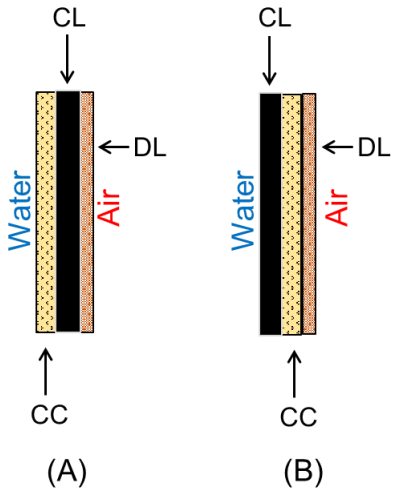

Figure 2-2. Two cathode configurations with (A) current collector facing water (B) catalyst layer facing water. (CL, catalyst layer; CC, current collector; DL, diffusion layer)

2.1.2 Cathode fabrication

2.1.2.1 Current collector

Electrically conductive current collectors have been commonly used to collect electrons transferred from the anode and function as the backbone of cathode *(7, 13, 14)*. Currently there are three commonly used current collectors: carbon cloth, copper mesh, and stainless steel mesh (Figure 2-3). Carbon cloth is traditionally used in fuel cell studies and is commercially available *(15-17)*. An early MFC study using carbon cloth as current collector with platinum catalyst produced a maximum power density of ~ 766 mW m^{-2} *(13)*. The power density produced with carbon cloth cathode was later improved to between 1100 and 1500 mW m^{-2} by using improved reactor configurations *(18, 19)*. However, the commercial grade of carbon cloth is very expensive (~ \$625 m^{-2}), which greatly limits applications of carbon cloth based cathodes *(8)*.

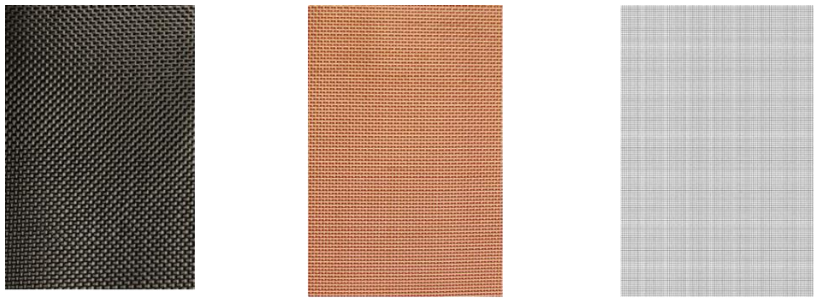

Figure 2-3. Three main cathode supporting materials: carbon cloth, copper mesh and stainless steel mesh.

As an alternative to replace the expensive carbon cloth, metal mesh has been emerging as a new type of cathode current collector *(20, 21)*. Metal mesh made of copper or stainless steel usually exhibit high electron conductivity of ~ 1.5×10^6 S m^{-1}, which is very useful for scaled up cathodes. Cathodes built using stainless steel mesh as a current collector produced similar power density to the cathode built using carbon cloth both with platinum as catalyst *(21)*. Another advantage of a

metal mesh current collector was the low cost of ~ \$10 m^{-2} for stainless steel mesh, which is much cheaper than carbon cloth *(8)*. However, one study claimed that corrosion might take place in metal based cathodes under water conditions *(22)*. To date, a metal mesh current collector is still considered to the cheapest cathode support material, and its use helps to lower the overall cathode cost.

Other materials have also been used as current collectors and support for cathodes. Graphite paste was coated as a conductive layer on ion exchange membranes or ultrafiltration membranes to act as current collector *(23, 24)*. However, the conductivity of this graphite layer was low and greatly limited the maximum power density to just 449 mW m^{-2}. For comparison, adding a piece of stainless steel onto the AEM membrane improved power production by 28% and reduced internal resistance by 38%, suggesting that graphite layer alone was not as conductive as the metal mesh *(24)*. Carbon mesh was also tested as cathode current collector, and it produced a power density similar to carbon cloth, but a more conductive current collector is still needed for larger size cathodes *(25)*.

In addition to being conductive, the current collectors have also to be porous for ion (protons or hydroxide) or oxygen diffusion. A mesh optimization study showed a decreased power production when using a finer stainless steel mesh (120-mesh) compared to coarser stainless steel mesh (30-mesh) *(26)*. The lower power production resulted from increased diffusion resistance and lower oxygen permeability with the finer stainless steel mesh. Therefore, the selection of current collector with an appropriate porous structure is also important when fabricating the cathode.

2.1.2.2 Catalyst layer

The catalyst layer is the core functioning part of the cathode, and it is usually fabricated from a mixture of catalyst and binding agent. Currently, the commercially available oxygen reduction

reaction catalysts for MFC cathodes use platinum, activated carbon, or certain metal oxides, which are all in particulate form. A polymer is usually needed to bind the catalysts together and form a catalyst layer.

Besides acting solely as a binding agent, the binder also plays an important role in maintaining a three-phase interface between air (oxygen), water (protons) and solid (catalyst) for the oxygen reduction reaction *(27)*. In order to facilitate proton diffusion, proton conductive polymers are usually used as binder for the cathode catalyst layer in fuel cells. Nafion is the mostly widely used cathode binder due to the high proton conductivity and chemical stability even at high temperature *(13, 28)*. However, Nafion is expensive as it costs ~ \$360 m^{-2} when used in the cathode (based on cathode area), which limits its applications in MFCs *(8)*. Alternatives to Nafion, including poly(phenlsulfone) and some cation fluorinated polymer binders such as poly(arylene ether) (Q-FPAE), were shown to have similar performance to Nafion in MFCs *(29, 30)*. However, cathodes using anion exchange polymers of quaternary 1,4-diazabicyclo-[2.2.2]-octane (DABCO) polysulfone (QDPSU) showed better performance compared than Nafion due to better interaction between the ionomer and oxygen, and improved OH^- transfer *(31)*. Another study using neutral hydrophilic polystyrene-b-poly(ethylene oxide) (PS-b-PEO) polymer as cathode binder reported lower initial power production compared to Nafion, but similar power production after 40 days *(32)*. Besides those hydrophilic polymer binders, there have been other studies that used hydrophobic poly(vinylidene fluoride) (PVDF) and poly(dimethylsiloxane) (PDMS) as cathode binders *(33, 34)*. From these studies, it appears that various polymers (cationic vs. anionic, and hydrophilic vs. hydrophobic) have been successfully used as cathode binders, and there is no strict conclusion about the best type of polymer as a cathode binder. However, hydrophilic binders are generally preferred *(32)*, and a hydrophobic binder cannot be added at a too high loading as it would impede ion transport.

A catalyst layer is usually fabricated by spreading a mixture of catalyst and binder onto the current collector via brushing, pressing, rolling, or dip coating. Brushing is the most commonly used method for applying a platinum catalyst mixture onto either carbon cloth or stainless steel mesh *(13, 35)*. The platinum loading is usually around 0.5 mg cm^{-2}, and can easily be brushed onto current collector forming a thin catalyst layer. However, brushing did not work very well with an activated carbon catalyst, when the loading increased to 25 mg cm^{-2}, as this led to a thick catalyst layer that was difficult to brush onto the current collector *(12)*. Considering that activated carbon is not highly electrically conductive, a dense packing structure is needed to ensure good electrical contact to adjacent carbon particles and the current collector. Therefore, pressing methods are more suitable for activated carbon catalyst layer fabrication as high pressures are needed to ensure good contact between particles *(11, 12)*. Roller pressing could enable easier fabrication as roller machines can operate continuously and automatically. One study also reported the use of a dip coating method for applying activated carbon catalyst layer onto carbon cloth current collector, which is also convenient, but the stability of this material on the current collector needs to be further investigated *(36)*.

2.1.2.3 Diffusion layer

The cathode diffusion layer serves dual purposes of being both oxygen permeable and waterproof. To facilitate the oxygen reduction reaction, the diffusion layer has to be porous so that oxygen molecules can diffuse through it. The diffusion layer should also be waterproof and serve as a barrier between the liquid phase and air phase. Therefore, the dual roles of diffusion layer place high demands on the production of an efficient and economical diffusion layer. In order for the diffusion layer to be waterproof, hydrophobic polymers are usually used for its fabrication. Polytetrafluoroethylene (PTFE) shows very strong hydrophobicity as the backbone is fully

fluorinated. In a platinum/carbon cloth cathode, 70% (w/v) of a PTFE solution was brushed onto the carbon cloth current collector, which was then sintered at 370 °C *(13)*. The sintering process helped to melt the PTFE and generated a homogeneous diffusion layer. The resulting PTFE diffusion layer showed good oxygen permeability and it could withstand 1.2 m water pressure *(37)*.

The PTFE diffusion layer, however, cannot be applied to metal mesh current collectors due to large mesh size. For larger cathodes, the diffusion layer has to be fabricated as a separate layer and placed on the air side of the cathode. Poly(dimethylsiloxane) mixed with carbon black was brushed onto a porous wipe cloth to form a separate diffusion layer with good oxygen permeability *(38)*. This layer was pressed onto the metal mesh based cathode using a pressing machine, but the waterproof capability of the cathode was not good due to the large pore size *(19)*. Another type of PTFE/carbon black diffusion layer was developed by mixing PTFE and carbon black, which are both hydrophobic *(11)*, and then pressing the mixture using a roller onto stainless steel mesh, followed by sintering at 370 °C to melt PTFE. The PTFE/carbon black diffusion layer showed a high pressure tolerance of ~ 3 m water height, but the loading of PTFE was very high of ~ 450 g m^{-2}, which would make the cathode expensive *(8, 37)*.

2.2 Cathode catalyst

A catalyst with high oxygen reduction reaction (ORR) reactivity is critical for high power production in an MFC, but the catalyst has to also be cheap for commercialization of MFCs. Platinum has been long used as the "ideal" oxygen reduction reaction catalyst, but it has a very high cost of ~ \$100 g^{-1}. Moreover, platinum is contaminated in a phosphate buffer solution or wastewater, and undergoes significant degradation in performance *(39, 40)*. Activated carbon has emerged as a low cost oxygen reduction reaction catalyst that costs only ~ \$1.4 kg^{-1} and it performs similarly to platinum in MFCs *(8)*. Many researchers have focused on improving the reactivity of

activated carbon or other carbon materials, including carbon black, carbon nanotubes or graphene. Therefore, much effort has been directed at developing alternative catalysts to platinum with high reaction activity.

2.2.1 Carbon based catalyst

Activated carbon

Activated carbon (AC) is a porous carbon material with high surface area that ranges from 800 to 1500 m^2 g^{-1}, and it has long been used as adsorbents in water treatment *(41, 42)*. It was found that AC could also catalyze oxygen reduction and served as a promising alternative catalyst to platinum *(20, 43)*. AC derived from different precursors can result in different ORR activities, and it was determined that coal derived AC produced the highest power density among peat, coconut shell, hardwood carbon, phenolic resin and bituminous coal derived ACs *(44)*. Surface oxygen functional groups such as carboxylic groups impeded ORR activity, while nitrogen functional groups facilitated ORR. Another study successfully identified pyridinic nitrogen as the ORR catalytic site using graphite as a model catalyst with stepwise nitrogen doping *(45)*.

Incorporation of nitrogen atoms in AC has been an effective method to boost the ORR activity, and AC is usually treated using nitrogen containing chemicals. AC treated with ammonia gas at 700 °C for 1 h increased the surface N content to 1.8% and produced a maximum power density of 2450 mW m^{-2} *(46)*. Ammonia gas removed oxygen functional groups on the AC surface and helped introduce nitrogen functional groups. Carbonization of cyanamide and activated carbon (750 °C for 4 h) increased the pyridinic nitrogen content up to 5%, resulting in a four electron transfer (electron-transfer number of 3.9) *(47)*. Acid/base treatment of AC was also reported to boost the ORR catalytic activity. AC treated with potassium hydroxide resulted in a 16% increase in maximum power density compared to untreated AC due to reduced internal resistance *(48)*.

Phosphoric acid treated AC at 400 °C showed a 55% increase in the maximum power density due to P atom incorporation *(49)*.

Loading AC with different metal oxides has also been reported to enhance the ORR activity of AC. Manganese oxides (MnO_2) was mixed with AC at 1:1 ratio and showed reduced internal resistance *(50)*. Electrochemical deposition of MnO_2 on AC was reported to increase the meso-pore surface area, and achieved 1.5 times higher power production compared to untreated AC *(51)*. Copper oxide (Cu_xO) was also deposited on AC to change AC surface roughness and pore structure, and it improved ORR catalysis *(52, 53)*. AC mixed with 10% of CeO_2, an oxygen storage metal oxides, also showed enhanced MFC performance likely due to improved oxygen diffusion as oxygen was pre-stored within CeO_2 matrix *(54)*.

AC is not very electrically conductive, but blending it with carbon black decreased ohmic and charge transfer resistances, resulting in a 16% increase in power production *(9)*. Ammonium bicarbonate was used as a pore former to increase the porosity of AC, and its use enhanced MFC power production due to a reduced charge transfer resistance *(55)*.

Carbon black/Graphite

Carbon black (CB) and graphite are electrically conductive and therefore they have been used as catalyst support materials *(56, 57)*. CB has an amorphous structure with large specific area and a very low cost of ~ \$3.3 kg^{-1} *(8)*. Graphite has a multi layered planar structure and is also cheap at ~ \$2 kg^{-1}. CB and graphite intrinsically exhibit no or low ORR activity, therefore different modifications have been made to create active sites on the CB or graphite surfaces. In one study, nitric acid treated CB produced a maximum power density of 170 mW m^{-2}, which was 22% lower than that of platinum *(58)*. In another study, nitric acid treated CB and ammonia gas treatment also enhanced the MFC performance due to incorporation of nitrogen *(59)*. The co-doping of nitrogen and fluorine onto carbon black improved the maximum power density of 672 mW m^{-2}, which was

17% higher than that of platinum *(60)*. Graphite treated with nitric acid also introduced nitrogen or oxygen functional groups on the surface, which enhanced ORR activity *(61, 62)*.

Carbon nanotube/nanofiber and graphene

Carbon nanotubes (CNTs), carbon nanofibers (CNFs), and graphene are all highly conductive nano-carbon materials that have low ORR activity. Although the costs of these nano materials are very high, and not competitive with activated carbon, carbon black or graphite, studies have also been conducted to enhance their ORR activity due to their high surface area and conductivities. For example, carbon nanotube doped with nitrogen produced a maximum power density of 1600 mW m^{-2} compared to 1393 mW m^{-2} with platinum *(63)*. A nitrogen doped CNT catalyzed ORR in a four electron transfer pathway, which was probably due to charge delocalization from the heteroatom doping. Metal catalysts such as platinum, MnO_2, NiO and Co_3O_4 were also immobilized on the CNT surface either by mechanical mixing or chemical reduction, which all boosted the ORR activity of CNT *(64-69)*. Carbon nanofibers were doped with nitrogen via pyrolysis with pyridine, and achieved similar power performance to a platinum catalyst *(70)*. Co-doping of nitrogen and sulfur onto CNF derived from natural spider silk improved the maximum power density to 1800 mW m^{-2}, which was 1.6 times higher than a platinum catalyst *(71)*. Graphene was also modified by doping with nitrogen using a denotation process with cyanuric chloride and trinitrophenol, resulting in a maximum power density of 1350 mW m^{-2}, which was similar compared to the 1420 mW m^{-2} produced with the platinum catalyst *(72)*.

2.2.2 Metal based catalyst

Due to the high cost of platinum, metal based catalysts have been examined that have lower costs using pure platinum. A platinum-iron alloy catalyst produced a maximum power density of

1097 mW m^{-2}, which was similar to 1030 mW m^{-2} using a pure platinum catalyst *(73)*. Other platinum-cobalt or platinum-nickel alloy catalysts have also been used as alternatives for ORR catalysts in MFCs *(74, 75)*.

Some metal oxides can catalyze the ORR, and are considered to be promising alternatives to platinum. MnO_2 was used as a cathode catalyst in an MFC, and it produced a maximum power density of 937 mW m^{-2}, which was slightly lower than 1037 mW m^{-2} for platinum *(76)*, Another study further demonstrated that β–MnO_2 exhibited higher ORR activity than α–MnO_2 and γ–MnO_2 *(77)*. A composite MnO_2/polypyrrole/MnO_2 nanowire catalyst was prepared via hydrothermal and in-situ polymerization for MFCs and produced a maximum power density of 721 mW m^{-2} *(78)*. Other metal oxides such as perovskite oxides, vanadium oxides, cobalt oxide and zirconium oxide have also been examined as cathode catalysts in MFCs but the stability of these metal oxides needs to be further investigated *(79-83)*.

2.2.3 Metal-nitrogen-carbon catalyst

Metal-nitrogen-carbon (M-N-C) catalysts are made by carbonizing an inexpensive metal and a nitrogen containing ligand at high temperatures (700 to 1000 °C) *(84)*. Different from metal or nitrogen doping, M-N-C catalysts can form chemical bonds between the metal, nitrogen, and carbon atoms, which could catalyze ORR in a quasi-four electron pathway or a direct four electron pathway *(84)*. Pyrolysis of iron phthalocyanine at 700 °C produced a Fe-N-C catalyst that performed similarly to a platinum catalyst in MFCs *(85)*. Pyrolysis cobalt naphthalocyanine and cobalt tetramethylphenylporphyrin produced a Co-N-C type catalyst, but it had lower power production compared to platinum in MFCs *(86, 87)*. The exact catalytic site for metal-nitrogen-carbon has not been determined yet and the application of this catalyst needs further investigation.

2.3 Cathode stability

MFCs are currently being examined mainly for use in wastewater treatment, and therefore the costs of the materials should be low for practical applications *(10, 88)*. As the cathode can be 50% of the total MFC cost, studies have been conducted to lower the cathode cost by using low cost catalysts, current collectors, and diffusion layers. However, cathode degradation over time can also hinder MFC applications. One study showed that an activated carbon cathode performance degraded up to 40% after one year operation in MFCs *(89)*. Therefore, it is also important to increase the lifetime of the cathode, as this would significantly lower overall MFC capital costs. Understanding the degradation mechanism of cathode would help develop better cathodes with longer lifetimes.

Biofilm growth on cathode surface has been identified to cause cathode degradation in performance. In typical single chamber MFCs, the cathode is directly exposed to both organic matter and oxygen, leading to biofilm growth on the cathode surface that can be 2~3 mm thick *(40)*. A one year operation of activated carbon cathode showed a 40% decrease in power production, from 1214 mW m^{-2} to 734 mW m^{-2} *(89)*. Removal of the biofilm increased the power production to 822 mW m^{-2}, which was a 67% recovery.

Cathodes are made to be oxygen permeable, and thus water evaporation can occur during cathode operation. The wastewater or synthetic phosphate buffer solutions used in MFCs contain salts. As the water is evaporated in the cathode, observable salt precipitation can be seen on the air side of cathode surface *(90)*, but to date no conclusions have been made as to whether such salt precipitation would affect cathode performance.

2.4 Conclusions

A review of the cathode structure and fabrication, catalyst and long term stability has shown recent progress in cathode materials and architecture, which could result in practical applications of MFCs. The fabrication of the cathode is has been improved in terms of cathode structure and by using low cost materials, but these cathodes still need to be tested in larger scale systems. The catalytic activity of a cathode has been greatly improved by modifying current catalysts or developing new catalysts. Many low cost catalysts have emerged as alternatives to platinum, with treated activated carbon showing the most promise. However, the long term stability of the cathodes still remains unclear, and a deeper understanding of cathode degradation mechanism is necessary. A highly active cathode with long lifetime and low cost would be beneficial for implementing MFCs for real wastewater treatment.

2.5 Literature cited

1. Logan, B. E., *Microbial fuel cells*. John Wiley & Sons, Inc.: Hoboken, NJ, 2008; p 300.
2. Niessen, J.; Schröder, U.; Scholz, F., Exploiting complex carbohydrates for microbial electricity generation- a bacterial fuel cell operating on starch. *Electrochem. Commun.* **2004,** *6*, 955-958.
3. Allen, R. M.; Bennetto, H. P., Microbial fuel cells: Electricity production from carbohydrates. *Appl. Biochem. Biotechnol.* **1993,** *39*, 27-40.
4. Bond, D. R.; Holmes, D. E.; Tender, L. M.; Lovley, D. R., Electrode-reducing microorganisms that harvest energy from marine sediments. *Science* **2002,** *295*, 483-485.
5. Lovley, D. R., Bug juice: harvesting electricity with microorganisms. *Nat. Rev. Microbiol.* **2006,** *4*, 497-508.
6. Xia, X.; Zhang, F.; Zhang, X.; Liang, P.; Huang, X.; Logan, B. E., Use of Pyrolyzed Iron Ethylenediaminetetraacetic Acid Modified Activated Carbon as Air–Cathode Catalyst in Microbial Fuel Cells. *ACS Appl. Mater. Interfaces* **2013,** *5*, 7862-7866.
7. Dong, H.; Yu, H.; Wang, X., Catalysis kinetics and porous analysis of rolling activated carbon-PTFE air-cathode in microbial fuel cells. *Environ. Sci. Technol.* **2012,** *46*, 13009-13015.
8. Yang, W.; He, W.; Zhang, F.; Hickner, M. A.; Logan, B. E., Single step fabrication using a phase inversion method of poly (vinylidene fluoride)(PVDF) activated carbon air cathodes for microbial fuel cells. *Environ. Sci. Technol. Lett.* **2014,** *1*, 416-420.
9. Zhang, X.; Xia, X.; Ivanov, I.; Huang, X.; Logan, B. E., Enhanced activated carbon cathode performance for microbial fuel cell by blending carbon black. *Environ. Sci. Technol.* **2014,** *48*, 2075-2081.

10. Logan, B. E.; Wallack, M. J.; Kim, K.-Y.; He, W.; Feng, Y.; Saikaly, P. E., Assessment of microbial fuel cell configurations and power densities. *Environ. Sci. Technol. Lett.* **2015,** *2*, 206-214.
11. Dong, H.; Yu, H.; Wang, X.; Zhou, Q.; Feng, J., A novel structure of scalable air-cathode without Nafion and Pt by rolling activated carbon and PTFE as catalyst layer in microbial fuel cells. *Water Res.* **2012,** *46*, 5777-5787.
12. Wei, B.; Tokash, J. C.; Chen, G.; Hickner, M. A.; Logan, B. E., Development and evaluation of carbon and binder loading in low-cost activated carbon cathodes for air-cathode microbial fuel cells. *RSC Adv* **2012,** *2*, 12751-12758.
13. Cheng, S.; Liu, H.; Logan, B. E., Increased performance of single-chamber microbial fuel cells using an improved cathode structure. *Electrochem. Commun.* **2006,** *8*, 489-494.
14. Garino, N.; Sacco, A.; Castellino, M.; Muñoz-Tabares, J. A.; Chiodoni, A.; Agostino, V.; Margaria, V.; Gerosa, M.; Massaglia, G.; Quaglio, M., Microwave-assisted synthesis of reduced graphene oxide/SnO2 nanocomposite for oxygen reduction reaction in microbial fuel cells. *ACS Appl. Mater. Interfaces* **2016,** *8*, 4633-4643.
15. Lee, H.-K.; Park, J.-H.; Kim, D.-Y.; Lee, T.-H., A study on the characteristics of the diffusion layer thickness and porosity of the PEMFC. *J.Power Sources* **2004,** *131*, 200-206.
16. Williams, M. V.; Kunz, H. R.; Fenton, J. M., Operation of Nafion®-based PEM fuel cells with no external humidification: influence of operating conditions and gas diffusion layers. *J.Power Sources* **2004,** *135*, 122-134.
17. Gamburzev, S.; Appleby, A. J., Recent progress in performance improvement of the proton exchange membrane fuel cell (PEMFC). *J.Power Sources* **2002,** *107*, 5-12.
18. Yang, W.; Zhang, F.; He, W.; Liu, J.; Hickner, M. A.; Logan, B. E., Poly (vinylidene fluoride-co-hexafluoropropylene) phase inversion coating as a diffusion layer to enhance the cathode performance in microbial fuel cells. *J. Power Sources* **2014,** *269*, 379-384.

19. Zhang, X.; He, W.; Yang, W.; Liu, J.; Wang, Q.; Liang, P.; Huang, X.; Logan, B. E., Diffusion layer characteristics for increasing the performance of activated carbon air cathodes in microbial fuel cells. *Environ. Sci.: Water Res. Technol.* **2016**, 266-273.
20. Zhang, F.; Cheng, S.; Pant, D.; Bogaert, G. V.; Logan, B. E., Power generation using an activated carbon and metal mesh cathode in a microbial fuel cell. *Electrochem. Commun.* **2009,** *11*, 2177-2179.
21. Zhang, F.; Saito, T.; Cheng, S.; Hickner, M. A.; Logan, B. E., Microbial Fuel Cell Cathodes With Poly(dimethylsiloxane) Diffusion Layers Constructed around Stainless Steel Mesh Current Collectors. *Environ. Sci. Technol.* **2010,** *44*, 1490-1495.
22. Janicek, A.; Fan, Y.; Liu, H., Performance and stability of different cathode base materials for use in microbial fuel cells. *J. Power Sources* **2015,** *280*, 159-165.
23. Zuo, Y.; Cheng, S.; Call, D.; Logan, B. E., Tubular membrane cathodes for scalable power generation in microbial fuel cells. *Environ. Sci. Technol.* **2007,** *41*, 3347-3353.
24. Zuo, Y.; Cheng, S.; Logan, B. E., Ion exchange membrane cathodes for scalable microbial fuel cells. *Environ. Sci. Technol.* **2008,** *42*, 6967-6972.
25. Luo, Y.; Zhang, F.; Wei, B.; Liu, G.; Zhang, R.; Logan, B. E., Power generation using carbon mesh cathodes with different diffusion layers in microbial fuel cells. *J. Power Sources* **2011,** *196*, 9317-9321.
26. Zhang, F.; Merrill, M. D.; Tokash, J. C.; Saito, T.; Cheng, S.; Hickner, M. A.; Logan, B. E., Mesh optimization for microbial fuel cell cathodes constructed around stainless steel mesh current collectors. *J.Power Sources* **2011,** *196*, 1097-1102.
27. Logan, B. E., Scaling up microbial fuel cells and other bioelectrochemical systems. *Appl. Microbiol. Biotechnol.* **2010,** *85*, 1665-1671.
28. Kraytsberg, A.; Ein-Eli, Y., Review of advanced materials for proton exchange membrane fuel cells. *Energy & Fuels* **2014,** *28*, 7303-7330.

29. Saito, T.; Merrill, M. D.; Watson, V. J.; Logan, B. E.; Hickner, M. A., Investigation of ionic polymer cathode binders for microbial fuel cells. *Electrochimica Acta* **2010,** *55*, 3398-3403.
30. Chen, G.; Wei, B.; Logan, B. E.; Hickner, M. A., Cationic fluorinated polymer binders for microbial fuel cell cathodes. *RSC ADV* **2012,** *2*, 5856-5862.
31. Yu, E. H.; Burkitt, R.; Wang, X.; Scott, K., Application of anion exchange ionomer for oxygen reduction catalysts in microbial fuel cells. *Electrochem. Commun.* **2012,** *21*, 30-35.
32. Saito, T.; Roberts, T. H.; Long, T. E.; Logan, B. E.; Hickner, M. A., Neutral hydrophilic cathode catalyst binders for microbial fuel cells. *Energy Environ Sci.* **2011,** *4*, 928-934.
33. Huang, L.; Tian, Y.; Li, M.; He, G.; Li, Z. Performance of stainless stell mesh cathode and PVDF-graphite cathode in microbial fuel cells. 2nd International Symposium on Aqua Science, Water Resource and Low Carbon Energy, 2010; AIP Publishing: 2010; pp 316-319.
34. Zhang, F.; Chen, G.; Hickner, M. A.; Logan, B. E., Novel anti-flooding poly(dimethylsiloxane) (PDMS) catalyst binder for microbial fuel cell cathodes. *J.Power Sources* **2012,** *218*, 100-105.
35. Hoskins, D. L.; Zhang, X.; Hickner, M. A.; Logan, B. E., Spray-on polyvinyl alcohol separators and impact on power production in air-cathode microbial fuel cells with different solution conductivities. *Biores. Technol.* **2014,** *172*, 156-161.
36. Ge, Z.; He, Z., An effective dipping method for coating activated carbon catalyst on the cathode electrodes of microbial fuel cells. *RSC Adv* **2015,** *5*, 36933-36937.
37. He, W.; Liu, J.; Li, D.; Wang, H.; Qu, Y.; Wang, X.; Feng, Y., The electrochemical behavior of three air cathodes for microbial electrochemical system (MES) under meter scale water pressure. *J.Power Sources* **2014,** *267*, 219-226.
38. Zhang, F.; Saito, T.; Cheng, S.; Hickner, M. A.; Logan, B. E., Microbial fuel cells cathodes constructed from stainless steel mesh that use poly(dimethylsiloxane) diffusion layers. *Environ. Sci. Technol.* **2010,** *44*, 1490-1495.

39. Savizi, I. S. P.; Janik, M. J., Acetate and phosphate anion adsorption linear sweep voltammograms simulated using density functional theory. *Electrochim Acta* **2011,** *56*, 3996-4006.

40. Kiely, P. D.; Rader, G.; Regan, J. M.; Logan, B. E., Long-term cathode performance and the microbial communities that develop in microbial fuel cells fed different fermentation endproducts. *Biores. Technol.* **2011,** *102*, 361-366.

41. Sontheimer, H.; Crittenden, J. C.; Summers, R. S., *Activated carbon for water treatment*. DVGW-Forschungsstelle, Engler-Bunte-Institut, Universitat Karlsruhe (TH): 1988.

42. Lambert, T. W.; Holmes, C. F.; Hrudey, S. E., Adsorption of microcystin-LR by activated carbon and removal in full scale water treatment. *Water Res.* **1996,** *30*, 1411-1422.

43. Iwazaki, T.; Obinata, R.; Sugimoto, W.; Takasu, Y., High oxygen-reduction activity of silk-derived activated carbon. *Electrochem. Commun.* **2009,** *11*, 376-378.

44. Watson, V. J.; Nieto Delgado, C.; Logan, B. E., Influence of chemical and physical properties of activated carbon powders on oxygen reduction and microbial fuel cell performance. *Environ. Sci. Technol.* **2013,** *47*, 6704-6710.

45. Guo, D.; Shibuya, R.; Akiba, C.; Saji, S.; Kondo, T.; Nakamura, J., Active sites of nitrogen-doped carbon materials for oxygen reduction reaction clarified using model catalysts. *Science* **2016,** *351*, 361-365.

46. Watson, V. J.; Nieto Delgado, C.; Logan, B. E., Improvement of activated carbons as oxygen reduction catalysts in neutral solutions by ammonia gas treatment and their performance in microbial fuel cells. *J. Power Sources* **2013,** *242*, 756-761.

47. Zhang, B.; Wen, Z.; Ci, S.; Mao, S.; Chen, J.; He, Z., Synthesizing nitrogen-doped activated carbon and probing its active sites for oxygen reduction reaction in microbial fuel cells. *ACS Appl. Mater. Interfaces* **2014,** *6*, 7464-7470.

48. Wang, X.; Gao, N.; Zhou, Q.; Dong, H.; Yu, H.; Feng, Y., Acidic and alkaline pretreatments of activated carbon and their effects on the performance of air-cathodes in microbial fuel cells. *Bioresour. Technol.* **2013,** *144*, 632-636.

49. Chen, Z.; Li, K.; Pu, L., The performance of phosphorus (P)-doped activated carbon as a catalyst in air-cathode microbial fuel cells. *Biores. Technol.* **2014,** *170*, 379-384.

50. Singh, I.; Chandra, A., Need for optimizing catalyst loading for achieving affordable microbial fuel cells. *Biores. Technol.* **2013,** *142*, 77-81.

51. Zhang, P.; Li, K.; Liu, X., Carnation-like MnO 2 modified activated carbon air cathode improve power generation in microbial fuel cells. *J.Power Sources* **2014,** *264*, 248-253.

52. Liu, Z.; Li, K.; Zhang, X.; Ge, B.; Pu, L., Influence of different morphology of three-dimensional CuxO with mixed facets modified air–cathodes on microbial fuel cell. *Biores. Technol.* **2015,** *195*, 154-161.

53. Zhang, X.; Li, K.; Yan, P.; Liu, Z.; Pu, L., N-type Cu 2 O doped activated carbon as catalyst for improving power generation of air cathode microbial fuel cells. *Biores. Technol.* **2015,** *187*, 299-304.

54. Singh, I.; Chandra, A., Use of the oxygen storage material CeO 2 as co-catalyst to improve the performance of microbial fuel cells. *International Journal of Hydrogen Energy* **2015**.

55. Li, D.; Qu, Y.; Liu, J.; He, W.; Wang, H.; Feng, Y., Using ammonium bicarbonate as pore former in activated carbon catalyst layer to enhance performance of air cathode microbial fuel cell. *J.Power Sources* **2014,** *272*, 909-914.

56. Lin, G.; Du, H.-d.; Li, B.-h.; Kang, F.-y., The effect of particle size on the interaction of Pt catalyst particles with a carbon black support. *New Carbon Mater* **2010,** *25*, 53-59.

57. Liang, Y.; Dai, H.-B.; Ma, L.-P.; Wang, P.; Cheng, H.-M., Hydrogen generation from sodium borohydride solution using a ruthenium supported on graphite catalyst. *Int. J. Hydrogen* **2010,** *35*, 3023-3028.

58. Duteanu, N.; Erable, B.; Kumar, S. S.; Ghangrekar, M. M.; Scott, K., Effect of chemically modified Vulcan XC-72R on the performance of air-breathing cathode in a single-chamber microbial fuel cell. *Bioresour. Technol.* **2010,** *101*, 5250-5255.

59. Yang, G.; Sun, Y.; Yuan, Z.; Lü, P.; Kong, X.; Li, L.; Chen, G.; Lu, T., Application of surface-modified carbon powder in microbial fuel cells. *Chinese J. Catal. Journal* **2014,** *35*, 770-775.

60. Meng, K.; Liu, Q.; Huang, Y.; Wang, Y., Facile synthesis of nitrogen and fluorine co-doped carbon materials as efficient electrocatalysts for oxygen reduction reactions in air-cathode microbial fuel cells. *J. Mater. Chem. A* **2015,** *3*, 6873-6877.

61. Erable, B.; Duteanu, N.; Kumar, S. S.; Feng, Y.; Ghangrekar, M. M.; Scott, K., Nitric acid activation of graphite granules to increase the performance of the non-catalyzed oxygen reduction reaction (ORR) for MFC applications. *Electrochem. Commun.* **2009,** *11*, 1547-1549.

62. Shi, X.; Feng, Y.; Wang, X.; Lee, H.; Liu, J.; Qu, Y.; He, W.; Kumar, S. M. S.; Ren, N., Application of nitrogen-doped carbon powders as low-cost and durable cathodic catalyst to air–cathode microbial fuel cells. *Biores. Technol.* **2012,** *108*, 89-93.

63. Feng, L.; Yan, Y.; Chen, Y.; Wang, L., Nitrogen-doped carbon nanotubes as efficient and durable metal-free cathodic catalysts for oxygen reduction in microbial fuel cells. *Energy Environ Sci.* **2011,** *4*, 1892-1899.

64. Lu, M.; Kharkwal, S.; Ng, H. Y.; Li, S. F. Y., Carbon nanotube supported MnO 2 catalysts for oxygen reduction reaction and their applications in microbial fuel cells. *Biosens. Bioelectron* **2011,** *26*, 4728-4732.

65. Lu, M.; Guo, L.; Kharkwal, S.; Ng, H. Y.; Li, S. F. Y., Manganese–polypyrrole–carbon nanotube, a new oxygen reduction catalyst for air-cathode microbial fuel cells. *J.Power Sources* **2013,** *221*, 381-386.

66. Liew, K. B.; Daud, W. R. W.; Ghasemi, M.; Loh, K. S.; Ismail, M.; Lim, S. S.; Leong, J. X., Manganese oxide/functionalised carbon nanotubes nanocomposite as catalyst for oxygen reduction reaction in microbial fuel cell. *Int. J. Hydrogen* **2015,** *40*, 11625-11632.

67. Chen, Y.; Lv, Z.; Xu, J.; Peng, D.; Liu, Y.; Chen, J.; Sun, X.; Feng, C.; Wei, C., Stainless steel mesh coated with MnO 2/carbon nanotube and polymethylphenyl siloxane as low-cost and high-performance microbial fuel cell cathode materials. *J. Power Sources* **2012,** *201*, 136-141.

68. Huang, J.; Zhu, N.; Yang, T.; Zhang, T.; Wu, P.; Dang, Z., Nickel oxide and carbon nanotube composite (NiO/CNT) as a novel cathode non-precious metal catalyst in microbial fuel cells. *Biosens. Bioelectron* **2015,** *72*, 332-339.

69. Song, T.-S.; Wang, D.-B.; Wang, H.; Li, X.; Liang, Y.; Xie, J., Cobalt oxide/nanocarbon hybrid materials as alternative cathode catalyst for oxygen reduction in microbial fuel cell. *Int. J. Hydrogen* **2015,** *40*, 3868-3874.

70. Chen, S.; Chen, Y.; He, G.; He, S.; Schröder, U.; Hou, H., Stainless steel mesh supported nitrogen-doped carbon nanofibers for binder-free cathode in microbial fuel cells. *Biosens. Bioelectron* **2012,** *34*, 282-285.

71. Zhou, L.; Fu, P.; Cai, X.; Zhou, S.; Yuan, Y., Naturally derived carbon nanofibers as sustainable electrocatalysts for microbial energy harvesting: A new application of spider silk. *Appl. Catal., B* **2016,** *188*, 31-38.

72. Feng, L.; Chen, Y.; Chen, L., Easy-to-operate and low-temperature synthesis of gram-scale nitrogen-doped graphene and its application as cathode catalyst in microbial fuel cells. *ACS nano* **2011,** *5*, 9611-9618.

73. Zhang, J.-N.; You, S.-J.; Yuan, Y.-X.; Zhao, Q.-L.; Zhang, G.-D., Efficient electrocatalysis of cathodic oxygen reduction with Pt–Fe alloy catalyst in microbial fuel cell. *Electrochem. Commun.* **2011,** *13*, 903-905.

74. Yan, Z.; Wang, M.; Lu, Y.; Liu, R.; Zhao, J., Ethylene glycol stabilized NaBH4 reduction for preparation carbon-supported Pt–Co alloy nanoparticles used as oxygen reduction electrocatalysts for microbial fuel cells. *J. Solid State Electrochem.* **2014,** *18*, 1087-1097.

75. Chang, Y.-Y.; Zhao, H.-Z.; Zhong, C.; Xue, A., Effects of different Pt-M (M= Fe, Co, Ni) alloy as cathodic catalyst on the performance of two-chambered microbial fuel cells. *Russ J. Electrochem.* **2014,** *50*, 885-890.

76. Roche, I.; Katuri, K.; Scott, K., A microbial fuel cell using manganese oxide oxygen reduction catalysts. *Journal of applied electrochemistry* **2010,** *40*, 13-21.

77. Zhang, L.; Liu, C.; Zhuang, L.; Li, W.; Zhou, S.; Zhang, J., Manganese dioxide as an alternative cathodic catalyst to platinum in microbial fuel cells. *Biosens. Bioelectron* **2009,** *24*, 2825-2829.

78. Yuan, H.; Deng, L.; Tang, J.; Zhou, S.; Chen, Y.; Yuan, Y., Facile synthesis of MnO2/Polypyrrole/MnO2 multiwalled nanotubes as advanced electrocatalysts for the oxygen reduction reaction. *ChemElectroChem* **2015,** *2*, 1152-1158.

79. Dong, H.; Yu, H.; Wang, X.; Zhou, Q.; Sun, J.,Carbon-supported perovskite oxide as oxygen reduction reaction catalyst in signle chamered microbial fuel cells. *J. Chem. Technol. Biotechnol.* **2013,** *88*, 774-778.

80. Ghoreishi, K. B.; Ghasemi, M.; Rahimnejad, M.; Yarmo, M. A.; Daud, W. R. W.; Asim, N.; Ismail, M., Development and application of vanadium oxide/polyaniline composite as a novel cathode catalyst in microbial fuel cell. *Int. J. Energy Res.* **2014,** *38*, 70-77.

81. Noori, M. T.; Ghangrekar, M.; Mukherjee, C., V 2 O 5 microflower decorated cathode for enhancing power generation in air-cathode microbial fuel cell treating fish market wastewater. *Int. J. Hydrogen* **2016,** *41*, 3638-3645.

82. Gong, X.-B.; You, S.-J.; Wang, X.-H.; Zhang, J.-N.; Gan, Y.; Ren, N.-Q., A novel stainless steel mesh/cobalt oxide hybrid electrode for efficient catalysis of oxygen reduction in a microbial fuel cell. *Biosens. Bioelectron* **2014,** *55*, 237-241.

83. Mecheri, B.; Iannaci, A.; D'Epifanio, A.; Mauri, A.; Licoccia, S.,Carbon-supported zirconium oxide as a cathode for microbial fuel cell applications. *ChemPlusChem* **2016,** *81*, 80-85.

84. Bezerra, C. W.; Zhang, L.; Lee, K.; Liu, H.; Marques, A. L.; Marques, E. P.; Wang, H.; Zhang, J., A review of Fe–N/C and Co–N/C catalysts for the oxygen reduction reaction. *Electrochim Acta* **2008,** *53*, 4937-4951.

85. Zhao, F.; Harnisch, F.; Schröder, U.; Scholz, F.; Bogdanoff, P.; Herrmann, I., Challenges and constraints of using oxygen cathodes in microbial fuel cells. *Environ. Sci. Technol.* **2006,** *40*, 5193-5199.

86. Cheng, S.; Liu, H.; Logan, B. E., Power densities using different cathode catalysts (Pt and CoTMPP) and polymer binders (Nafion and PTFE) in single chamber microbial fuel cells. *Environ. Sci. Technol.* **2006,** *40*, 364-369.

87. Kim, J. R.; Kim, J.-Y.; Han, S.-B.; Park, K.-W.; Saratale, G.; Oh, S.-E., Application of Co-naphthalocyanine (CoNPc) as alternative cathode catalyst and support structure for microbial fuel cells. *Bioresource technology* **2011,** *102*, 342-347.

88. Li, W.-W.; Yu, H.-Q.; He, Z., Towards sustainable wastewater treatment by using microbial fuel cells-centered technologies. *Energy Environ Sci.* **2014,** *7*, 911-924.

89. Zhang, F.; Pant, D.; Logan, B. E., Long-term performance of activated carbon air cathodes with different diffusion layer porosities in microbial fuel cells. *Biosens. Bioelectron* **2011,** *30*, 49-55.

90. Zhang, X.; Pant, D.; Zhang, F.; Liu, J.; He, W.; Logan, B. E., Long-term performance of chemically and physically modified activated carfbon in air cathodes of microbial fuel cells. *ChemElectroChem* **2014,** *1*, 1859-1866.

Chapter 3

Poly(vinylidene fluoride-co-hexafluoropropylene) phase inversion coating as a diffusion layer to enhance the cathode performance in microbial fuel cells

Abstract

A low cost poly(vinylidene fluoride-co-hexafluoropropylene) (PVDF-HFP) phase inversion coating was developed as a cathode diffusion layer to enhance the performance of microbial fuel cells (MFCs). A maximum power density of 1430 ± 90 mW m^{-2} was achieved at a PVDF-HFP loading of 7.1 mg cm^{-2} (4:1 polymer:carbon black), with activated carbon as the oxygen reduction cathode catalyst. This power density was 31% higher than that obtained with a more conventional platinum (Pt) catalyst on carbon cloth (Pt/C) cathode with a poly(tetrafluoroethylene) (PTFE) diffusion layer (1090 ± 30 mW m^{-2}). The improved performance was due in part to a larger oxygen mass transfer coefficient of 3×10^{-3} cm s^{-1} for the PVDF-HFP coated cathode, compared to 1.7×10^{-3} cm s^{-1} for the carbon cloth/PTFE-based cathode. The diffusion layer was resistant to electrolyte leakage up to water column heights of 41 ± 0.5 cm (7.1 mg cm^{-2} loading of 4:1 polymer:carbon black) to 70 ± 5 cm (14.3 mg cm^{-2} loading of 4:1 polymer:carbon black). This new type of PVDF-HFP/carbon black diffusion layer could reduce the cost of manufacturing cathodes for MFCs.

3.1 Introduction

Microbial fuel cell (MFC) technologies can be used to convert organic and inorganic substrates to electrical power *(1-5)*. Exoelectrogenic bacteria on the anode oxidize substrates to generate electrons, which flow through an external circuit to the cathode where typically oxygen reduction occurs. Platinum is often used as the oxygen reduction catalyst in these cathodes *(6, 7)*, although different catalysts have also been investigated such as carbon nanotubes, cobalt oxides, and FeNC *(8-10)*. Activated carbon (AC) has emerged as the most attractive alternative catalyst to platinum due to its low cost ($2.6 kg^{-1}), and it can have comparable or superior performance to Pt-based catalysts over time in MFCs *(11-13)*.

A typical AC cathode consists of an AC catalyst layer on the electrolyte side that is directly attached to a current collector, and a diffusion layer on the air side. The diffusion layer has two important roles in cathode performance: it serves as a barrier to separate the solution phase from air phase, and therefore to avoid water leakage through the cathode; and it can be used to limit oxygen transfer into the anode solution, but it must allow oxygen to reach the cathode catalyst sites. Hydrophobic polymers, such as polytetrafluoroethylene (PTFE) and poly(dimethylsiloxane) (PDMS), are often used to make diffusion layers *(11, 14)*. Carbon black (CB) is added into these polymers to enhance porosity and thereby improve oxygen mass transfer to the catalyst. A PTFE/CB diffusion layer was previously developed that had good structural rigidity, but forming the cathode required sintering at a high temperature of 340 °C *(11)*. An alternative diffusion layer made of a PDMS/CB mixture was shown to achieve good oxygen permeability, but no information was provided relative to possible water leakage at higher water pressures that would be encountered when making larger cathodes *(14)*. Improvements in both the oxygen transfer and water leakage properties of diffusion layers could be useful in improving power production by MFCs, as long as these materials are inexpensive and can easily be formed into the desired cathode profile.

Two polymers that exhibit good physical stability and chemical resistance *(15)* that could be useful as diffusion layers in MFCs are poly(vinylidene fluoride) (PVDF) and poly(vinylidene fluoride-co-hexafluoropropylene) (PVDF-HFP). These materials are both hydrophobic fluorinated polymers that have long been used for membrane-based processes such as membrane distillation *(16, 17)*. PVDF-HFP may be more useful in MFC applications as the hexafluropropylene (HFP) group increases the fluorine content, which makes PVDF-HFP more hydrophobic than PVDF *(18)*. Preparation of porous membranes from these polymers is easily accomplished by the phase inversion process *(19)*. During phase inversion casting, PVDF-HFP polymer chains precipitate due to non-solvent interactions and form a more flexible structure compared to PVDF as a result of the lower crystallinity of the PVDF-HFP *(18)*. In order to improve the performance of MFCs, a PVDF-HFP coating was examined as a new type of water resistant diffusion layer that could easily be made using the phase inversion method. The typical preparation of the polymer diffusion layer coating was modified to include inexpensive CB as filler particles to improve the oxygen permeability of the diffusion layer. Different thicknesses and mass ratios of PVDF-HFP and CB in the diffusion layer were tested to improve oxygen transfer and power production, and to minimize water leakage. The effects of different preparation conditions were examined in terms of the mechanical stability of the material relative to oxygen transfer and performance properties.

3.2 Materials and Methods

3.2.1 Cathode Fabrication

The catalyst layer was prepared by mixing AC powder (Norit SX plus, Norit Americas Inc., TX) with a 60% PTFE emulsion and CB at a ratio of 9:1:0.9 (w/w), except as noted. The AC mixture was then spread with a spatula onto a 7 cm^2 circular section of stainless steel mesh

(corrosion-resistant 304 stainless steel woven wire cloth, 42 × 42 mesh, 0.014 cm wire diameter; McMaster-Carr, USA) and dried in a fume hood for >2 h at room temperature (23 ± 1 °C).

Poly(vinylidene fluoride-co-hexafluoropropylene) (Kynar® Flex 2801, 12 wt.% HFP) was purchased from Arkema, Inc. N, N-Dimethylacetamide (DMAc) was used as the solvent to dissolve the PVDF-HFP. A 10% (w/v) PVDF-HFP solution was stirred vigorously at room temperature for >8 h to completely dissolve the polymer. The diffusion layer casting solution was then made by adding PVDF-HFP (100 mg, 1 mL of 10% PVDF-HFP solution) with CB at mass ratios of 4:1, 4:2 and 4:3 of PVDF-HFP:CB. After vortexing for 20 s, the solution was spread directly onto the AC catalyst layer with a spatula. The cathodes were then immersed into deionized (DI) water for 10 min at room temperature to induce phase inversion. The cathodes were dried in an oven at 80 °C for 5 min, followed by additional air drying in a fume hood for 6 h. The cathodes were stored in DI water prior to testing. Cathodes with different PVDF-HFP loadings (4.3 mg cm^{-2}, 7.1 mg cm^{-2} and 14.3 mg cm^{-2}) were also prepared at a ratio of 4:1 of PVDF-HFP:CB.

Scanning electron microscopy (SEM; FEI model XL30, tungsten filament, 5 KeV electron beam) was used to examine the morphology of the PVDF-HFP diffusion layers. The cathodes were dried and then sputter coated with gold particles for SEM imaging. SEM was not done for 4.3 mg cm^{-2} loading due to the difficulty to obtain useful images at this low loading.

A carbon cloth-based cathode with platinum catalyst (ETEK C1-10 10% Pt on Vulcan XC-72) and a PTFE diffusion layer was prepared as previously described, and used as a control to evaluate performance relative to the AC *(6)*. A poly(dimethylsiloxane) (PDMS) wipe diffusion layer was also prepared as previously described *(20)* to provide a comparison to the diffusion layers tested here. Two layers of PDMS solution were applied to a cloth wipe material (DuPont Sontara, Style 8864), and then this wipe diffusion layer was placed toward the AC catalyst layer.

3.2.2 Electrochemical Measurements

All electrochemical measurements were conducted in an electrochemical cell (2 cm length, 3 cm diameter) containing two chambers separated by a Nafion® membrane. The electrolyte was a 50 mM phosphate buffer solution (PBS) (Na_2HPO_4, 4.58 g L^{-1}; $NaH_2PO_4 \cdot H_2O$, 2.45 g L^{-1}; NH_4Cl, 0.31 g L^{-1}; KCl, 0.31 g L^{-1}; pH = 6.9; κ = 6.94 mS cm^{-1}). The counter electrode was a 7 cm^2 round platinum plate. An Ag/AgCl reference electrode (RE-5B, BASi, West Lafayette, IN; + 0.209 V versus a standard hydrogen electrode) was placed close to cathode and kept in the same position for each test. All potentials were reported here versus SHE. A potentiostat (VMP3 Multichannel Workstation, Biologic Science Instruments, USA) was used for all measurements in a constant temperature room (30 °C).

A step current method was used to obtain the cathode polarization curve by applying different currents after keeping the cell in an open circuit condition for 1 h. The lower currents (1 mA, 2 mA, 3 mA and 4 mA) were applied for 1 h and the higher currents (5 mA, 6 mA, 7 mA, 8 mA, 9 mA and 10 mA) were applied for 30 min to obtain steady-state conditions.

3.2.3 MFC construction and operation

MFCs were single-chamber, cubic reactors 4 cm in length with an inside diameter of 3 cm. The anodes were graphite fiber brushes heat treated at 450 °C in air for 30 min *(21)*. The MFC anodes were fully acclimated through operation for over one year at a fixed external resistance of 1000 Ω in a constant temperature room (30 °C). The medium contained 1 g L^{-1} sodium acetate dissolved in 50 mM PBS buffer with trace minerals and vitamins *(22)*.

Single cycle polarization tests were conducted by varying the external resistance from 1000 to 20 Ω at 20 min intervals. Voltage drops (U) across external resistors were recorded by a computer

based data acquisition system (2700, Keithley Instrument, OH). Current densities (i) and power densities (P) were normalized to the projected cathode area (A = 7 cm^2), and calculated as $i = U/RA$ and $P = iU/A$, where R is the external resistance. To avoid power overshoot in PVDF-HFP diffusion layer loading tests, multiple cycle polarization tests were conducted by using a different external resistance (1000 to 20 Ω) over a complete fed-batch cycle (as indicated). All polarization data were obtained after 5 fed-batch cycles to ensure steady state. Current densities and power densities were based on the maximum power during each cycle. Cathode impedance was calculated from the slope of cathode polarization curve, and normalized by projected cathode area. Coulombic efficiencies were calculated for each resistance as previously described based on changes in chemical oxygen demand (COD) concentration *(23)*. All tests were conducted in duplicate.

3.2.4 Oxygen permeability

Oxygen transport through the cathode was calculated in terms of an oxygen mass transfer coefficient (k, cm s^{-1}) based on the change in the dissolved oxygen (DO) concentration in a 4 cm long single-chamber reactor as previously described (duplicate measurements) *(6)*. Dissolved oxygen (DO) concentrations were measured using a non-consumptive DO probe (Foxy-18G, Ocean Optics Inc., USA).

3.2.5 Pressure tests

A fully assembled reactor was used to determine the maximum water pressure (in cm of static head) that would produce water leakage through the cathodes. A cubic single chamber MFC was connected through a hole on its side using a rubber tube to a water storage bottle. The height of water was changed by raising the storage container until water droplets were observed on the air

side of the cathode diffusion layer. The static pressure head (cm) was calculated as the difference in height between the cathode and the top of the water level in the storage container.

3.3 Results and Discussion

3.3.1 MFC performance with different polymer ratios

MFC tests were first conducted with cathodes made with different polymer to carbon black ratios. A maximum power density of 1390 ± 175 mW m^{-2} was achieved with the 4:1 PVDF-HFP:CB diffusion layer, which contained 14.3 mg cm^{-2} of PVDF-HFP and 3.6 mg cm^{-2} of CB. Similar maximum power density of 1430 ± 150 mW m^{-2} was achieved with the 4:2 PVDF-HFP:CB diffusion layer, which contained 14.3 mg cm^{-2} of PVDF-HFP and 7.1 mg cm^{-2} of CB. The lowest power density of 1280 ± 330 mW m^{-2} was produced using the 4:3 polymer:CB diffusion layer (Figure 3-1A). Increasing the ratio of polymer to CB led to a less mechanically stable diffusion layer, as cracks were observed for layers with 4:3 PVDF-HFP:CB. Generally, no large differences in power performance were observed with different diffusion layer polymer:CB composition ratios, based on similar cathode potentials (Figure 3-1B).

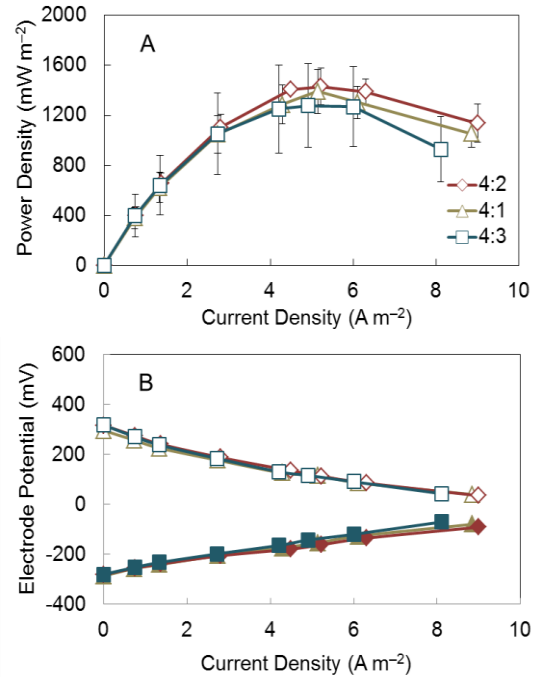

Figure 3-1. (A) Power density curve for ratio test (4:1, 4:2 and 4:3 coresponding to PVDF-HFP:CB in mass ratio) (B) Electrode potentials (solid symbols for anode potentials and open symbols for cathode potentials).

3.3.2 Electrochemical Performance of cathodes as a function of polymer loading

Further tests were conducted to examine the effect of polymer loading, all at the 4:1 ratio for PVDF-HFP:CB. Cathode polarization tests conducted using an abiotic electrochemical cell showed that the AC cathode with a diffusion layer polymer loading of 7.1 mg cm^{-2} PVDF-HFP had the best electrochemical performance (Figure 3-2). The AC cathode with a diffusion layer of the same polymer loading and phase inversion processing, but without CB, had the poorest electrochemical performance. The use of CB as filler particles in the PVDF-HFP polymer therefore greatly improved cathode performance, likely by introducing porosity in the polymer layer. The cathode with a polymer loading of 14.3 mg cm^{-2} (4:1 polymer:CB) showed slightly better performance than the one with the lowest loading (4.3 mg cm^{-2}, 4:1 polymer:CB).

The Pt/C-based cathode had better electrochemical performance than the AC-based cathode with a 4.3 mg cm^{-2} loading at both high and low current densities, but it performed worse at intermediate current densities (4 ~ 6 A m^{-2}), perhaps due to dihydrogen phosphate adsorption on catalytic sites *(24)*.

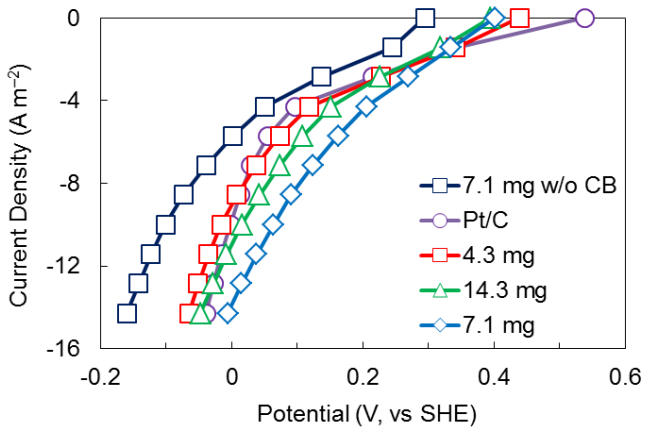

Figure 3-2. Current-voltage (polarization) curves using AC cathodes with different loading of PVDF-HFP and Pt/C cathode.

3.3.3 MFC performance as a function of polymer loading

When the cathodes with different PVDF-HFP loading were used in MFCs, the best performance was obtained using the diffusion layer with 7.1 mg cm^{-2} loading (4:1 ratio of PVDF-HFP:CB), in agreement with abiotic electrochemical tests (Figure 3-3A). The largest maximum power density for this cathode was 1430 ± 90 mW m^{-2}. Increasing or decreasing this PVDF-HFP loading reduced performance. The maximum power densities were 1280 ± 60 mW m^{-2} with a higher loading (14.3 mg cm^{-2}), and 1140 ± 60 mW m^{-2} at the lower loading (4.3 mg cm^{-2}). All of these power densities were slightly better than those produced with the Pt/C cathode of 1090 ± 30 mW m^{-2}. The cathodic polarization curves also showed that Pt/C cathode had a lower cathode potential than the other three AC cathodes (Figure 3-3B), indicating the anode performance was not a factor.

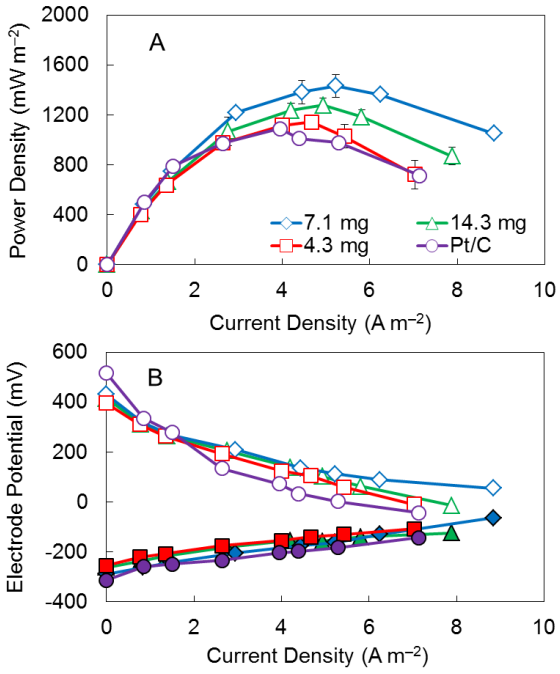

Figure 3-3. (A) Power density curve for PVDF-HFP loading test (normalized to cm^2) at 4:1 ratio and Pt/C cathode (B) Electrode potentials (solid symbols for anode potentials and open symbols for cathode potentials.

The cathode resistances followed a trend consistent with whole cell polarization data, with the resistances varying inversely with maximum power. The Pt/C based cathode had the largest resistance of 110 ± 6 Ω, followed by the AC cathodes with different PVDF-HFP loadings that had resistances of 75 ± 6 Ω (4.3 mg cm^{-2}), 69 ± 7 Ω (14.3 mg cm^{-2}), and 61 ± 2 Ω (7.1 mg cm^{-2}).

MFCs with the cathode PVDF-HFP diffusion layer developed here produced a higher power density, and used less polymer, than MFCs with diffusion layers made of other polymers such as PDMS and PTFE. A diffusion layer consisting of PDMS and CB applied to a wipe cloth, with a similar cathode structure and the same type of MFC, produced a maximum power density of 1310 ± 70 mW m^{-2} *(20)*. A PTFE/CB diffusion layer rolled onto stainless steel mesh produced a maximum of 1360 ± 30 mW m^{-2} *(25)*. Both of these power densities are lower than the maximum power densities obtained here. The optimum PVDF-HFP diffusion layer required less polymer and CB (7.1 mg cm^{-2} of polymer and 1.8 mg cm^{-2} of CB), compared to the PDMS wipe (12.1 mg cm^{-2}

of PDMS and 3.1 mg cm^{-2} of CB) *(14)* or the PTFE (37.5 mg cm^{-2} of polymer) *(26)* diffusion layers. The PVDF polymer was also less expensive, so that polymer costs for these this diffusion layers was only \$1.8 m^{-2} for PVDF-HFP (\$25 kg^{-1}), compared to \$0.36 m^{-2} for PDMS (\$3 kg^{-1}) and \$9.4 m^{-2} for PTFE (\$25 kg^{-1}) diffusion layers *(27)*. In addition, the PTFE/CB diffusion layer requires sintering at 340 °C for 25 min, which makes its preparation more complicated and expensive *(25)* than the other types of diffusion layers.

3.3.4 Coulombic efficiencies

MFCs with Pt/C-based cathodes showed the highest CEs at all current densities and reached a maximum CE of 79% at a current density of 7.1 A m^{-2} (Figure 3-5A). This CE was much larger than the highest CE of 60% produced using the 7.1 mg cm^{-2} PVDF-HFP loading (4:1 polymer:CB). The CEs all increased with the current density, which is commonly observed with MFCs using acetate *(28)*.

3.3.5 Surface morphology

Based on the SEM images, the addition of the CB resulted in a more porous PVDF-HFP diffusion layer, and the CB particles were well-distributed within the PVDF-HFP network. A diffusion layer made with the pure polymer showed small surface pore sizes of <500 nm (Figure 3-4A). When CB was added, larger surface pores were observed at both PVDF-HFP loadings of 14.3 mg cm^{-2} (4:1 polymer:CB) and 7.1 mg cm^{-2} (4:1 polymer:CB) (Figure 3-4B and Figure 3-4C). The number of pores appeared to have increased with CB addition.

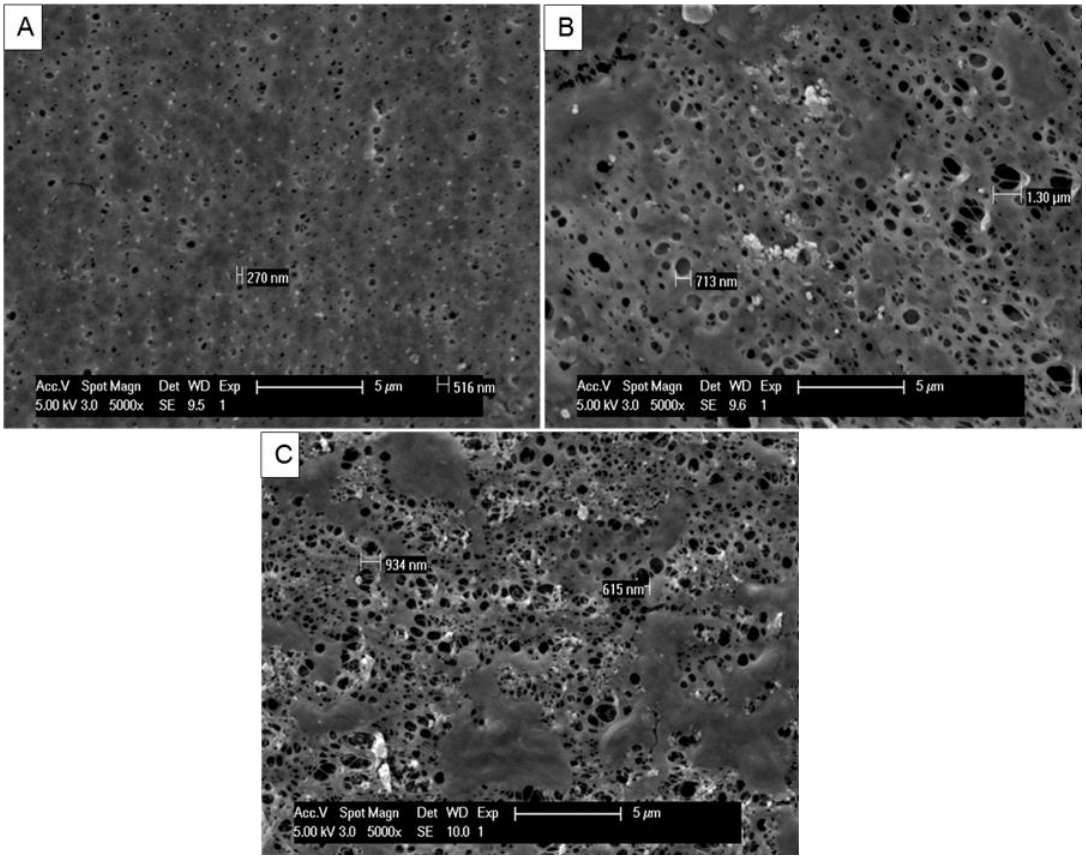

Figure 3-4. SEM images of PVDF-HFP diffusion layer with (A) 7.1 mg cm^{-2} loading without CB (B) 14.3 mg cm^{-2} loading with CB at the ratio of 4:1 PVDF-HFP:CB (C) 7.1 mg cm^{-2} loading with CB at the ratio of 4:1 PVDF-HFP:CB.

3.3.6 Oxygen Permeability

The oxygen mass transfer coefficient of AC cathodes was inversely related to the loading of PVDF-HFP. With the highest PVDF-HFP loading of 14.3 mg cm^{-2}, at a ratio of 4:1 PVDF-HFP:CB, the oxygen permeability was $1.4 \pm 0.7 \times 10^{-3}$ cm s^{-1}, which was comparable to the standard Pt/C carbon cloth/PTFE-based cathode with a value of $1.7 \pm 0.8 \times 10^{-3}$ cm s^{-1}. AC cathodes with an intermediate PVDF-HFP loading of 7.1 mg cm^{-2} and a polymer:CB ratio of 4:1 had an oxygen mass transfer coefficient of $3.1 \pm 0.7 \times 10^{-3}$ cm s^{-1}, which was the second largest among

the cathodes. The mass transfer coefficient increased to 5.4 ± 1.2 × 10^{-3} cm s^{-1} using the lowest PVDF-HFP loading (Figure 3-5B).

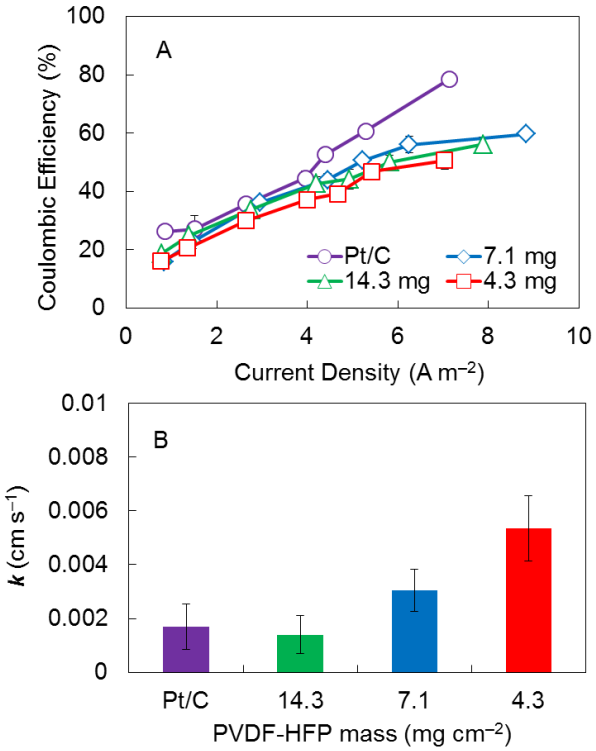

Figure 3-5. (A) Coulombic efficiencies (CEs) obtained for PVDF-HFP loading test at 4:1 ratio and Pt/C cathode (B) Oxygen mass transfer coefficient of AC cathodes with different PVDF-HFP loadings and Pt/C cathode.

High oxygen mass transfer should be beneficial for the oxygen reduction reaction, but oxygen transfer alone did not account for the differences in the maximum power densities. AC cathodes with the highest power of 1430 ± 90 mW m^{-2} had an intermediate oxygen mass transfer coefficient (3.1 ± 0.7 × 10^{-3} cm s^{-1}) (Figure 3-5B). Although 4.3 mg cm^{-2} PVDF-HFP loading with a polymer:CB ratio of 4:1 showed the highest oxygen permeability of the cathodes tested, this diffusion layer resulted in low power (1140 ± 60 mW m^{-2}), perhaps as a result of water intrusion (flooding) of the catalyst *(29)*.

3.3.7 Water Pressure Tests

The microporous structure of PVDF-HFP diffusion layers (Figure 3-4B and 3-4C) prevented liquid water leakage through the pores where oxygen enters the cathode structure. Water leakage was only detected on the diffusion layer edges where the cathode was clamped using a gasket to the cell, suggesting the primary reason for leakage was weak tensile strength and cracking at the seal edges. Higher loadings of PVDF-HFP greatly increased the water pressure that the cathode sustained without leaking around the edges. For the PVDF-HFP diffusion layer with 14.3 mg cm^{-2} loading and a polymer:CB ratio of 4:1, the AC-based cathode withstood 70 ± 5 cm of water pressure (Figure 3-6). With lower loadings of 7.1 and 4.3 mg cm^{-2} at the same polymer:CB ratio, the water pressures that AC cathode was able to withstand before leakage decreased to 41 ± 0.5 cm and 2 ± 0.5 cm, respectively, suggesting further decreases of the PVDF-HFP loading might compromise the physical and mechanical strength of this coating. The PDMS/CB wipe-based diffusion layer withstood a water pressure of only 19 ± 1 cm, while the Pt/C-based standard cathode started leaking through the pores at 120 ± 7 cm (Figure 3-6).

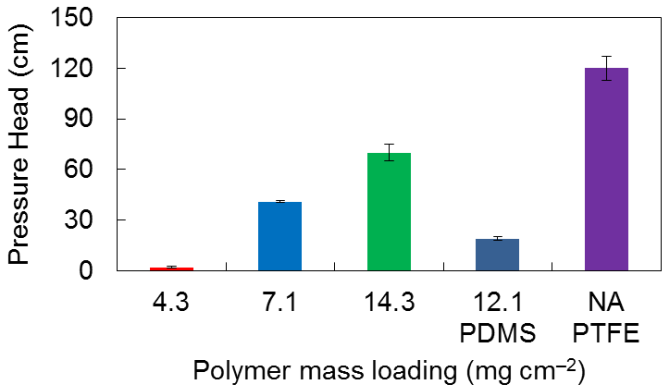

Figure 3-6. Water pressure resistance of cathodes with different diffusion layer polymer loadings

3.4 Conclusions

A microporous diffusion layer with a PVDF-HFP loading of 7.1 mg cm^{-2} and CB loading of 1.8 mg cm^{-2} (mass ratio of 4:1 of PVDF-HFP:CB) had good electrochemical performance and required less polymer than previously prepared cathodes. The maximum power was 1430 ± 90 mW m^{-2} with 7.1 mg cm^{-2} PVDF-HFP loading (4:1 loading ratio), compared to 1090 ± 30 mW m^{-2} for the Pt/C cathode with a PTFE diffusion layer. The PVDF-HFP diffusion layer withstood a water pressure resistance of 41 ± 0.5 cm water height with a polymer loading of 4:1 (polymer:CB), with leakage around the cathode edges but not through the pores. These results suggest that PVDF-HFP phase inversion diffusion layer could be useful as a lower cost way to construct MFC cathodes.

3.5 Acknowledgments

This research was supported by Award KUS-I1-003-13 from the King Abdullah University of Science and Technology (KAUST), and a graduate scholarship from the China Scholarship Council (CSC) to W. Y.

3.6 Literature cited

1. Logan, B. E., *Microbial fuel cells*. John Wiley & Sons, Inc.: Hoboken, NJ, 2008; p 300.
2. Niessen, J.; Schröder, U.; Scholz, F., Exploiting complex carbohydrates for microbial electricity generation- a bacterial fuel cell operating on starch. *Electrochem. Commun.* **2004,** *6*, 955-958.
3. Allen, R. M.; Bennetto, H. P., Microbial fuel cells: Electricity production from carbohydrates. *Appl. Biochem. Biotechnol.* **1993,** *39*, 27-40.
4. Bond, D. R.; Holmes, D. E.; Tender, L. M.; Lovley, D. R., Electrode-reducing microorganisms that harvest energy from marine sediments. *Science* **2002,** *295*, 483-485.
5. Lovley, D. R., Bug juice: harvesting electricity with microorganisms. *Nat. Rev. Microbiol.* **2006,** *4*, 497-508.
6. Cheng, S.; Liu, H.; Logan, B. E., Increased performance of single-chamber microbial fuel cells using an improved cathode structure. *Electrochem. Commun.* **2006,** *8*, 489-494.
7. Santoro, C.; Li, B.; Cristiani, P.; Squadrito, G., Power generation of microbial fuel cells (MFCs) with low cathodic platinum loading. *Int. J. Hydrogen* **2013,** *38*, 692-700.
8. Ghasemi, M.; Ismail, M.; Kamarudin, S. K.; Saeedfar, K.; Daud, W. R. W.; Hassan, S. H. A.; Heng, L. Y.; Alam, J.; Oh, S.-E., Carbon nanotube as an alternative cathode support and catalyst for microbial fuel cells. *Appl. Energy* **2013,** *102*, 1050-1056.
9. Ahmed, J.; Yuan, Y.; Zhou, L.; Kim, S., Carbon supported cobalt oxide nanoparticles–iron phthalocyanine as alternative cathode catalyst for oxygen reduction in microbial fuel cells. *J. Power Sources* **2012,** *208*, 170-175.
10. Jaouen, F.; Goellner, V.; Lefevre, M.; Herranz, J.; Proietti, E.; Dodelet, J. P., Oxygen reduction activities compared in rotating-disk electrode and proton exchange membrane fuel cells for highly active Fe-N-C catalysts. *Electrochim Acta* **2013,** *87*, 619-628.

11. Dong, H.; Yu, H.; Wang, X.; Zhou, Q.; Feng, J., A novel structure of scalable air-cathode without Nafion and Pt by rolling activated carbon and PTFE as catalyst layer in microbial fuel cells. *Water Res.* **2012**.
12. Cheng, S.; Wu, J., Air-cathode preparation with activated carbon as catalyst, PTFE as binder and nickel foam as current collector for microbial fuel cells. *Bioelectrochemistry* **2013,** *92*, 22-26.
13. Zhang, F.; Cheng, S.; Pant, D.; Bogaert, G. V.; Logan, B. E., Power generation using an activated carbon and metal mesh cathode in a microbial fuel cell. *Electrochem. Commun.* **2009,** *11*, 2177-2179.
14. Zhang, F.; Saito, T.; Cheng, S.; Hickner, M. A.; Logan, B. E., Microbial fuel cells cathodes constructed from stainless steel mesh that use poly(dimethylsiloxane) diffusion layers. *Environ. Sci. Technol.* **2010,** *44*, 1490-1495.
15. Liu, F.; Hashim, N. A.; Liu, Y. T.; Abed, M. R. M.; Li, K., Progress in the production and modification of PVDF membranes. *J Membr. Sci* **2011,** *375*, 1-27.
16. Garcia-Payo, M. C.; Essalhi, M.; Khayet, M., Effects of PVDF-HFP concentration on membrane distillation performance and structural morphology of hollow fiber membranes. *J. Membr. Sci.* **2010,** *347*, 209-219.
17. Wang, K. Y.; Chung, T. S.; Gryta, M., Hydrophobic PVDF hollow fiber membranes with narrow pore size distribution and ultra-thin skin for the fresh water production through membrane distillation. *Chem Eng Sci* **2008,** *63*, 2587-2594.
18. Shi, L.; Wang, R.; Cao, Y. M.; Feng, C. S.; Liang, D. T.; Tay, J. H., Fabrication of poly(vinylidene fluoride-co-hexafluropropylene) (PVDF-HFP) asymmetric microporous hollow fiber membranes. *J. Membr. Sci.* **2007,** *305*, 215-225.
19. Tomaszewska, M., Preparation and properties of flat-sheet membranes from poly(vinylidene fluoride) for membrane distillation. *Desalination* **1996,** *104*, 1-11.

20. Wei, B.; Tokash, J. C.; Chen, G.; Hickner, M. A.; Logan, B. E., Development and evaluation of carbon and binder loading in low-cost activated carbon cathodes for air-cathode microbial fuel cells. *RSC ADV* **2012**.

21. Logan, B. E.; Cheng, S.; Watson, V.; Estadt, G., Graphite fiber brush anodes for increased power production in air-cathode microbial fuel cells. *Environ. Sci. Technol.* **2007,** *41*, 3341-3346.

22. Lovley, D. R.; Phillips, E. J. P., Novel mode of microbial energy metabolism: organic carbon oxidation coupled to dissimilatory reduction of iron or manganese. *Appl. Environ. Microbiol.* **1988,** *54*, 1472-1480.

23. Logan, B. E.; Aelterman, P.; Hamelers, B.; Rozendal, R.; Schröder, U.; Keller, J.; Freguiac, S.; Verstraete, W.; Rabaey, K., Microbial fuel cells: methodology and technology. *Environ. Sci. Technol.* **2006,** *40*, 5181-5192.

24. Savizi, I. S. P.; Janik, M. J., Acetate and phosphate anion adsorption linear sweep voltammograms simulated using density functional theory. *Electrochim Acta* **2011,** *56*, 3996-4006.

25. Dong, H.; Yu, H.; Wang, X., Catalysis kinetics and porous analysis of rolling activated carbon-PTFE air-cathode in microbial fuel cells. *Environ. Sci. Technol.* **2012,** *46*, 13009-13015.

26. Weihua He, J. L., Da Li, Haiman Wang, Youpeng Qu, Xin Wang, Yujie Feng, The electrochemical behavior of three air cathodes for microbial electrochemical system (MES) under meter scale water pressure *J. Power Sources* **2014,** *In Press*.

27. www.alibaba.com.cn, *Plastic source market*.

28. Fan, Y.; Hu, H.; Liu, H., Enhanced coulombic efficiency and power density of air-cathode microbial fuel cells with an improved cell configuration. *J. Power Sources* **2007,** *171*, 348-354.

29. Zhang, F.; Chen, G.; Hickner, M. A.; Logan, B. E., Novel anti-flooding poly(dimethylsiloxane) (PDMS) catalyst binder for microbial fuel cell cathodes. *J. Power Sources* **2012,** *218*, 100-105.

Chapter 4

Single step fabrication using a phase inversion method of poly(vinylidene fluoride) (PVDF) activated carbon air cathodes for microbial fuel cells

Abstract

Air cathodes used in microbial fuel cells (MFCs) need to have high catalytic activity for oxygen reduction, but they must also be easy to manufacture, inexpensive, and watertight. A simple one-step, phase inversion process was used here to construct an inexpensive MFC cathode using a poly(vinylidene fluoride) (PVDF) binder and an activated carbon catalyst. The phase inversion process enabled cathode preparation at room temperatures, without the need for additional heat treatment, and it produced for the first time a cathode that did not require a separate diffusion layer to prevent water leakage. MFCs using this new type of cathode produced a maximum power density of 1470 ± 50 mW m^{-2} with acetate as a substrate, and 230 ± 10 mW m^{-2} with domestic wastewater. These power densities were similar to those obtained using cathodes made using more expensive materials or more complex procedures, such as cathodes with a polytetrafluoroethylene (PTFE) binder and a poly(dimethylsiloxane) (PDMS) diffusion layer, or a Pt catalyst. Even though the PVDF cathodes did not have a diffusion layer, they withstood up to 1.22 ± 0.04 m of water head (~12 kPa) without leakage, compared to 0.18 ± 0.02 m for cathodes made using PTFE binder and PDMS diffusion layer. The cost of PVDF and activated carbon ($3 m^{-2}) was less than that of the stainless steel mesh current collector ($12 m^{-2}). PVDF-based AC cathodes therefore are inexpensive, have excellent performance in terms of power and water leakage, and they can be easily manufactured using a single phase inversion process at room temperature.

4.1 Introduction

Microbial fuel cells (MFCs) are being developed to recover energy during wastewater treatment by generating electricity from organic matter using exoelectrogenic bacteria *(1-5)*. Air cathodes are used in MFCs to avoid the energy demands needed for aerating wastewater *(6, 7)*. Platinum catalysts promote high oxygen reduction reaction activity in MFC cathodes, but practical MFC applications on larger scales will need to avoid using cathodes containing precious metals or other expensive materials. Activated carbon (AC) has been shown to be an effective catalyst for oxygen reduction in MFCs, as it produces power densities similar to cathodes made with Pt, the performance of AC is relatively well maintained over time *(6, 8, 9)*, and AC is inexpensive (~\$1.4 Kg^{-1}). Different temperature and pressure treatments of AC have been used to further enhance cathode performance, but increase energy input and complicate fabrication procedures, resulting in higher cost materials *(10)*.

In addition to having good performance with inexpensive materials, cathodes used in MFCs must be watertight so that they do not leak when used in larger-scale reactors, and they must be easy to mass produce. Polytetrafluoroethylene (PTFE) is often used as a catalyst binder, but some of these types of cathodes cannot withstand high water pressures. For example, cathodes made by a common batch-pressing method using a PTFE/AC mixture on stainless steel mesh current collector, with a diffusion layer of poly(dimethylsiloxane) (PDMS)/ carbon black (CB) to minimize water leakage, produced a good maximum power density of 1310 ± 70 mW m^{-2} *(11)*. However, these cathodes leaked with less than one meter head of water pressure *(12)*. Cathodes made by a rolling-press method using the same binder but with a PTFE/CB diffusion layer on stainless steel mesh current collector had similar power densities but much improved water retention (up to 3 m of water head) *(13, 14)*. The PTFE used in the diffusion layer (\$9.4 m^{-2}) is relatively expensive as it costs almost as much as the stainless steel current collector (~\$12 m^{-2}). The sintering process

needed for the diffusion layer (340°C for 25 min) *(12, 13)* also makes PTFE-based cathodes difficult to mass produce. Poly(vinylidene fluoride) (PVDF) has previously been used in making cathodes, but only as a diffusion layer added on to the air-side of a cathode. Thus, the cathode itself was made using a paste and press type of process, with the diffusion layer added following cathode construction *(12)*.

A new type of AC cathode was developed in this work using a phase inversion process with a PVDF binder. This new preparation procedure enabled cathode production in a one-step process, without the need for further heat-treatment or the addition of a separate diffusion layer. PVDF is a semicrystalline fluoropolymer that exhibits good physical stability and chemical resistance. It has been used as a binder material in the electrodes of batteries and fuel cells *(15, 16)* and capacitors *(17)*, but it has always been prepared for these applications as a paste. There has only been one report on the use of PVDF in an MFC cathode, but the cathode was prepared using a typical "mix and paste" approach, rather than a phase inversion approach used here, and the peak power density was relatively low (286 mW m^{-2}) for an air cathode under the tested conditions *(18)*. PVDF is also used to make microfiltration and ultrafiltration membranes using a diffusion-induced, phase inversion method *(19-21)*. The phase inversion process occurs at room temperature, making membrane production simple and flexible, allowing large-scale production of low-cost production of membranes *(19)*. During the phase inversion process in a water bath, the PVDF diffuses out from the catalyst mixture and precipitates on the cathode surface, forming a thin but dense hydrophobic PVDF skin layer on the surface that is relatively waterproof. Therefore, making a cathode with PVDF by a phase inversion process was hypothesized to be able to accomplish both binding of the catalyst to the current collector, and formation of a polymer layer that could withstand high water pressure to avoid the need for a separate diffusion layer. The low cost of the polymer and the ease of the phase inversion process would make the production of the MFC cathodes both simple and inexpensive.

4.2 Materials and Methods

4.2.1 Cathode Fabrication and Operation

PVDF solutions with different concentrations of 5%, 7.5% and 10% (w/v) were prepared by dissolving PVDF powder (~534,000 Da; Sigma Aldrich) in N, N-dimethylacetamide (DMAc), with vigorous stirring using a stir bar at room temperature (23 ± 1 °C) for over 8 h to completely dissolve the polymer. AC powder (Norit SX plus, Norit Americas Inc., TX) was applied at an optimum AC loading of 26.5 mg cm^{-2}, based on previous experiments. Catalyst mixtures were prepared with different PVDF loadings (all mass ratios) of: (1) 8.8 mg cm^{-2}, AC:CB (Vulcan XC-72, Cabot Corporation, USA):PVDF (10% as prepared) = 30:3:10; (2) 6.6 mg cm^{-2}, AC:CB:PVDF (7.5%) = 30:3:7.5; (3) 4.4mg cm^{-2}, AC:CB:PVDF (7.5%) = 30:3:5. The mixtures were spread directly onto an 11.3 cm^2 circular section of stainless steel mesh (50 × 50, type 304, McMaster-Carr, USA) with a spatula (except as noted). The cathodes were then immersed into deionized (DI) water for 15 min at room temperature to induce phase inversion. Cathodes were then air dried in a fume hood for >6 h, and stored in DI water prior to tests. The performance of the PVDF cathodes was compared to controls made with an AC (26.5 mg cm^{-2}), CB, and a PTFE (60%) emulsion at a AC:CB:PTFE ratio of 9:1:0.9 (w/w) with a PDMS (12.1 mg cm^{-2}) wipe diffusion layer *(11)*.

Cubic single-chamber MFCs were used in all tests (except as noted). They were constructed from a Lexan block 4 cm in length, with an inside cylindrical chamber having a diameter of 3 cm *(22)*. The anodes were graphite fiber brushes (2.5 cm in both diameter and length, heat treated at 450 °C in air for 30 min) that were placed horizontally in the middle of the MFC chambers *(22)*. Anodes were fully acclimated by operation for over one year at a constant temperature (30 °C) and a fixed external resistance (1000 Ω). The medium contained 1 g L^{-1} sodium acetate dissolved in 50 mM PBS buffer amended with 12.5 mL L^{-1} minerals and 5 mL L^{-1} vitamins (except as noted).

In larger-scale MFC tests, PVDF cathodes (7 cm × 10 cm, with 5 cm × 7 cm exposed to the air) were constructed and tested in a multi-brush anode reactor (130 mL) fed with domestic wastewater as previously described (see also Appendix A, Figure S4-3) *(23)*. Carbon cloth-based cathodes with a platinum catalyst (ETEK C1-10 10% Pt on Vulcan XC-72) and a PTFE diffusion layer was prepared as previously described,*(24)* and used as a Pt catalyst control.

4.2.2 Measurements

MFC power curves were obtained by decreasing the external resistance from 1000 through 500, 200, 100, 75, 50 to 20 Ω at 20 min intervals. Coulombic efficiencies were calculated at a resistance of 1000 Ω based on changes in chemical oxygen demand (COD) concentration, as previously described. Cathode polarization measurements were conducted with new cathodes in a two chamber electrochemical cell (2 cm length, 3 cm diameter, with a Nafion® membrane and Pt counter electrode) using a step current method, with a series of different set currents after the cell was acclimated under open circuit conditions for 1 h. The lower currents (1 mA, 2 mA, 3 mA and 4 mA) were applied for 1 h and the higher currents (5 mA, 6 mA, 7 mA, 8 mA, 9 mA and 10 mA) were applied for 30 min to obtain steady-state conditions. A fully assembled reactor was used to determine the maximum water pressure (in cm of static head) that would produce water leakage through the cathodes as previously described *(12)*. A rubber ring covered with at least three layers of Teflon tape was used to seal the edge during the pressure test. All tests were conducted with duplicate cathodes.

4.3 Results and Discussion

4.3.1 Cathode Performance Using Acetate

A maximum power density of 1470 ± 50 mW m^{-2} was produced by MFCs with PVDF cathodes (8.8 mg cm^{-2}) with the SS mesh facing the water side, and the PVDF-AC catalyst layer facing the air side of the cell, using acetate as the fuel (Figure 4-1A). A similar power density (1450 ± 10 mW m^{-2}) was produced using a cathode made with a PTFE binder, but this cathode required a diffusion layer to avoid water leakage. The columbic efficiency of the PTFE cathode was 20 ± 5%, which was higher than PVDF or reversed PVDF cathode (both had CEs of 13 ± 1%). Although the decrease in the CE results in less production of electricity from the substrate, this can lead to faster removal of the organic matter which can be desirable in wastewater treatment as that can reduce the time needed for wastewater treatment *(25)*. Future studies employing separators could be conducted to increase CE while minimizing bio-fouling *(26)*. Using less PVDF for the cathode (4.4 or 6.6 mg cm^{-2}) did not alter power production (Appendix A, Figure S4-1). When the PVDF cathode orientation was reversed, with the PVDF-AC layer in contact with the electrolyte (SS mesh on the air side), the maximum power density decreased to 1170 ± 10 mW m^{-2} (Figure 4-1A). The change in performance was due to more negative cathode potentials, as the anode potentials were not altered by changing the cathode orientation (Figure 4-1B). The reduction in power when the catalyst faced the electrolyte showed that the cathode composition was asymmetric. During the phase inversion process, it was expected that a more hydrophobic skin layer would form on the cathode. This type of layer would therefore hinder ion diffusion to and from the catalyst surface, which would reduce cathode performance.

Abiotic electrochemical tests with the cathodes similarly showed improved performance of the PVDF cathodes when the catalyst layer was exposed to the air side of the cell, compared to the

catalyst layer facing the electrolyte (Figure 4-1C). Similar overpotentials were obtained using the PVDF cathode and the PTFE cathode with a diffusion layer (Figure 4-1C).

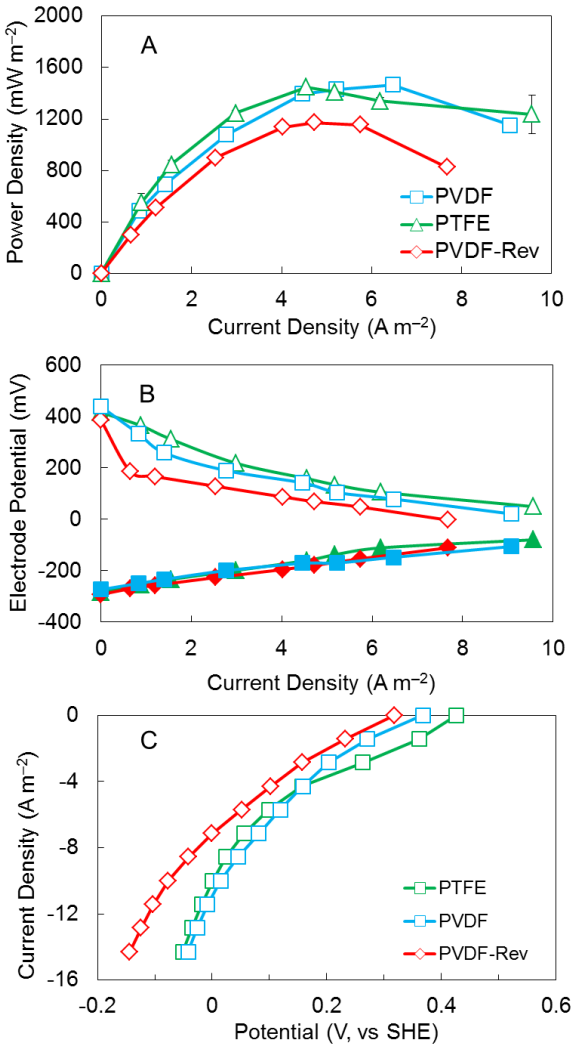

Figure 4-1. MFC tests: (A) power density curves for a PVDF cathode, reversed-side PVDF cathode, and a PTFE cathode; (B) electrode potentials (solid symbols, anode potentials; open symbols, cathode potentials). (C) Current-voltage (polarization) curves for the same cathodes in an abiotic electrochemical cell.

4.3.2 Water Pressure Resistance

The PVDF cathodes showed good water pressure resistance, tolerating a water pressure head of 1.22 ± 0.04 m (~12 kPa) for the cathode with 8.8 mg cm^{-2} PVDF loading before showing any

water leakage (Figure 4-2). In contrast, the PTFE cathode showed water leakage at a very low water height of 0.18 ± 0.02 m, despite the use of a diffusion layer. Further evidence of the asymmetric nature of the PVDF cathode was shown by water leakage at a lower water height of 1.02 ± 0.02 m when the cathode orientation was reversed, and the catalyst layer was oriented towards the electrolyte.

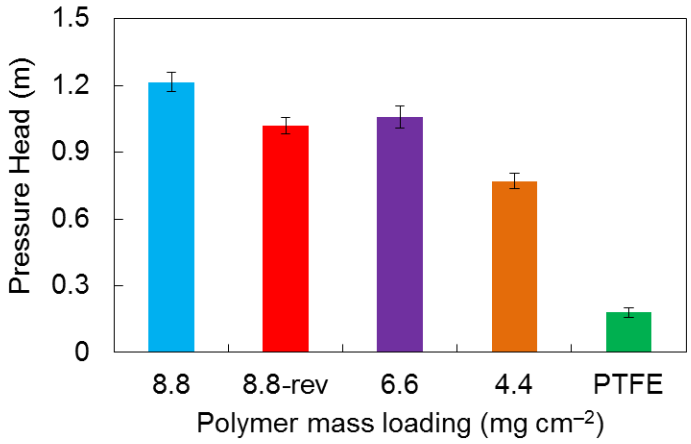

Figure 4-2. Water pressure resistance of PVDF cathodes with different polymer loadings (8.8, 6.6 and 4.4 mg cm^{-2}) with the polymer layer facing the air, compared to the reversed orientation of a PVDF cathode (8.8 mg cm^{-2}), and a PTFE cathode.

A reduction in the PVDF loadings resulted in water leakage at lower water heights of 1.06 ± 0.06 m (6.6 mg cm^{-2}) and 0.77 ± 0.04 m (4.4 mg cm^{-2}) compared to higher PVDF loadings. Cathodes with lower PVDF loadings likely had less tolerance to water pressure due to formation of a less dense PVDF network (Appendix A, Figure S4-2), even though power production was not affected by the polymer loading (Appendix A, Figure S4-1). Thus, the higher PVDF loading of 8.8 mg cm^{-2} was required to avoid water leakage.

4.3.3 MFC Performance with Larger Cathodes and Domestic Wastewater

To demonstrate the scalability of the PVDF cathodes, and their suitability for use with actual wastewaters, larger PVDF cathodes were tested in multi-brush anode reactors *(23)*. The maximum power density with the domestic wastewater was 230 ± 10 mW m^{-2} (Figure S4-4). This lower power density is consistent with previous reports showing that power production is lower with a domestic wastewater compared to more optimal conditions obtained using acetate in well buffered solutions. This power density was the same as that produced using carbon cloth cathodes with a platinum catalyst (PTFE as diffusion layer) in a separator-free configuration. No water leakage was observed in tests using these larger sized the PDVF cathodes, confirming the stability of the process when making larger cathodes. Additional tests with these cathodes have shown that there was no water leakage, even after two months of operation (data not shown).

4.3.4 Materials and Cost Analysis

The PVDF cathodes not only tolerate relatively higher water pressures, but they are also economical to manufacture due to the use of relatively small amounts of inexpensive polymer (Table 4-1). The overall cost of the PVDF cathode was \$15 m^{-2}, but \$12 m^{-2} of this cost is for the stainless steel mesh. The catalyst layer of the best performing PVDF cathodes required 88 g m^{-2} of polymer, compared to a range of 30 g m^{-2} (PTFE) to 100 g m^{-2} (Nafion) for other cathodes. However, the PVDF cathode did not have a diffusion layer which greatly reduced polymer requirements. For example, while the cathode prepared by a rolling method used only 45 g m^{-2} for the catalyst layer, 450 g m^{-2} of PTFE was used for the diffusion layer (Table 4-1), resulting in an overall much higher materials cost. Although the cathode made using a pressing method with PTFE

and PDMS cost only \$14 m^{-2} for the materials, the water tolerance was relatively poor (0.18 m) compared to that of the PVDF cathode (1.22 m).

Table 4-1. Material and cost analysis of current activated carbon cathodes and Pt/C cathode

Cathode	Catalyst layer (g m^{-2})				Diffusion layer (g m^{-2})		Current collector ($ m^{-2})			Max. Power (mW m^{-2})	Pressure tolerance (m)	Cost ($ m^{-2})	Ref.
	Pt	AC	Polymer	CB	CB	Polymer	Carbon Cloth	SS mesh	Nickel foam				
Phase inversion	-	265	88 (PVDF)	26.5	-	-	-	12	-	1470 ± 50	1.22 ± 0.04	15	This study
Rolling	-	273	45 (PTFE)	-	191	450 (PTFE)	-	12	-	1355 ± 26	3	25	(13, 14)
	-	200	60 (PTFE)	8	60	454 (PTFE)	-	-	20	1190 ± 50	-	33	*(6)*
Pressing	-	270	30 (PTFE)	-	31	121 (PDMS)	-	12	-	1310 ± 70	0.18 ± 0.02	14	*(11)*
Brushing	5	-	100 (Nafion)	-	15.6	555 (PTFE)	625	-	-	1320	1.2 ± 0.07	1814	*(6, 12)*

(Cost estimations were all based on commercial price of materials in bulk quantity and unit price was provided in Appendix A, Table S4-1)

4.4 Conclusions

Inexpensive PVDF cathodes, fabricated via a simple one-step phase inversion process, withstood high water pressures while achieving good power performance. The cathode fabrication was accomplished by spreading the AC/PVDF/CB mixture onto a stainless steel mesh, followed by immersion in water, making the procedure simple yet efficient compared to previous methods requiring high temperature heat treatments *(13)*. The durability of the cathodes will now need to be further examined over time, but preliminary tests have shown that the cathodes can produce power levels comparable to other AC or Pt catalyst cathodes, with both acetate and wastewater solutions, and that they do not leak even after two months of operation.

4.5 Acknowledgments

This research was supported by the Strategic Environmental Research and Development Program (SERDP), Award KUS-I1-003-13 from the King Abdullah University of Science and Technology (KAUST), and a graduate scholarship from the China Scholarship Council (CSC) to W. Y.

4.6 Literature cited

1. Logan, B. E., *Microbial fuel cells*. John Wiley & Sons, Inc.: Hoboken, NJ, 2008; p 300.
2. Niessen, J.; Schröder, U.; Scholz, F., Exploiting complex carbohydrates for microbial electricity generation- a bacterial fuel cell operating on starch. *Electrochem. Commun.* **2004,** *6*, 955-958.
3. Allen, R. M.; Bennetto, H. P., Microbial fuel-cells - electricity production from carbohydrates. *Appl. Biochem. Biotechnol.* **1993,** *39*, 27-40.
4. Bond, D. R.; Holmes, D. E.; Tender, L. M.; Lovley, D. R., Electrode-reducing microorganisms that harvest energy from marine sediments. *Science* **2002,** *295*, 483-485.
5. Lovley, D. R., Bug juice: harvesting electricity with microorganisms. *Nat. Rev. Microbiol.* **2006,** *4*, 497-508.
6. Cheng, S. A.; Wu, J. C., Air-cathode preparation with activated carbon as catalyst, PTFE as binder and nickel foam as current collector for microbial fuel cells. *Bioelectrochemistry* **2013,** *92*, 22-26.
7. Wang, X.; Feng, C. J.; Ding, N.; Zhang, Q. R.; Li, N.; Li, X. J.; Zhang, Y. Y.; Zhou, Q. X., Accelerated OH- transport in activated carbon air cathode by modification of quaternary ammonium for microbial fuel cells. *Environ. Sci. Technol.* **2014,** *48*, 4191-4198.
8. Dong, H.; Yu, H.; Wang, X.; Zhou, Q.; Feng, J., A novel structure of scalable air-cathode without Nafion and Pt by rolling activated carbon and PTFE as catalyst layer in microbial fuel cells. *Water Res.* **2012,** *46*, 5777-87.
9. Zhang, F.; Cheng, S.; Pant, D.; Bogaert, G. V.; Logan, B. E., Power generation using an activated carbon and metal mesh cathode in a microbial fuel cell. *Electrochem. Commun.* **2009,** *11*, 2177-2179.

10. Santoro, C.; Artyushkova, K.; Babanova, S.; Atanassov, P.; Ieropoulos, I.; Grattieri, M.; Cristiani, P.; Trasatti, S.; Li, B.; Schuler, A. J., Parameters characterization and optimization of activated carbon (AC) cathodes for microbial fuel cell application. *Biores. Technol.* **2014,** *163*, 54-63.
11. Wei, B.; Tokash, J. C.; Chen, G.; Hickner, M. A.; Logan, B. E., Development and evaluation of carbon and binder loading in low-cost activated carbon cathodes for air-cathode microbial fuel cells. *RSC Adv* **2012,** *2*, 12751-12758.
12. Yang, W.; Zhang, F.; He, W.; Liu, J.; Hickner, M. A.; Logan, B. E., Poly (vinylidene fluoride-co-hexafluoropropylene) phase inversion coating as a diffusion layer to enhance the cathode performance in microbial fuel cells. *J. Power Sources* **2014,** *269*, 379-384.
13. Dong, H.; Yu, H.; Wang, X., Catalysis kinetics and porous analysis of rolling activated carbon-PTFE air-cathode in microbial fuel cells. *Environ. Sci. Technol.* **2012,** *46*, 13009-13015.
14. He, W.; Liu, J.; Li, D.; Wang, H.; Qu, Y.; Wang, X.; Feng, Y., The electrochemical behavior of three air cathodes for microbial electrochemical system (MES) under meter scale water pressure. *J.Power Sources* **2014,** *267*, 219-226.
15. Barsykov, V.; Khomenko, V., The influence of polymer binders on the performance of cathodes for lithium-ion batteries. *Scientific proceedings of riga technical university, series 1: material science and applied chemistry* **2010,** *21*, 2010.
16. Su, H. N.; Pasupathi, S.; Bladergroen, B.; Linkov, V.; Pollet, B. G., Optimization of gas diffusion electrode for polybenzimidazole-based high temperature proton exchange membrane fuel cell: Evaluation of polymer binders in catalyst layer. *Int. J. Hydrogen* **2013,** *38*, 11370-11378.
17. Fonseca, C. P.; Benedetti, J. E.; Neves, S., Poly (3-methyl thiophene)/PVDF composite as an electrode for supercapacitors. *J.Power Sources* **2006,** *158*, 789-794.

18. Huang, L.; Tian, Y.; Li, M.; He, G.; Li, Z. Performance of stainless steel mesh cathode and PVDF-graphite cathode in microbial fuel cells, 2nd International Symposium on Aqua Science, Water Resource and Low Carbon Energy, 2010; AIP Publishing: 2010; pp 316-319.
19. Liu, F.; Hashim, N. A.; Liu, Y. T.; Abed, M. R. M.; Li, K., Progress in the production and modification of PVDF membranes. *J. Membr. Sci.* **2011,** *375*, 1-27.
20. Venault, A.; Chang, Y.; Yang, H. S.; Lin, P. Y.; Shih, Y. J.; Higuchi, A., Surface self-assembled zwitterionization of poly(vinylidene fluoride) microfiltration membranes via hydrophobic-driven coating for improved blood compatibility. *J. Membrane. Sci* **2014,** *454*, 253-263.
21. Danxi, H.; Lei, W.; Xiaorong, M.; Xudong, W.; Juanli, B., Study on the effect of modified PVDF ultrafiltration membrane for secondary effluent of urban sewage. *Desalin. Water. Treat.* **2014,** *52*, 1-8.
22. Logan, B. E.; Cheng, S.; Watson, V.; Estadt, G., Graphite fiber brush anodes for increased power production in air-cathode microbial fuel cells. *Environ. Sci. Technol.* **2007,** *41*, 3341-3346.
23. Ahn, Y.; Logan, B. E., Domestic wastewater treatment using multi-electrode continuous flow MFCs with a separator electrode assembly design. *Appl. Microbiol. Biotechnol.* **2013,** *97*, 409-416.
24. Cheng, S.; Liu, H.; Logan, B. E., Increased performance of single-chamber microbial fuel cells using an improved cathode structure. *Electrochem. Commun.* **2006,** *8*, 489-494.
25. Ahn, Y.; Hatzell, M. C.; Zhang, F.; Logan, B. E., Different electrode configurations to optimize performance of multi-electrode microbial fuel cells for generating power or treating domestic wastewater. *J.Power Sources* **2014,** *249*, 440-445.

26. Ren, L.; Ahn, Y.; Logan, B. E., A two-stage microbial fuel cell and anaerobic fluidized bed membrane bioreactor (MFC-AFMBR) system for effective domestic wastewater treatment. *Environ. Sci. Technol.* **2014,** *48*, 4199-4206.

Chapter 5

Development of carbon free diffusion layer for activated carbon air cathode of microbial fuel cells

Abstract

The fabrication of activated carbon air cathodes for larger-scale microbial fuel cells requires a diffusion layer (DL) that is highly resistant to water leakage, oxygen permeable, and made using inexpensive materials. A hydrophobic polyvinylidene fluoride (PVDF) membrane synthesized using a simple phase inversion process was examined as a low cost ($0.9 m^{-2}), carbon-free DL that prevented water leakage at high pressure heads compared to a polytetrafluoroethylene/carbon black DL ($11 m^{-2}). The power density produced with a PVDF (20% ,w/v) DL membrane of 1400 ± 7 mW m^{-2} was similar to that obtained using a wipe DL [cloth coated with poly(dimethylsiloxane)]. Water head tolerance reached 1.9 m (~19 kPa) with no mesh supporter, and 2.1 m (~21 kPa, maximum testing pressure) with a mesh supporter, compared to 0.2 ± 0.05 m for the wipe DL. The elimination of carbon black from the DL greatly simplified the fabrication procedure and further reduced overall cathode costs.

5.1 Introduction

Microbial fuel cells (MFCs) are devices that can be used to sustainably harvest energy during wastewater treatment by directly extracting electricity from organic matter using exoelectrogenic bacteria *(1-5)*. Electrons released by exoelectrogenic bacteria on the anode are transferred via an external circuit to the cathode, where typically oxygen is reduced *(6, 7)*. Air cathodes are used to avoid energy demands needed for aeration of wastewater. Activated carbon (AC) air cathodes are now frequently used in MFCs due to the low price of AC ($1.4 kg^{-1}) and its good catalytic activity as AC performs similar to or better than Pt catalysts in these systems *(8, 9)*. Oxygen reduction is a three-phase reaction, in which protons in the solution phase and oxygen in the air phase combine together on the solid AC catalyst phase *(10, 11)*. Therefore, a high performance AC cathode requires a binder that enables efficient proton transfer to the catalyst site but does not inhibit oxygen transfer. Cathodes must also be made using a diffusion layer (DL) so that water does not leak out of the cell.

Cathode materials need to be durable and inexpensive, and the construction of the cathode should require relatively simple procedures and inexpensive equipment with low energy consumption. The cost of the cathode was estimated to be up to 47% of the total cost of all MFC materials, and therefore it is critical to reduce the cathode cost *(12)*, as larger-scale MFCs will require high cathode specific surface areas (area per volume of the reactor) *(13)*. In order to achieve dual goals of being waterproof and oxygen permeable, however, complex procedures have often been used to fabricate DLs. Polytetrafluoroethylene (PTFE), a fluorinated hydrophobic polymer, is commonly applied to the air side of the cathode to produce a DL with the required hydrophobicity *(14, 15)*. However, PTFE requires high temperature treatment (i.e. 340 ºC) to melt the PTFE and form a uniform waterproof polymer film, which therefore results in a complex process that consumes a lot of energy for heating *(14)*. A PTFE film can be very dense, and impede oxygen

transport, and thus carbon black (CB) powder is usually added to increase the porosity, although this adds another mixing step to the cathode production process *(14)*. A pressurized process stage may also be required as PTFE is not expandable at room temperature *(16)*. A PTFE/CB diffusion layer with a PTFE loading of 450 g m^{-2} was estimated to cost \$11 m^{-2} *(14, 17)*. Therefore, fabrication of larger-scale cathodes using PTFE/CB can be both relatively expensive (compared to other DLs), and complex due to the need for both high temperatures and press equipment. Several other DLs have been developed using other materials, but they leak at relatively low water pressures. For example, an inexpensive polymer DL was made from poly(vinylidene fluoride-co-hexafluoropropylene)/CB (PVDF-HFP/CB) mixture at a low PVDF-HFP loading of 44 g/m^2, at an estimated materials cost of \$1.1 m^{-2}, but a cathode with this DL leaked at only 41 ± 0.5 cm of water pressure *(17)*. A cloth wipe DL [cloth coated with poly(dimethylsiloxane), PDMS], which costs only \$0.36 m^{-2} using 121 g m^{-2} PDMS, withstood only 19 ± 1 cm of water pressure *(17, 18)*. In general, the high cost of polymers and high polymer loadings required to make cathodes waterproof makes it a challenge to balance the need for avoiding water leakage but also ensuring sufficient cathode performance relative to power generation.

PVDF is highly hydrophobic fluorinated polymer that can be easily processed at room temperature *(19)*. Recently, a simple phase inversion method was used to fabricate an AC air cathode using PVDF to simultaneous form both the catalyst layer (CL) and the DL, which greatly simplified the fabrication procedure *(8)*. During the phase inversion process a porous film of PVDF was formed on the air side of cathode, and small cathodes were shown to not leak at up to 1.2 m of water pressure *(8)*. However, when larger PVDF cathode were used in subsequent tests (unpublished data), leaks developed at much lower water pressures due to an uneven DL formed by the PVDF that left small holes in the DL. Thus, larger-scale cathodes made with PVDF will require an additional DL in order to avoid water leakage.

In order to prevent water leakage through AC cathodes, the use of an additional and separate PVDF membrane was examined here as a DL that could be easily added to the cathode to make it consistently waterproof at relatively high (~ 2 m) water pressure. Hydrophobic PVDF membranes have long been used in membrane-based processes such as membrane distillation that allow for gas permeation but not liquid flow *(20, 21)*. The PVDF membrane properties have been thoroughly investigated for membranes made with established and commercialized fabrication procedures *(22)*. PVDF membranes are highly resistant to leakage, as shown by a critical liquid entry pressure (LEP) for water of 0.13 MPa for a 15% (w/w) PVDF hollow fiber membrane *(23)*. Thus, very large PVDF membranes could be used as a waterproof DL for an AC cathode. The performance of cathodes with DL membranes made with different amounts of PVDF was evaluated here under both abiotic in electrochemical tests, and under biotic conditions in MFCs. The mechanical stability of the DLs was examined relative to leakage using a lab-designed water pressure test system.

5.2 Materials and methods

5.2.1 Membrane fabrication

Membrane casting solutions of 15%, 20% and 25% (w/v) PVDF were prepared by dissolving PVDF powder (~534,000 Da; Sigma Aldrich) in N, N-dimethylacetamide (DMAc, anhydrous, 99.8%, Sigma Aldrich) and vigorously stirring using a stir bar at 60 °C for over 6 h, until the solution became homogeneous and transparent. A slow stirring process was continued for another 2 h to remove bubbles in the solution. The solution was then cast onto a clean glass plate with a doctor blade (Microm II, Gardco, USA) set at a height of 200 µm, and exposed to air for 30 s. The glass plate was then immersed in a distilled water bath, in which the phase inversion process took place. After 10 min, the membrane was transferred to an ethanol/water (1:1, v/v) bath for 6 h and

then to a pure ethanol bath for another 24 h (Appendix B, Figure S5-1). This solvent exchange procedure was adopted to prevent the shrinkage of the PVDF membranes. The PVDF membrane was then air dried in a fume hood for 10 min to restore hydrophobicity, and stored in sealed plastic bag at room temperature prior to use.

5.2.2 Cathode fabrication and operation

The AC catalyst layer was prepared by mixing AC powder (Norit SX plus, Norit Americas Inc., TX) with PVDF (5% w/v) PVDF and carbon black (CB; Vulcan XC-72, Cabot Corporation, USA) powder at a mass ratio of AC:CB:PVDF = 30:3:5, with an AC catalyst loading of 26.5 mg cm^{-2} as previously described . The mixture was spread directly onto an 11.3 cm^2 circular section of stainless steel mesh (50 × 50, type 304, McMaster-Carr, USA) with a spatula (except as noted). The mesh with the catalyst was then immersed into deionized (DI) water for 15 min at room temperature to leach out DMAc solvent, and air dried in a fume hood overnight prior to use. The final cathode was produced by attaching the DL onto the CL (fixed by rubber O ring) with the dense skin layer facing the CL. The cathode was positioned in the reactor with the DL facing the air side and CL towards the solution side. A PDMS/CB wipe DL [cloth coated with PDMS/CB mixture] was used as an established control as it has been used in many other studies *(24, 25)*; it was prepared as previously described *(18)*.

The cathodes were operated in cubic single-chamber MFCs (except as noted) constructed from a Lexan block 4 cm in length, with an inner chamber diameter of 3 cm *(26)*. The anodes were graphite fiber brushes (2.5 cm in both diameter and length, heat treated at 450 °C in air for 30 min) placed horizontally in the center of MFC chambers *(26)*. Anodes were acclimated by operation for over one year in a previous MFC at a constant temperature (30 °C), with a fixed external resistance (1000 Ω). The medium contained 1 g/L sodium acetate dissolved in 50 mM phosphate buffer

solution (PBS; Na_2HPO_4, 4.58 g L^{-1}; $NaH_2PO_4 \cdot H_2O$, 2.45 g L^{-1}; NH_4Cl, 0.31 g L^{-1}; KCl, 0.31 g L^{-1}; pH = 6.9; conductivity of κ = 6.9 mS cm^{-1}) amended with 12.5 mL L^{-1} minerals and 5 mL L^{-1} vitamins *(8)*.

5.2.3 Cathode performance characterization

Electrochemical cathode tests were conducted in a two-chamber electrochemical cell assembled by bolting two 2-cm wide cubes separated by an anion exchange membrane (AEM; AMI-7001, Membrane International Inc., USA). The counter electrode was a 7 cm^2 diameter platinum plate. An Ag/AgCl reference electrode (RE-5B, BASi, West Lafayette, IN; + 0.209 V vs a standard hydrogen electrode, SHE) was placed in the cathode chamber close to cathode. Electrochemical measurements were conducted with a multichannel potentiostat (VMP3 Workstation, Biologic Science Instruments, USA) in a constant temperature room at 30 °C. A step current method was used to obtain the cathode polarization curve by applying lower currents (0 mA, 1 mA, 2 mA, and 3 mA) for 30 min and higher currents (4 mA, 5 mA, 6 mA, 7 mA, 8 mA, 9 mA and 10 mA) for 20 min to obtain steady-state conditions. All potentials were reported here versus SHE.

Single cycle polarization tests of cathodes under 0 m and 1 m water pressure were conducted in cubic, single-chamber MFCs using the single-cycle method by varying the external resistance from 1000 to 20 Ω at 20 min intervals *(8)*. A lab designed water pressure system was used to apply the water pressure against a cathode (Appendix B, Figure S5-2).Voltage drops (U) across resistors in the circuit were recorded by a computer based data acquisition system (2700, Keithley Instrument, OH). Current densities (i) and power densities (P) were normalized to the projected cathode area (A = 7 cm^2), and calculated as $i = U/RA$ and $P = iU/A$, where R is the external resistance.

5.2.4 Membrane stability

The mechanical stability and waterproof capability of the PVDF membrane DL were tested in a lab made water pressure system (Appendix B, Figure S5-2). A cathode was placed in a cubic reactor with the same dimensions as indicated above for the MFC. A channel drilled in the side of the cubic chamber was connected to a 2.1 meter long PVC tube, which was filled with DI water pumped by a peristaltic pump (MPII, Harvard Apparatus, MA) to maintain a certain water height. Water column height was raised at 10 cm (PVDF) or 5 cm (PDMS wipe DL) intervals, and maintained for 1 min at each water height. The final water height was recorded when water leakage was observed. The water leakage test was conducted with and without a plastic mesh layer (25 × 25 mesh sizes, New York Wire, USA) held against the air-side of the cathode to investigate the effect of membrane deformation on leakage. The PVDF content of each of the samples was measured using circular samples, each 11.3 ± 0.2 cm^2, in triplicate.

5.2.5 Oxygen permeability and membrane morphology

Oxygen permeability through the cathodes was evaluated in terms of an oxygen mass transfer coefficient (**k**, cm s^{-1}) calculated from the change in the dissolved oxygen (DO) concentration in a 4 cm cube reactor as previously described (duplicate measurements) *(6)*. Dissolved oxygen (DO) concentrations were measured with a non-consumptive DO probe (Foxy-18G, Ocean Optics Inc., USA).

Field Emission Scanning Electron (FE-SEM) Variable Pressure (VP) (Zeiss Sigma FE-SEM VP, 3 KeV electron beam) was used to investigate the porous morphology of the PVDF membrane surfaces. The membranes were first washed with DI water to remove any debris and then dried for 12 hours in air atmosphere before characterization.

5.3 Results and discussion

5.3.1 Membrane stability test

The water pressure resistance of cathodes, examined at PVDF loadings of the DL of 29 ± 2 g m^{-2} (15% w/v), 36 ± 2 g m^{-2} (20%) and 40 ± 2 g m^{-2} (25%), increased with PVDF loading (Figure 5-1). The 25% PVDF membrane reached the maximum water pressure possible in our tests of 2.1 m, indicating good mechanical strength and water containment. Slightly lower water pressure resistances of 1.9 m were obtained with the 20% PVDF membrane DL and 1.8 ± 0.1 m for the 15% PVDF membrane (Figure 5-1B). The maximum water pressure of the PDMS wipe DL was 0.2 ± 0.05 m. There was noticeable deformation of the membranes at the higher water pressures. Using a plastic mesh support to minimize membrane deformation, all the PVDF membrane DLs reached the maximum testing water pressure of 2.1 m while the PDMS wipe DL still leaked at the same water pressure.

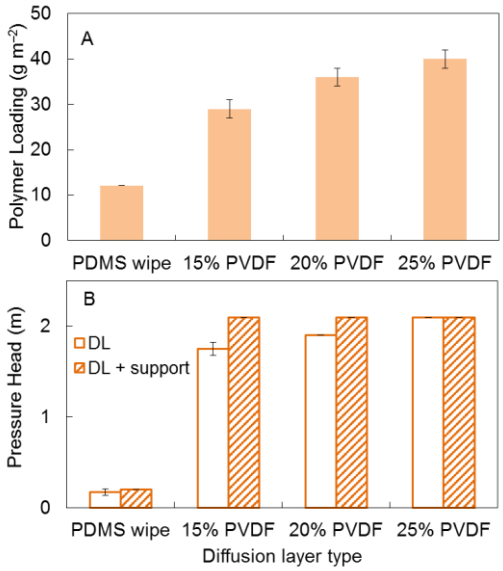

Figure 5-1. (A) Polymer loadings in PDMS wipe, 15%, 20%, 25% (w/v) PVDF membrane diffusion layers (B) Water pressure resistance of PDMS wipe and PVDF membrane diffusion layers with and without nylon spacer support.

5.3.2 Electrochemical performance of AC cathodes with membrane DLs

In abiotic step current tests, the best electrochemical performance among the AC cathodes with PVDF was achieved using the 20% PVDF membrane DL, as it had the highest potential under the tested current density range (Figure 5-2). The 25% PVDF membrane DL achieved a lower potential of 0.047 V compared to 0.084 V of 20% PVDF membrane DL at the at the current density of 5.7 A m^{-2}, where MFCs typically reached their maximum power performance *(8, 17)*. Slight higher potential of 0.055 V was achieved with the 15% PVDF membrane DL under same current density of 5.7 A m^{-2}, which was still 29 mV lower than the 20% PVDF membrane DL. The PDMS wipe DL had the highest potentials, but it was only 15 mV more than that of the 20% PVDF membrane DL at 5.7 A m^{-2}, and a maximum of 21 mV at higher current densities.

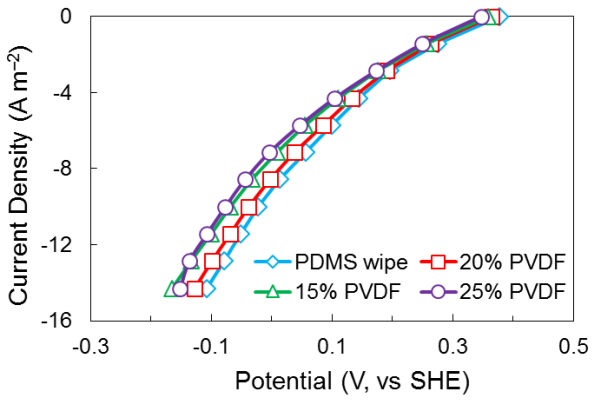

Figure 5-2. Current-voltage (polarization) curves for AC cathodes with PDMS wipe, 15%, 20% and 25% (w/v) PVDF membrane diffusion layers.

5.3.3 Power performance of MFCs with membrane DLs

The power produced using AC cathodes with the different DLs in MFCs was evaluated based on single cycle polarization data. A maximum power density of 1400 ± 7 mW m^{-2} was obtained with the 20% PVDF membrane DL and was similar to 1450 ± 7 mW m^{-2} achieved by the PDMS wipe DL (Figure 5-3A), which might be due to similar oxygen permeability of the two DLs

(Appendix B, Table S5-1). The oxygen mass transfer coefficient of 20% PVDF membrane DL was 2.9 ± 0.3 × 10^{-3} cm s^{-1} and close to 3.1 ± 0.5 × 10^{-3} cm s^{-1} for the PDMS wipe DL (Appendix B, Table S5-1). The 25% PVDF membrane DL produced a lower maximum power density of 1260 ± 80 mW m^{-2}, likely due to a denser polymer network in the DL which would reduce oxygen transport to the catalyst. The lowest power density of 1180 ± 120 mW m^{-2} was obtained with the 15% PVDF membrane, with a large standard deviation among tests suggesting uneven PVDF content in the DL. The PDMS wipe DL and 20% PVDF membrane had similar cathode potentials (Figure 5-3B), further supporting the similar electrochemical performance of these two types of DLs. Cathodes with 15% and 25% PVDF membrane DLs had the lowest potentials in the current density range of 3 to 7 A m^{-2}.

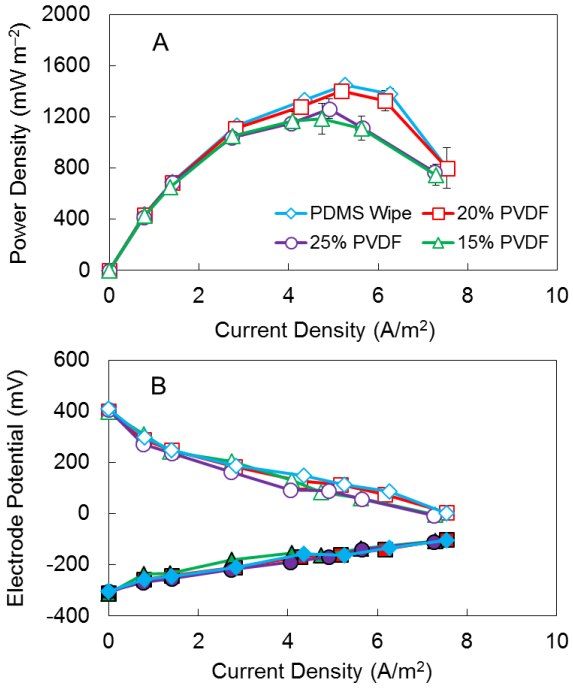

Figure 5-3. (A) Power density curve for AC cathodes with PDMS wipe, 15%, 20% and 25% (w/v) PVDF membrane diffusion layers (B) Electrode potentials (solid symbols for anode potentials and open symbols for cathode potentials)

Additional water pressure did not affect the performance of the MFC with the 20% PVDF membrane. When 1 m of water pressure applied to the cathode, the power density was 1380 ± 60

mW m^{-2}, indicating performance was not significantly different compared to operation due only to the water pressure of the fluid inside the MFC (Figure 5-4A). In addition, cathode potentials were also unaffected under elevated water pressure (Figure 5-4B). Further tests of this membrane in a larger MFC (130 mL, projected cathode membrane area of 35 cm^2) also has shown stable voltage generation for over 20 days (Appendix B, Figure S5-3).

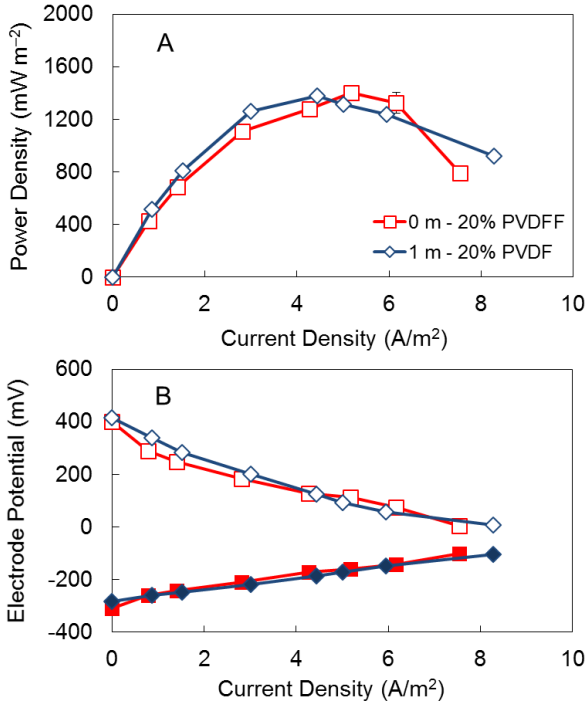

Figure 5-4. (A) Power density curve for AC cathodes with 20% (w/v) PVDF membrane diffusion layer under 0 m and 1 m water pressures (B) Electrode potentials (solid symbols for anode potentials and open symbols for cathode potentials).

5.3.4 Surface morphology

The surface pore sizes of the PVDF membrane diffusion layers appeared to decrease inversely with PVDF concentration. The largest pore sizes observed varied between 110 nm to 170 nm, with a loose polymer network, for the 15% PVDF membrane (Appendix B, Figure S5-4A). With a higher PVDF concentration of 20% (w/v), the membrane had a more uniform appearance, with pore sizes

of ~100 nm (Appendix B, Figure S5-4B). A further increase in the PVDF concentration to 25% (w/v) led to a denser membrane surface with the smallest pore sizes (between 70 and 90 nm, Appendix B, Figure S5-4C). Very small pore sizes suggested a dense polymer network that might have limited the oxygen permeability and resulted in a decrease of the power density using the 25% PVDF membrane (Appendix B, Figure S5-4C).

5.3.5. Membrane cost

In terms of polymer consumption, less PVDF (29 to 40 ± 2 g m^{-2}) was needed to make a DL than that needed for PDMS (121 g m^{-2}) (Figure 5-1A). This amount of PVDF is also lower than the amount of polymer used to make other types of DLs, for example the PTFE/CB DL (450 g m^{-2} of PTFE) . The material cost of PDMS was only \$0.4 m^{-2} (\$3 kg^{-1} for PDMS) but the water pressure resistance was only 0.2 ± 0.05 m (Figure 5-1B). The 20% PVDF membrane DL had slightly higher cost of \$0.9 m^{-2} (\$24 kg^{-1} for PVDF) but the water pressure resistance was 9 times higher compared to a PDMS wipe DL (Figure 5-1B). This PVDF cost of \$0.9 m^{-2} was significantly lower than the PTFE (\$11 m^{-2}, based on \$25 kg^{-1} for PTFE) needed to make a PTFE/CB DL, which is a 92% cost reduction. The 20% PVDF membrane is therefore a cost effective DL for preventing water leakage through an AC cathode, and it maintained a good balance between being waterproof and power production.

Maximum power density normalized to polymer cost also suggested higher power production per unit cost using PVDF membranes as DLs (Table 5-1). Cathodes with PVDF membrane DLs had maximum power densities between 1260 mW $\$^{-1}$ with 25% PVDF DL, and 1690 mW $\$^{-1}$ with 15% PVDF DL, which were all much higher than 120 mW $\$^{-1}$ using the PTFE/CB DL. Moreover, the PVDF membrane DL avoided the need for heat treatment or additional mixing steps needed to mix polymers with CB, used in the PTFE/CB DL, which greatly simplified the fabrication

procedure. The use of this new PVDF membrane DL shows great promise for enabling the fabrication of inexpensive AC cathodes for larger-scale MFC systems. When normalized to polymer cost, maximum power production of 1690 mW $\$^{-1}$ with 15% PVDF DL was 8% higher than the 20% PVDF DL (1560 mW $\$^{-1}$). Therefore, 15% PVDF DL would provide better cost savings for MFC operation compared to the 20% PVDF DL. The 20% PVDF DL exhibited higher power densities than the 15% PVDF DL (Table 5-1), so the use of the greater PVDF content might be warranted in applications requiring higher voltage or current.

Table 5-1. Maximum power density normalized to cathode surface area and DL polymer cost

DL type	Polymer cost ($\$ m^{-2}$)	mWm^{-2}	mW $\$^{-1}$	Ref.
15% PVDF	0.7	1180	1690	this study
20% PVDF	0.9	1400	1560	this study
25% PVDF	1	1260	1260	this study
PDMS wipe	0.4	1450	3620	this study
PTFE/CB	11	1355	120	(14)

5.4 Conclusions

A hydrophobic PVDF membrane was fabricated as a carbon free DL for a cathode to achieve both high water pressure resistance capability and low polymer cost. With a low PVDF loading of 36 ± 2 g m^{-2}, the membrane DL resisted 1.9 m of water pressure, and 2.1 m with a mesh supporter. The power performance of AC cathodes with this membrane DL was similar to AC cathodes made with a PDMS wipe DL. The application of this PVDF membrane DL shows great promise for the fabrication of inexpensive AC cathodes for larger-scale MFC systems.

5.5 Acknowledgement

This research was supported by the Strategic Environmental Research and Development Program (SERDP), and a graduate scholarship from the China Scholarship Council (CSC) to W. Y.

5.6 Literature cited

1. Logan, B. E., *Microbial fuel cells*. John Wiley & Sons, Inc.: Hoboken, NJ, 2008; p 300.
2. Niessen, J.; Schröder, U.; Scholz, F., Exploiting complex carbohydrates for microbial electricity generation: a bacterial fuel cell operating on starch. *Electrochem. Commun.* **2004,** *6*, 955-958.
3. Bond, D. R.; Holmes, D. E.; Tender, L. M.; Lovley, D. R., Electrode-reducing microorganisms that harvest energy from marine sediments. *Science* **2002,** *295*, 483-485.
4. Kim, J. R.; Jung, S. H.; Regan, J. M.; Logan, B. E., Electricity generation and microbial community analysis of alcohol powered microbial fuel cells. *Bioresour. Technol.* **2007,** *98*, 2568-2577.
5. Ahn, Y.; Logan, B. E., Effectiveness of domestic wastewater treatment using microbial fuel cells at ambient and mesophilic temperatures. *Bioresour. Technol.* **2010,** *101*, 469-475.
6. Cheng, S.; Liu, H.; Logan, B. E., Increased performance of single-chamber microbial fuel cells using an improved cathode structure. *Electrochem. Commun.* **2006,** *8*, 489-494.
7. Cheng, S.; Logan, B. E., Increasing power generation for scaling up single-chamber air cathode microbial fuel cells. *Bioresour. Technol.* **2011,** *102*, 4468-4473.

8. Yang, W.; He, W.; Zhang, F.; Hickner, M. A.; Logan, B. E., Single step fabrication using a phase inversion method of poly (vinylidene fluoride)(PVDF) activated carbon air cathodes for microbial fuel cells. *Environ. Sci. Technol. Lett.* **2014,** *1*, 416-420.
9. Wang, X.; Gao, N.; Zhou, Q.; Dong, H.; Yu, H.; Feng, Y., Acidic and alkaline pretreatments of activated carbon and their effects on the performance of air-cathodes in microbial fuel cells. *Bioresour. Technol.* **2013,** *144*, 632-636.
10. Nie, L.; Liu, J.; Zhang, Y.; Liu, M., Effects of pore formers on microstructure and performance of cathode membranes for solid oxide fuel cells. *J. Power Sources* **2011,** *196*, 9975-9979.
11. Duteanu, N.; Erable, B.; Kumar, S. S.; Ghangrekar, M. M.; Scott, K., Effect of chemically modified Vulcan XC-72R on the performance of air-breathing cathode in a single-chamber microbial fuel cell. *Bioresour. Technol.* **2010,** *101*, 5250-5255.
12. Rozendal, R. A.; Hamelers, H. V. M.; Rabaey, K.; Keller, J.; Buisman, C. J. N., Towards practical implementation of bioelectrochemical wastewater treatment. *Trends Biotechnol.* **2008,** *26*, 450-459.
13. Logan, B. E.; Wallack, M. J.; Kim, K.-Y.; He, W.; Feng, Y.; Saikaly, P. E., Assessment of microbial fuel cell configurations and power densities. *Environ. Sci. Technol. Lett.* **2015,** *2*, 206-214.
14. Dong, H.; Yu, H.; Wang, X.; Zhou, Q.; Feng, J., A novel structure of scalable air-cathode without Nafion and Pt by rolling activated carbon and PTFE as catalyst layer in microbial fuel cells. *Water Res.* **2012,** *46*, 5777-87.
15. Cheng, S. A.; Wu, J. C., Air-cathode preparation with activated carbon as catalyst, PTFE as binder and nickel foam as current collector for microbial fuel cells. *Bioelectrochemistry* **2013,** *92*, 22-26.
16. Dong, H.; Yu, H.; Wang, X., Catalysis kinetics and porous analysis of rolling activated carbon-PTFE air-cathode in microbial fuel cells. *Environ. Sci. Technol.* **2012,** *46*, 13009-13015.

17. Yang, W.; Zhang, F.; He, W.; Liu, J.; Hickner, M. A.; Logan, B. E., Poly (vinylidene fluoride-co-hexafluoropropylene) phase inversion coating as a diffusion layer to enhance the cathode performance in microbial fuel cells. *J. Power Sources* **2014,** *269*, 379-384.
18. Wei, B.; Tokash, J. C.; Chen, G.; Hickner, M. A.; Logan, B. E., Development and evaluation of carbon and binder loading in low-cost activated carbon cathodes for air-cathode microbial fuel cells. *RSC Adv* **2012,** *2*, 12751-12758.
19. Liu, F.; Hashim, N. A.; Liu, Y. T.; Abed, M. R. M.; Li, K., Progress in the production and modification of PVDF membranes. *J. Membr. Sci.* **2011,** *375*, 1-27.
20. Wang, K. Y.; Chung, T. S.; Gryta, M., Hydrophobic PVDF hollow fiber membranes with narrow pore size distribution and ultra-thin skin for the fresh water production through membrane distillation. *Chem Eng Sci* **2008,** *63*, 2587-2594.
21. Tomaszewska, M., Preparation and properties of flat-sheet membranes from poly(vinylidene fluoride) for membrane distillation. *Desalination* **1996,** *104*, 1-11.
22. Nejati, S.; Boo, C.; Osuji, C. O.; Elimelech, M., Engineering flat sheet microporous PVDF films for membrane distillation. *J. Membr. Sci.* **2015,** *492*, 355-363.
23. Tan, X.; Tan, S. P.; Teo, W. K.; Li, K., Polyvinylidene fluoride (PVDF) hollow fibre membranes for ammonia removal from water. *J. Membr. Sci.* **2006,** *271*, 59-68.
24. Luo, Y.; Zhang, F.; Wei, B.; Liu, G.; Zhang, R.; Logan, B. E., Power generation using carbon mesh cathodes with different diffusion layers in microbial fuel cells. *J. Power Sources* **2011,** *196*, 9317-9321.
25. Zhang, F.; Saito, T.; Cheng, S.; Hickner, M. A.; Logan, B. E., Microbial Fuel Cell Cathodes With Poly(dimethylsiloxane) Diffusion Layers Constructed around Stainless Steel Mesh Current Collectors. *Environ. Sci. Technol.* **2010,** *44*, 1490-1495.

26. Logan, B. E.; Cheng, S.; Watson, V.; Estadt, G., Graphite fiber brush anodes for increased power production in air-cathode microbial fuel cells. *Environ. Sci. Technol.* **2007,** *41*, 3341-3346.

Chapter 6

Engineering a Membrane Based Air Cathode for Microbial Fuel Cells via Hot Pressing and Using Multi-Catalyst Layer Stacking

Abstract

Microbial fuel cell (MFC) cathodes must have high performance and be resistant to water leakage. Hydrophobic poly(vinylidene fluoride) (PVDF) membranes have shown great advantages in providing a waterproof diffusion layer for MFCs and reducing the cathode costs. However, previous approaches have lacked a method to integrate the diffusion layer into the cathode structure. Here, a hot pressing was used to bind the PVDF diffusion layer onto the air side of the activated carbon cathode, and additional catalyst layers were added to improve performance. Cathodes pressed at 60 °C produced a 16% higher maximum power density of 1630 ± 10 mW m^{-2} than non-pressed controls (1400 ± 7 mW m^{-2}). Cathode performance was further increased to 1850 ± 90 mW m^{-2} by catalyst stacking, through the addition of an extra catalyst layer (CL), which better utilized the available surface area of the stainless steel mesh (SS) current collector. The use of one stainless steel current collector and two catalyst layers (SS/2CLs) produced more positive cathode potentials compared to other designs (SS/CL or 2SS/2CL). Low material costs and high power production for MFCs using these cathodes could enable more cost effective power production using MFCs.

6.1 Introduction

Microbial fuel cells (MFCs) are devices that convert organic substrates into electricity using exoelectrogenic bacteria *(1-5)*. Electrons are released to the anode through degradation of organics and transferred to the cathode, where oxygen reduction is used to generate power. Low-cost cathodes with high catalytic performance are critical for applications of MFCs for wastewater treatment and electricity production *(6-12)*. Previous studies have concluded that cathode materials need to cost less than \$100 m^{-2} to make MFCs an economically viable method of power generation, at production scales of hundreds or more square meters for pilot scale reactors *(13)*. Activated carbon (AC) is often used as an oxygen reduction catalyst, due to its low cost (\$1.4 kg^{-1}), in air cathode-type MFCs to avoid the need to provide oxygen to the cathode by energy intensive water aeration *(6, 14-16)*. However, fabrication of AC cathodes for commercial applications is still hindered by the difficulty of producing square meter-sized cathodes in large quantities.

One of the main obstacles for scaling up AC cathodes is integrating a diffusion layer (DL) that is both oxygen permeable and waterproof into the cathode structure. It was recently shown that the use of a hydrophobic poly(vinylidene fluoride) (PVDF) membrane as external DL could provide these qualities, as cathodes withstood up to 2 m of water pressure, and they had oxygen permeabilities comparable to existing PDMS (polydimethylsiloxane) cloth diffusion layers, enabling good catalytic performance *(17)*. However, the AC catalyst layer (CL) fabrication required an organic solvent (dimethyacetamide) that dissolved the PVDF membrane DL, therefore the PVDF membrane was placed on top of the CL but not bonded to it *(14)*. That non-bonded configuration could result in water accumulation retention between catalyst and DL layer, which would adversely impact cathode performance by reducing oxygen permeability *(18)*. Previous studies showed that water accumulation on the other side of the cathode, between the catalyst layer and a separator (on the water side), adversely affected cathode performance *(19)*. Therefore,

physical integration of PVDF membrane DL into cathode structure is critical for stable performance of a membrane-based DL on the cathode, and an alternative binder or procedure is needed that does not require dimethylacetamide.

Another factor in cathode construction is the AC catalyst loading *(14)*. It was previously shown that increasing the AC catalyst loading from 27 to 62 mg cm^{-2} did not appreciably impact the cathode performance *(20)*. However, the additional AC was pasted only on one side of the current collector. This approach could have increased electrical resistance of the most distant catalyst as activated carbon is not highly electrically conductive, and so this single-sided cathode approach might have negated any advantage of the additional catalyst.

In this study, new cathode construction methods were developed to improve cathode performance while keeping the cost of making the cathodes low. In order to better integrate the DL into the cathode, a hot pressing method was examined at 60 and 120 °C, and compared to pressing at room temperature (25 °C), to physically integrate the DL (PVDF membrane) into the air side of the cathode. We further hypothesized that cathode performance could be improved by adding additional catalyst material if better electrical connections were made between the added catalyst and the current collector. Therefore, we tested adding an additional catalyst layer onto the other (water) side of the cathode, as well as adding a second current collector onto the water side. These additional cathode layers, referred to a multi-layer stacked cathodes, were tested for their performance in both abiotic and biotic (MFC) conditions.

6.2 Materials and methods

6.2.1 Cathode fabrication

The CL was prepared by dispersing AC (Norit SX plus, Norit Americas Inc., TX) in ethanol and stirring at 60 °C on a hot plate as previously described *(21)*. Ethanol was used to facilitate the fabrication process as ethanol evaporates faster than water. A 60% PTFE emulsion (Sigma Aldrich, USA) was added dropwise at a mass ratio of AC: PTFE = 6:1. The mixture was stirred until most ethanol evaporated to form a wet gel. The AC/PTFE gel was then pressed to expand under 1×10^7 Pa for 2 s at 25, 60 or 120 °C (Model 4388, CARVER, INC., USA), and then re-folded and re-pressed two more times (Appendix C, Figure S6-1). The resulting CL had a thickness of 780 ± 60 µm, corresponding to an AC loading of 27 ± 1 mg cm^{-2}. The CL was placed between stainless steel (SS) mesh (42 × 42, type 304, McMaster-Carr, USA) and hydrophobic PVDF membrane DL (0.45 µm, MILLIPORE, USA) and rinsed with ethanol. The sandwiched SS/CL/DL cathode was then pressed under 3×10^7 Pa for at least 15 s at 60 °C until the membrane surface became dry (Figure 6-1A). The pressed cathodes were then taken out and dried in a fume hood for later use. Multi-layer (stacked) AC cathodes were fabricated in three different configurations: using one SS current collector and two CLs (SS/2CL); two SS current collectors and two CLs (2SS/2CL) (Figure 6-1B and 6-1C).

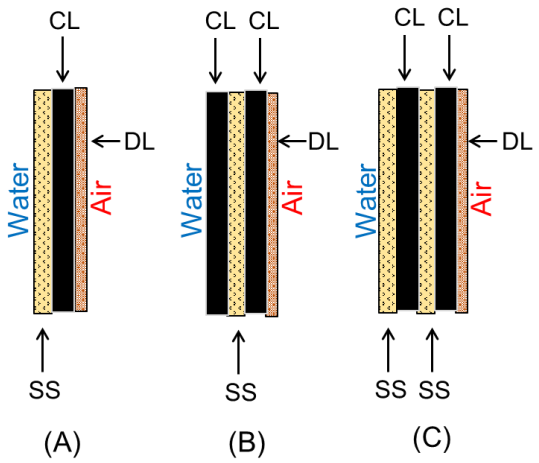

Figure 6-1. Cathode configurations: (A) SS/CL (B) SS/2CL (C) 2SS/2CL. (SS: Stainless steel mesh; CL: Catalyst layer; DL: Diffusion layer)

6.2.2 Cathode performance characterization

Step current tests were conducted using two-chamber, electrochemical cells assembled by bolting together two cubes (2-cm wide) containing 3-cm diameter cylindrical chambers, separated by an anion exchange membrane (AEM; AMI-7001, Membrane International Inc., USA). The counter electrode was a 7 cm^2 diameter platinum plate. An Ag/AgCl reference electrode (RE-5B, BASi, West Lafayette, IN; + 0.209 V vs a standard hydrogen electrode, SHE) was placed in the cathode chamber close to the electrode. All potentials reported here were corrected to SHE. Electrochemical measurements were conducted with a multichannel potentiostat (VMP3 Workstation, Biologic Science Instruments, USA) in a constant temperature room at 30 °C. The lower currents (1 mA, 2 mA, 3 mA and 4 mA) were applied for 1 h and the higher currents (5 mA, 6 mA, 7 mA, 8 mA, 9 mA and 10 mA) were applied for 30 min to achieve steady-state conditions, as previously described *(17)*. Impedance measurements of cathodes were conducted at 0.1 V vs SHE over a frequency range of 100 kHz to 100 mHz with a sinusoidal perturbation of 14.2 mV amplitude. All electrochemical tests were conducted in 50 mM phosphate buffer solution (PBS;

Na_2HPO_4, 4.58 g/L; $NaH_2PO_4 \cdot H_2O$, 2.45 g/L; NH_4Cl, 0.31 g/L; KCl, 0.31 g/L; pH = 6.9; conductivity of κ = 6.9 mS/cm).

Single cycle polarization tests of AC cathodes were conducted by varying the external resistance from 1000 to 20 Ω at 20 min intervals in cubic single-chamber MFCs (except as noted) constructed from a single Lexan block 4 cm in length, with an inner chamber diameter of 3 cm, as previously described *(22)*. The anodes were graphite fiber brushes (2.5 cm in both diameter and length, heat treated at 450 °C in air for 30 min) placed horizontally in the center of the MFC chambers *(22)*. Anodes were acclimated by operation for over one year in previous MFCs at a constant temperature (30 °C), with a fixed external resistance (1000 Ω). The medium contained 1 g/L sodium acetate dissolved in 50 mM PBS amended with 12.5 mL/L minerals and 5 mL/L vitamins *(14)*.

6.2.3 Physical characterization

The surface areas of cathode CLs pressed at different temperatures were determined from nitrogen adsorption isotherms (at 77.3 K) by progressively increasing relative pressures of 5×10^{-6} to 0.99 atm atm^{-1} (ASAP 2420, Micromeritics Instrument Corp., GA). All samples were degassed at 100 °C for 16 h prior to measurements. The Brunauer-Emmet-Teller (BET) specific surface area was evaluated using adsorption data in a relative pressure range between 5×10^{-6} to 0.2 atm atm^{-1}.

The morphologies of the PVDF membrane DLs pressed at different temperatures were examined using scanning electron microscopy (SEM; FEI model XL30, tungsten filament, 5 KeV electron beam). The membranes were sputter coated with gold particles before SEM imaging.

Oxygen transport through the cathode was calculated in terms of an oxygen mass transfer coefficient (**k**, cm s^{-1}) based on the change in the dissolved oxygen (DO) concentration in a 4 cm long single-chamber reactor as previously described (duplicate measurements) *(23)*. Dissolved

oxygen (DO) concentrations were measured using a non-consumptive DO probe (Foxy-18G, Ocean Optics Inc., USA).

6.3 Results and discussion

6.3.1 Effect of pressing temperature on cathode performance

The maximum power density of the AC cathode pressed at 60 °C was 1630 ± 10 mW m^{-2}, which was similar to that obtained at 25 °C (1620 ± 70 mW m^{-2}) (Figure 6-2). However, the DL membrane on the cathode pressed at 25 °C did not tightly bind to the surface of the cathode, likely because too much of the ethanol solvent was retained on the cathode surface during the pressing process due to a low evaporation rate at this temperature. The highest maximum power density of 1840 ± 90 mW m^{-2} was achieved with the cathode pressed at 120 °C. Cathodes pressed under 25, 60 and 120 °C all produced higher maximum power densities than those previously reported for non-pressed cathodes containing the same DL (1400 ± 7 mW m^{-2}) *(17)*.

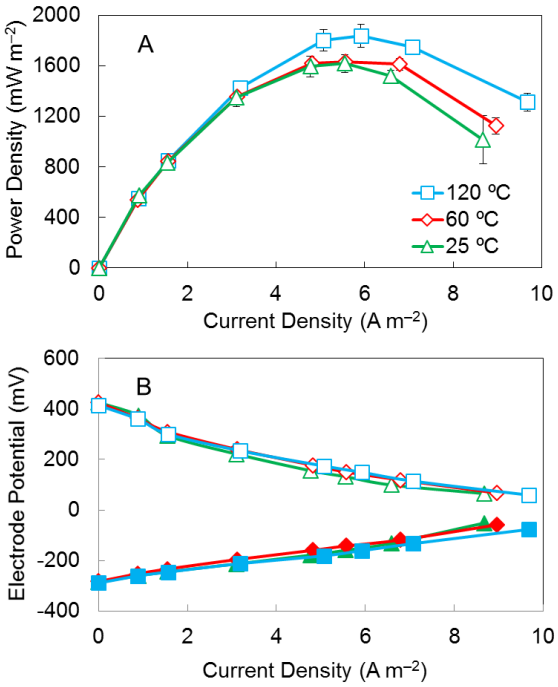

Figure 6-2. (A) Power density curves for AC cathodes pressed at 25, 60 and 120 °C. (B) Electrode potentials (solid symbols, anode potentials; open symbols, cathode potentials).

Increasing the pressing temperature had minimal impact on the CLs but impacted the morphology of the DLs. The BET surface area of the CLs pressed at different temperatures remained similar of 787 $m^2\ g^{-1}$ (25 °C), 791 $m^2\ g^{-1}$ (60 °C) and 781 (120 °C) $m^2\ g^{-1}$, suggesting no porosity change in the CLs (Figure 6-3). However, the higher pressing temperature of 120 °C led to a much denser membrane surface compared to membranes pressed at 25 and 60 °C (Figure 6-4A–6-4C), and some cracks were observed on the membrane pressed at 120 °C (Figure 6-4D). Therefore, a higher oxygen mass transfer coefficient of $3.0 \pm 0.3 \times 10^{-3}$ cm s^{-1} was achieved for membranes pressed at 120 °C even though the membrane surface was denser. The mass transfer coefficients for the other two membranes were $2.6 \pm 0.2 \times 10^{-3}$ cm s^{-1} (25 °C) and $2.5 \pm 0.1 \times 10^{-3}$ cm s^{-1} (60 °C) (Appendix C, Table S6-1). The occurrence of cracks on membranes when pressed at 120 °C also suggested that pressing at 60 °C was better in terms of maintaining membrane surface morphology. To minimize energy consumption for producing cathodes, and avoid the occurrence

of cracks in the membrane, a pressing temperature of 60 °C was selected for additional AC catalyst tests.

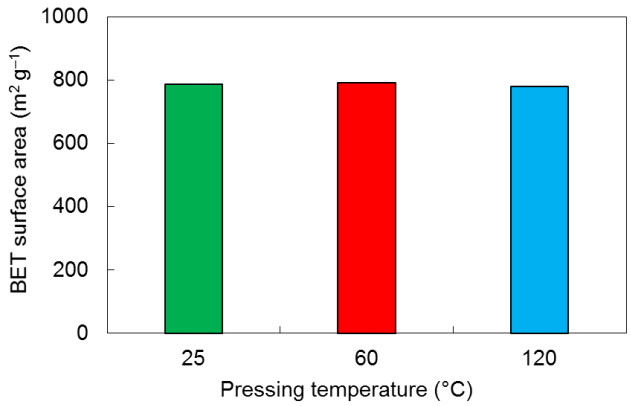

Figure 6-3. BET surface area for AC catalyst layers pressed at 25, 60 and 120 °C.

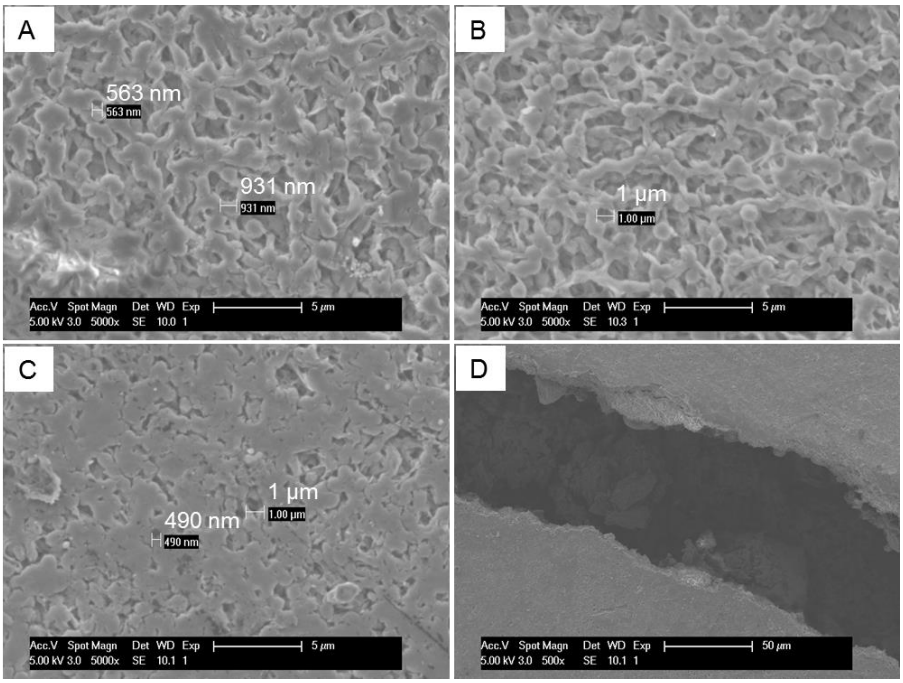

Figure 6-4. SEM images for PVDF membrane diffusion layers pressed at (A) 25, (B) 60, (C-D) 120 °C.

6.3.2 Multi-layer stacked cathode performance

To further optimize the membrane based AC cathode, a multi-layer stacking cathode structure was tested for making cathodes (Figure 6-1). The reactors with the AC cathode containing one SS current collector and two CLs (SS/2CL) produced the highest maximum power density of 1850 ± 90 mW m^{-2} (Figure 6-5). MFCs with other cathodes produced 13% lower maximum power densities, with 1630 ± 10 mW m^{-2} for the single (SS/CL) cathode structure, and 1640 ± 30 mW m^{-2} for the double (2SS/2CL) cathode structure (Figure 6-5). Although the 2SS/2CL cathode had the same AC loading as the SS/2CL cathode, it is likely that the additional SS current collector on the solution side blocked ion transport to and from the cathode, which could have resulted in the decreased power.

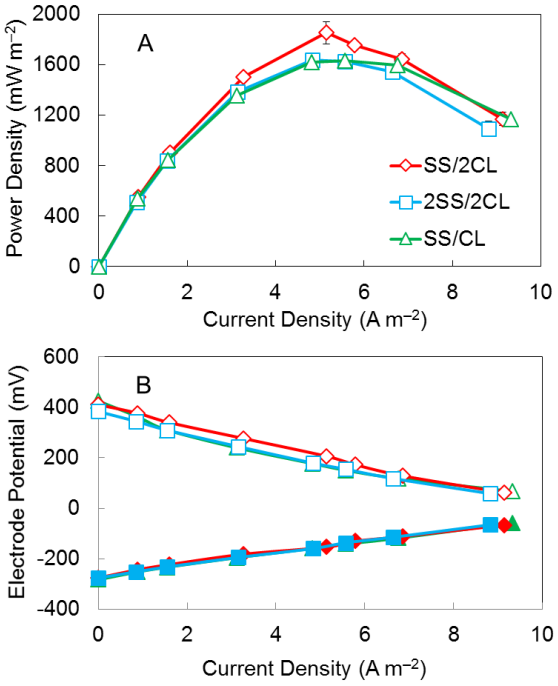

Figure 6-5. (A) Power density curves for AC cathodes with SS/CL, SS/2CL and 2SS/2CL. (B) Electrode potentials (solid symbols, anode potentials; open symbols, cathode potentials).

Higher electrode potentials were obtained in abiotic electrochemical tests with the SS/2CL cathode, compared to the SS/CL or 2SS/2CL cathodes, at current densities up to 10 A m^{-2} (Figure

6-6A), a current range typical for MFCs *(6, 8)*. At a current density of 6 A m^{-2} where the maximum power density was achieved (see below), the potential for the SS/2CL cathode was 150 mV, which was 25% higher than that obtained for both of the other cathodes (120 mV; SS/CL and 2SS/2CL) (Figure 6-6A). Similar cathode performance was achieved when a single CL was placed either at the solution side or air side, indicating CL position relative to the water phase did not affect the performance (Appendix C, Figure S6-2).

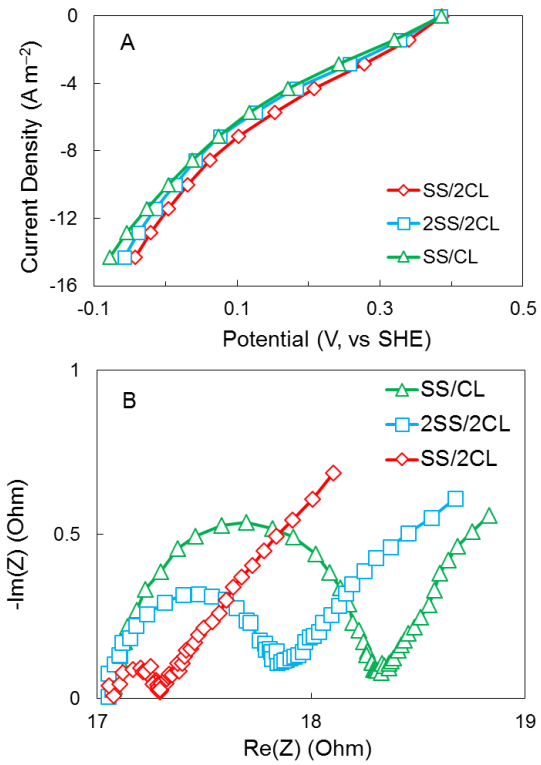

Figure 6-6. (A) Current-voltage (polarization) curves (B) EIS spectra for the AC cathodes with SS/CL, SS/2CL and 2SS/2CL in an abiotic electrochemical cell.

The EIS spectra showed that the SS/2CL cathode had a smaller arc and a charge transfer resistance of 0.3 Ω, which was 88% lower than 2.4 Ω for the SS/CL cathode (Figure 6-6B). Although the 2SS/2CL also lowered the charge transfer resistance to 1.2 Ω but was not enough to significantly boost the cathode performance (Figure 6-6B). The better electrochemical performance with SS/2CL cathode, indicated that increasing the AC loading increased performance, but only

when the additional catalyst was added on the other side of the existing layer so that it made good contact with the current collector. Thus, previous findings that additional catalyst did not improve performance were likely due to the additional catalyst only being placed on one side of the cathode *(20)*.

6.3.3 Energy cost projections for MFCs

Due to the low cost of AC catalyst, adding a second CL to the cathode did not appreciably increase the material costs of the cathode. The materials cost of the SS/2CL is estimated to be \$16.5 m^{-2}, which was only \$1.4 m^{-2} more compared to the original \$15.1 m^{-2} for the SS/CL cathode (Table 6-1). The unit power production, which is the power produced (mW m^{-2}) divided by the cost of the cathode materials (\$ m^{-2}), has been used to evaluate the economics of power production using MFCs *(17)*. The unit power production for the SS/2CL cathode was 112 mW $\$^{-1}$, which is quite similar to that for the SS/CL cathode of 108 mW $\$^{-1}$. Adding an extra SS currently collector substantially decreased the unit power production to 58 mW $\$^{-1}$ and thus was not considered to be economically viable (Table 6-1). To evaluate the overall cost of MFCs, cathode lifetime was estimated to be 5 years, and the cathode materials were estimated to be 50% of the overall MFC cost based on a previous study *(24)*. Using these values, the overall MFC cost normalized for 5 years is \$21 m^{-2}, which is below the target of \$100 m^{-2} *(13)*.

Table 6-1. Maximum power density normalized to cathode surface area and cathode cost

Cathode Configuration	Cathode Cost (\$ m^{-2})	mW m^{-2}	mW $\$^{-1}$
SS/CL	15.1	1630	108
SS/2CL	16.5	1850	112
2SS/2CL	28.5	1640	58

6.4 Conclusions

A hot pressing method of AC cathode fabrication was examined to integrate a hydrophobic PVDF membrane as the DL into the cathode structure, producing a maximum power density of 1630 ± 10 mW m^{-2} at a pressing temperature of 60 °C. Cathode performance was further increased by adding an extra CL onto the other side of the SS current collector, producing a maximum power density of 1850 ± 90 mW m^{-2}, which was 13% greater than that obtained without additional catalyst. The adoption of this new AC cathode procedure could enable more cost effective power production using MFCs.

6.5 Acknowledgments

This research was supported by the Strategic Environmental Research and Development Program (SERDP) and a graduate scholarship from the China Scholarship Council (CSC) to W. Y.

6.6 Literature cited

1. Logan, B. E., *Microbial fuel cells*. John Wiley & Sons, Inc.: Hoboken, NJ, 2008; p 300.
2. Niessen, J.; Schröder, U.; Scholz, F., Exploiting complex carbohydrates for microbial electricity generation: a bacterial fuel cell operating on starch. *Electrochem. Commun.* **2004,** *6*, 955-958.
3. Allen, R. M.; Bennetto, H. P., Microbial fuel cells: electricity production from carbohydrates. *Appl. Biochem. Biotechnol.* **1993,** *39*, 27-40.
4. Xu, B.; Ge, Z.; He, Z., Sediment microbial fuel cells for wastewater treatment: challenges and opportunities. *Environ. Sci.: Water Res. Technol.* **2015,** *1*, 279-284.
5. Lovley, D. R., Bug juice: harvesting electricity with microorganisms. *Nat. Rev. Microbiol.* **2006,** *4*, 497-508.
6. Cheng, S.; Wu, J., Air-cathode preparation with activated carbon as catalyst, PTFE as binder and nickel foam as current collector for microbial fuel cells. *Bioelectrochemistry* **2013,** *92*, 22-26.
7. Dong, H.; Yu, H.; Wang, X., Catalysis kinetics and porous analysis of rolling activated carbon-PTFE air-cathode in microbial fuel cells. *Environ. Sci. Technol.* **2012,** *46*, 13009-13015.
8. Wang, X.; Feng, C. J.; Ding, N.; Zhang, Q. R.; Li, N.; Li, X. J.; Zhang, Y. Y.; Zhou, Q. X., Accelerated OH- transport in activated carbon air cathode by modification of quaternary ammonium for microbial fuel cells. *Environ. Sci. Technol.* **2014,** *48*, 4191-4198.
9. Li, D.; Qu, Y.; Liu, J.; He, W.; Wang, H.; Feng, Y., Using ammonium bicarbonate as pore former in activated carbon catalyst layer to enhance performance of air cathode microbial fuel cell. *J.Power Sources* **2014,** *272*, 909-914.

10. He, W.; Zhang, X.; Liu, J.; Zhu, X.; Feng, Y.; Logan, B. E., Microbial fuel cells with an integrated spacer and separate anode and cathode modules. *Environ. Sci.: Water Res. Technol.* **2016,** *2*, 186-195.
11. Ge, Z.; He, Z., Long-term performance of a 200 liter modularized microbial fuel cell system treating municipal wastewater: treatment, energy, and cost. *Environ. Sci.: Water Res. Technol.* **2016,** *2*, 274-281.
12. Forrestal, C.; Haeger, A.; Dankovich, L.; Cath, T. Y.; Ren, Z. J., A Liter-scale Microbial Capacitive Deionization System for the Treatment of Shale Gas Wastewater. *Environ. Sci.: Water Res. Technol.* **2016**.
13. Logan, B. E.; Wallack, M. J.; Kim, K.-Y.; He, W.; Feng, Y.; Saikaly, P. E., Assessment of microbial fuel cell configurations and power densities. *Environ. Sci. Technol. Lett.* **2015,** *2*, 206-214.
14. Yang, W.; He, W.; Zhang, F.; Hickner, M. A.; Logan, B. E., Single step fabrication using a phase inversion method of poly (vinylidene fluoride)(PVDF) activated carbon air cathodes for microbial fuel cells. *Environ. Sci. Technol. Lett.* **2014,** *1*, 416-420.
15. Janicek, A.; Fan, Y.; Liu, H., Performance and stability of different cathode base materials for use in microbial fuel cells. *J. Power Sources* **2015,** *280*, 159-165.
16. Yang, W.; Zhang, F.; He, W.; Liu, J.; Hickner, M. A.; Logan, B. E., Poly (vinylidene fluoride-co-hexafluoropropylene) phase inversion coating as a diffusion layer to enhance the cathode performance in microbial fuel cells. *J. Power Sources* **2014,** *269*, 379-384.
17. Yang, W.; Kim, K.-Y.; Logan, B. E., Development of carbon free diffusion layer for activated carbon air cathode of microbial fuel cells. *Bioresour. Technol.* **2015,** *197*, 318-322.
18. Zhang, F.; Pant, D.; Logan, B. E., Long-term performance of activated carbon air cathodes with different diffusion layer porosities in microbial fuel cells. *Biosens. Bioelectron* **2011,** *30*, 49-55.

19. Zhang, X.; Cheng, S.; Wang, X.; Huang, X.; Logan, B. E., Separator characteristics for increasing performance of microbial fuel cells. *Environ. Sci. Technol.* **2009,** *43*, 8456-8461.

20. Wei, B.; Tokash, J. C.; Chen, G.; Hickner, M. A.; Logan, B. E., Development and evaluation of carbon and binder loading in low-cost activated carbon cathodes for air-cathode microbial fuel cells. *RSC Adv* **2012,** *2*, 12751-12758.

21. Dong, H.; Yu, H.; Wang, X.; Zhou, Q.; Feng, J., A novel structure of scalable air-cathode without Nafion and Pt by rolling activated carbon and PTFE as catalyst layer in microbial fuel cells. *Water Res.* **2012,** *46*, 5777-87.

22. Logan, B. E.; Cheng, S.; Watson, V.; Estadt, G., Graphite fiber brush anodes for increased power production in air-cathode microbial fuel cells. *Environ. Sci. Technol.* **2007,** *41*, 3341-3346.

23. Cheng, S.; Liu, H.; Logan, B. E., Increased performance of single-chamber microbial fuel cells using an improved cathode structure. *Electrochem. Commun.* **2006,** *8*, 489-494.

24. Rozendal, R. A.; Hamelers, H. V. M.; Rabaey, K.; Keller, J.; Buisman, C. J. N., Towards practical implementation of bioelectrochemical wastewater treatment. *Trends Biotechnol.* **2008,** *26*, 450-459.

Chapter 7

Immobilization of Metal-Nitrogen-Carbon Co-catalyst on Activated Carbon with Enhanced Cathode Performance in Microbial Fuel Cells

Abstract

Applications of microbial fuel cells (MFCs) are limited in part by low power densities mainly due to cathode performance. Successful immobilization of iron-nitrogen-carbon co-catalyst on activated carbon (Fe-N-C/AC) improved the oxygen reduction reaction to nearly a four electron transfer, compared to a two-electron transfer of activated carbon (AC). With acetate as the fuel, the maximum power density was 4.7 ± 0.2 W m^{-2}, which is higher than any previous report for an air-cathode MFC. With domestic wastewater as a fuel, MFCs with the Fe-N-C/AC cathode produced up to 0.8 ± 0.03 W m^{-2}, which was twice that obtained with a platinum-catalyzed cathode. The use of this Fe-N-C/AC catalyst can therefore substantially increase power production, and enable broader applications of MFCs for renewable electricity generation using waste materials.

7.1 Introduction

A microbial fuel cell is a nascent technology for harvesting electricity directly from organic matter in water, and thus it has great potential for treating wastewater economically without the use of energy derived from fossil fuels *(1-5)*. Bacteria on the anode oxidize organic matter and produce an electrical current, and typically oxygen is reduced at the cathode. However, the relatively low power density (0.4 ~ 1.5 W m^{-2}) of air-cathode MFCs still hinders wide applications, mainly due to poor cathode performance *(6-8)*. The oxygen reduction reaction (ORR) on the MFC cathode is limited by poor kinetics with activated carbon or even precious metal catalysts.*(9)* Functionalized carbon nanotubes or graphene based catalysts can be used to produce ORR rates comparable to platinum *(10-12)* but these materials are currently too expensive for MFC applications. Only activated carbon currently shows promise for MFC applications due to the need for an inexpensive catalyst *(13-15)*. Activated carbon costs ~\$1.4 kg^{-1} and it is relatively resistant to corrosion and fouling *(16, 17)*. Further improvements in the ORR for cathodes must therefore use activated carbon and other inexpensive materials *(18)*.

ORR catalysts that exhibit higher catalytic activities have a four-electron transfer rather, than a two-electron transfer *(9)*. The ORR catalyzed by activated carbon often takes place by a two-electron pathway, with an electron transfer number around 2.6, compared to a four electron transfer using platinum *(9)*. Nitrogen functional groups on activated carbon are critical for ORR but activated carbon usually has a low content of nitrogen species (< 1%) *(9, 19, 20)*. Using graphite as a model catalyst, it was shown that the number of electrons transferred can be increased by well-controlled nitrogen doping with the ORR active sites created by pyridinic nitrogen *(21)*.

Several of the more successful approaches to improve the catalytic activity of activated carbon have therefore been based on increasing the nitrogen content of activated carbon but exclusively with high material consumption. For example, carbonization of cyanamide and activated carbon

(750 °C for 4 h) increased the pyridinic nitrogen content up to 5%, resulting in a four electron transfer (electron-transfer number of 3.9) *(22)*. However, five times as much mass of cyanamide was used to treat the activated carbon, making it an expensive process. In another study, activated carbon was treated with ammonia gas (700 °C for 1 h) to increase the nitrogen content to 1.5% and the electron transfer number to 3.8, but this is also an expensive approach *(23)*. A more successful approach for producing a more cost-effective ORR catalyst is based on using a metal organic framework, which is made by carbonizing an inexpensive metal and organic ligand at high temperatures (700 to 1000 °C) *(24)*. These catalysts produce an increase in the O-O bond distance for oxygen, and thus facilitate the ORR in a near four-electron transfer pathway *(25)*. However, these catalysts have so far only been examined on expensive or non-reactive support materials, such as carbon nanotubes or porous silica rather than activated carbon and generally produced low power densities *(26, 27)*. In one study, the addition of both iron and nitrogen to the carbon was attempted using iron chloride and ethylenediamine *(28)*. However, only nitrogen was found on the carbon surface after treatment, so any improvements were due solely to the very high nitrogen doping (89:2, N:C), making it an expensive approach for improving the ORR reaction. Therefore, a low material consumption method to boost the ORR activity of activated carbon is essential to make MFCs economically viable.

In this study, we examined immobilization of a metal organic framework material onto activated carbon with significantly low material consumption. The advantage of activated carbon as a substrate is its very high surface area (700 to 1500 $m^2\ g^{-1}$) *(20)*. However, successful addition of a catalyst onto activated carbon was uncertain as the material addition could block the inner pores, resulting in decreased surface area and decreased power generation. Most tests were conducted using Fe, with Co examined as a possible alternative precursor and Na as a negative control. A low amount of the nitrogen precursor (1,10-phenanthroline) was used to minimize the cost, for example a ratio of 6:1:1 for a mass ratio of activated carbon:$FeCl_3$:organic precursor

(denoted as Fe-N-C/AC). To demonstrate the utility of these materials for MFCs, we examined power production in single-chamber, air-cathode MFCs using acetate in a standard 50 mM phosphate buffer solution (a typical benchmark for many new cathode material comparisons), acetate in a high conductivity (200 mM) PBS solution, and unamended domestic wastewater. The performance of the Fe-N-C/AC catalyst was also compared to controls prepared with only Fe or N addition, plain activated carbon, and cathodes made with a Pt catalyst.

7.2 Materials and methods

7.2.1 Catalyst synthesis and cathode fabrication

Three types of modified AC catalysts were synthesized: Fe-N-C immobilized AC (Fe-N-C/AC); nitrogen doped AC (N-AC); and iron doped AC (Fe-AC). To prepare the Fe-N-C/AC catalysts, 6 g of AC powder (Norit SX plus, Norit Americas Inc., TX) was dispersed and stirred for 30 min in 75 mL of water containing 1 g of $FeCl_3$ (anhydrous, Sigma Aldrich, USA) and 1 g of 1,10–phenanthroline (Sigma Aldrich, USA) at 60 °C. The mixture was dried in an oven at 80 °C, and then pyrolyzed at 800 °C for 15 min in an N_2 atmosphere. The resulting powder was soaked in 0.01 mol L^{-1} hydrochloric acid for 1 h and stirred to remove any iron residual, and then dried in a fume hood at room temperature for 48 h. The other two catalysts were prepared using the same procedure, but using only phenanthroline for the N-AC catalyst, and only $FeCl_3$ for the Fe-AC catalyst. Plain AC was used as a control (no treatment). Co-N-C/AC and Na-N-C/AC were also fabricated using 1 g of Cobalt chloride (Sigma Aldrich, USA) or 1 g of sodium chloride (Sigma Aldrich, USA) following the same procedure.

The AC-based cathodes were fabricated by placing a pre-made catalyst layer between stainless steel (SS) mesh (42 × 42, type 304, McMaster-Carr, USA) and a hydrophobic PVDF membrane

diffusion layer (0.45 μm, MILLIPORE, USA). The material was then rinsed with ethanol, pressed at 3×10^7 Pa. for at least 15 s at 60 °C (Model 4388, CARVER, INC., USA), and then dried in a fume hood. The AC catalyst layer was prepared by mixing activated carbon (modified or non-modified) and a 60% PTFE emulsion (Sigma Aldrich, USA) in ethanol at a mass ratio of AC: PTFE = 6:1 with stirring on a hot plate at 60 °C, as previously described *(14)*. The mixture was then continuously stirred at 60 °C to form a gel. The gel was then pressed under 1×10^7 Pa. for 2 s at 60 °C and folded for a second pressing, which was repeated for a total of three times. The prepared catalyst layer had a thickness of 780 ± 60 μm with a catalyst loading of 27 ± 1 mg cm^{-2}.

In order to compare the performance of the catalysts used here to previously studies, a carbon cloth-based cathode with made using a platinum catalyst (ETEK C1-10 10% Pt on Vulcan XC-72) and a PTFE diffusion layer was prepared, as previously described *(29)*.

7.2.2 MFC construction and operation

MFCs were single-chamber, cubic reactors constructed from a Lexan block 4 cm in length, with an inside chamber diameter of 3 cm (30). The anodes were graphite fiber brushes (2.5 cm in both diameter and length) heat treated at 450 °C in air for 30 min, and placed horizontally in the middle of MFC chambers (30). Anodes were fully pre-acclimated by use in MFCs for over one year at a fixed external resistance of 1000 Ω, in a constant temperature room (30 °C). The medium used here contained 1 g L–1 sodium acetate dissolved in a phosphate buffer solution (PBS) that was amended with 12.5 mL L–1 minerals and 5 mL L–1 vitamins (31). The two PBS buffers were: 50 mM (Na2HPO4, 4.58 g L–1; NaH2PO4·H2O, 2.45 g L–1; NH4Cl, 0.31 g L–1; KCl, 0.13 g L–1; pH = 6.9; κ = 6.94 mS cm–1) and 200 mM (Na2HPO4, 18.3 g L–1; NaH2PO4·H2O, 9.8 g L–1; NH4Cl, 1.24 g L–1; KCl, 0.52 g L–1; pH = 7; κ = 20.4 mS cm–1). Domestic waste water was collected from the primary clarifier of the Pennsylvania State University Waste Water Treatment

Plant, and stored at 4 °C prior to use. The total chemical oxygen demand (COD) of the wastewater was 540 ± 10 mg L–1 (sCOD, 275 ± 10 mg L–1; pH, 7.5; conductivity, 1.5 mS cm–1).

Single cycle polarization tests were conducted by varying the external resistance from 1000 Ω to 20 Ω at 20 min intervals *(32)*. The voltage drop (*U*) across an external resistor was recorded by a computer based data acquisition system (2700, Keithley Instrument, OH). Current densities (*i*) and power densities (*P*) were normalized to the exposed projected cathode area (A = 7 cm^2), and calculated as $i = U/RA$ and $P = iU/A$, where R is the external resistance. All tests were conducted in duplicate.

7.2.3 Electrochemical analysis

The electrochemical performance of cathodes were evaluated using linear sweep voltammetry (LSV) in an electrochemical cell (2 cm length, 3 cm diameter) containing two chambers separated by an anion exchange membrane (AEM; AMI-7001, Membrane International Inc., USA). The electrolyte was 50 mM PBS prepared as described above. The counter electrode was a 7 cm^2 round platinum plate. An Ag/AgCl reference electrode (RE-5B, BASi, West Lafayette, IN; + 0.209 V vs a standard hydrogen electrode) was placed close to cathode and kept in the same position for all tests. All potentials were reported versus a standard hydrogen electrode (SHE). A potentiostat (VMP3 Multichannel Workstation, Biologic Science Instruments, USA) was used for all measurements, and all tests were conducted in a constant temperature room (30 °C). The potentials on the cathodes were scanned from + 0.509 V to – 0.209 V versus SHE for 7 times to reach steady conditions. Impedance measurements of AC cathodes were conducted at 0.1 V vs SHE over a frequency range of 100 kHz to 100 mHz with a sinusoidal perturbation of 14.2 mV amplitude.

A rotating disk electrode (RDE) was used to evaluate the catalytic activity of the AC catalyst in the absence of appreciable external mass transfer limitation. An AC catalyst ink was prepared

by adding 30 mg of powdered AC into 3 mL of dimethylformamide (Sigma Aldrich, USA) with sonification (Model 450, Branson, USA) pulsed at 20% power for 8 min in an ice bath. Nafion (270 μL , 5 wt %, Sigma Aldrich, USA) was added into the solution and sonicated for another 8 min. After sonication, a drop (10 μL) of ink solution was coated onto a glassy carbon disk (Pine Instruments, USA) 5 mm in diameter, and dried overnight as previously described *(9)*. All RDE tests were conducted in 50 mM PBS sparged with nitrogen and then air. Solutions were sparged with a gas for 30 min before conducting linear sweep voltammetry tests and the gas was constantly streamed into the headspace during LSV runs. The potential of the disk electrode was scanned from 0.2 V to –1 V (vs. Ag/AgCl) at 10 mV s^{-1}, at rotation rates ranging from 100 rpm to 2100 rpm. The current generated under nitrogen sparging was subtracted from that obtained under air sparging to evaluate current generation due only to oxygen reduction *(33)*. All electrochemical tests were conducted at a constant temperature room (30 °C).

The electron-transfer number (n) for the ORR was calculated from the Koutecky–Levich plots derived from RDE data, based on the slope of fitting line (i^{-1} vs $\omega^{-1/2}$) according to Koutecky–Levich *(9)* equation:

$$\frac{1}{i} = \frac{1}{i_k} - \frac{1}{0.620nFAD^{2/3}cv^{-1/6}\omega^{1/2}} \qquad (1)$$

where i is the measured reduction current, i_k is the kinetic current, n is the number of electrons transferred in the reaction, F is the Faraday constant, A is the geometric surface area of the disk electrode, D is the oxygen diffusion coefficient, c is the concentration of oxygen in the solution, v is the kinematic viscosity, and ω is the rotation rate of the electrode *(34)*.

7.2.4 Surface characterization

A quick X-ray photoelectron spectroscopy (XPS) (Axis Ultra XPS, Kratos Analytical, UK, monochrome Al Kα source, 1486 eV) scan was first conducted for each sample to identify the elements present with a high generation energy, and short dwell time. High-resolution scans for quantification and chemical state information were collected afterward with a low generation energy and long dwell time. CASA XPS software was used for the elemental and peak fitting analysis of N1s (398 eV) and Fe2p ($2p_{3/2}$, 707 eV; $2p_{1/2}$, 720 eV) signals.

7.3 Results and discussion

7.3.1 Surface analysis of modified catalysts

Successful immobilization of iron into the Fe-N-C/AC catalyst was shown by Fe peaks at 707 eV ($Fe2p_{3/2}$) and 720 eV ($Fe2p_{1/2}$) on the surface of the treated activated carbon using x-ray photoelectron spectroscopy (XPS) (Figure 7-1A). Peak fitting indicated an Fe content of 1.5%, due to use of the 1,10-phenanthroline precursor to provide the nitrogen and carbon framework (Table 7-1, Figure 7-1A). No Fe peaks were observed on the AC surface treated with only Fe, indicating that use of only the $FeCl_3$ solution was unsuccessful in bonding the Fe to the carbon atoms within AC structure (Figure 7-1A). The nitrogen content, based on fitting the N1s peaks, was 0.6% for Fe-N-C/AC catalyst, compared to 0.7% for carbon prepared only with 1,10-phenanthroline (N-AC catalyst) (Table 7-1). As expected, the plain AC had very little nitrogen (0.01%, below the detection limit) (Figure 7-1B). These results show successful addition of both N and Fe into the carbon, with a very low amount of chemicals used (Figure 7-1).

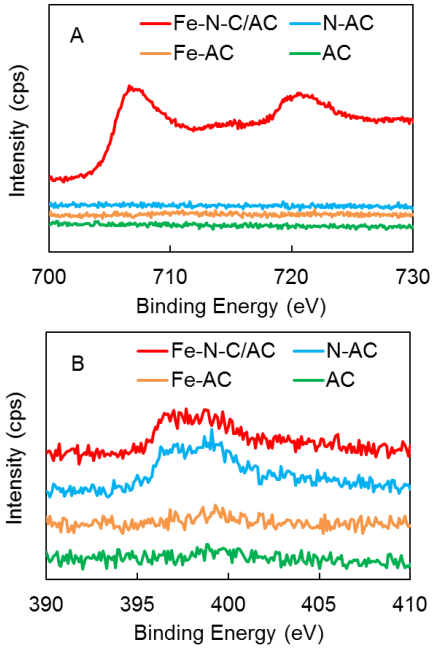

Figure 7-1. XPS spectra of AC, Fe-AC, N-AC and Fe-N-C/AC catalysts at (A) Fe2p peak, 700 ~ 730 eV, (B) N1s peak, 390 ~ 410 eV.

Table 7-1. Elemental compositions of AC, Fe-AC, N-AC and Fe-N-C/AC catalysts.

Catalyst	C [%]	O [%]	N [%]	Fe [%]
AC	94.52	5.47	0.01	–
Fe-AC	98.3	1.67	0.03	0
N-AC	96.8	2.4	0.7	–
Fe-N-AC	95.6	2.4	0.6	1.5

7.3.2 MFC tests with modified cathodes

The highest maximum power densities in MFC tests with the different cathodes were produced with the Fe-N-C/AC cathodes, with a maximum power density of 2.6 ± 0.05 W m^{-2} in 50 mM PBS.

This power density was 30% higher than that produced by the N-AC cathodes (2.0 ± 0.1 W m^{-2}) and 63% higher the Fe-AC or plain AC cathodes (1.6 ± 0.1 W m^{-2}) (Figure 7-2A). The electrode potentials also verified that the power differences mainly were mainly due to the different cathodes, as the anode potentials were similar for all tests (Figure 7-2B). The maximum power densities produced with the other two metals (2.0 ± 0.0 W m^{-2}, Co-N-C/AC; and 2.1 ± 0.1 W m^{-2}, Na-N-C/AC) was not significantly different from the N-only control, and therefore these were not further examined (Appendix D, Figure S7-1).

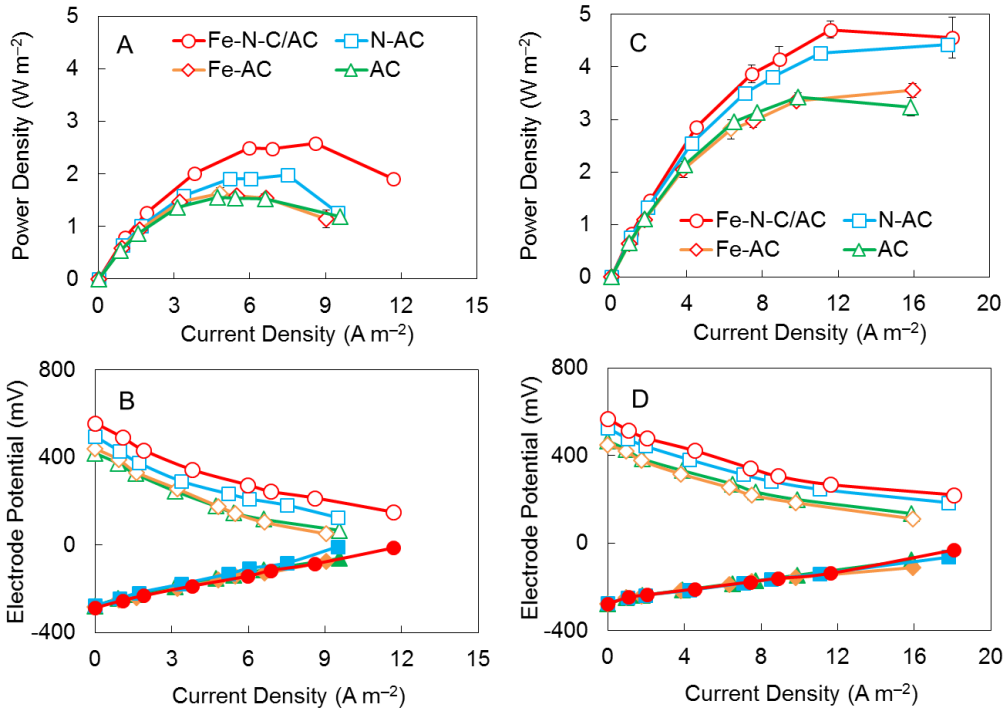

Figure 7-2. (A) Power density curves in 50 mM PBS for AC cathodes using AC, Fe-AC, N-AC and Fe-N-C/AC catalysts. (B) Electrode potentials in 50 mM PBS (solid symbols, anode potentials; open symbols, cathode potentials). (C) Power density curves in 200 mM PBS. (D) Electrode potentials in 200 mM PBS.

In tests using 200 mM PBS, all cathodes produced higher power densities, due to the reduced ohmic (solution) resistance. The MFCs with the Fe-N-C/AC cathodes produce 4.7 ± 0.2 W m^{-2}, higher than those obtained using Fe-AC or plain AC cathodes (3.4 ± 0.2 W $m^{-2)}$. (Figure 7-2C), which is higher than that achieved with any previous MFC using an air cathode. This maximum

power density of 4.7 W m^{-2} was much higher than any previous studies, including those conducted using a platinum catalysts *(29, 35)*. Although a power density of 6.9 W m^{-2} was reported with a Pt catalyst, this value was obtained by normalizing the power to the anode, which was much smaller than the cathode area *(36)*. If normalized to the cathode, the power density in that study would have been only 0.5 W m^{-2}. To confirm the improved performance of the Fe-N-C/AC cathodes, tests conducted using a platinum cathode here produced 3.2 ± 0.2 W m^{-2} (Appendix D, Figure S7-2). This is similar to untreated AC, and consistent with many previous studies showing similar power densities of plain AC compared to that using Pt in MFCs. Many studies have also used flat anodes, made of carbon cloth, felt or paper, compared to the high surface area brush anodes used here. However, the highest power density with a brush anode in this type of reactor (with 50 mM PBS) with a Pt catalyst, was previously reported to be only 1.6 W m^{-2} *(37)*.

7.3.3 Power production of MFCs fed domestic wastewater

Extracting electricity from domestic waste water is currently one of the most widely reported goals for using MFCs *(6, 38, 39)*. Therefore, tests were also conducted using the Fe-N-C/AC cathodes with domestic wastewater. A maximum power density of 0.8 ± 0.03 W m^{-2} was obtained with Fe-N-C/AC cathode, which was twice that produced using a Pt cathode (0.4 ± 0.03 W m^{-2}) (Figure 7-3A). At the maximum power point, the current density was 2.4 A m^{-2} for the MFC with the Fe-N-C/AC, compared to 1.8 A m^{-2} for Pt (Figure 7-3B).

The power density obtained here using domestic wastewater and the Fe-N-C/AC cathode was appreciably higher those previously reported using low-strength, domestic waste water from this same wastewater treatment plant, or other wastewaters. The low power produced using wastewater compared to acetate solutions, is due to a combination of its low conductivity (~ 1 mS cm^{-1}) and low concentration of organic matter (~ 500 mg L^{-1} of chemical oxygen demand). Thus, power

densities reported using domestic wastewater in MFCs have typically ranged from 0.3 to 0.5 W m^{-2} *(18)*. For example, 0.24 ± 0.02 W m^{-2} was reported using closely spaced electrodes (brush anode and AC cathode) in a smaller (14 mL) reactor with a design similar to that used here (28 mL), with domestic waste water from this same treatment plant *(40)*. A maximum power density of 0.33 ± 0.01 W m^{-2} was obtained using a larger, multi-brush anode reactor (130 mL) and a Pt/C cathode also with wastewater from this site *(38)*. which was comparable that obtained here using the Pt/C cathode (0.4 ± 0.03 W m^{-2}). The utilization of this modified AC cathode could therefore significantly increase the power density that can be harvested, enabling more effective production of electricity using wastewaters.

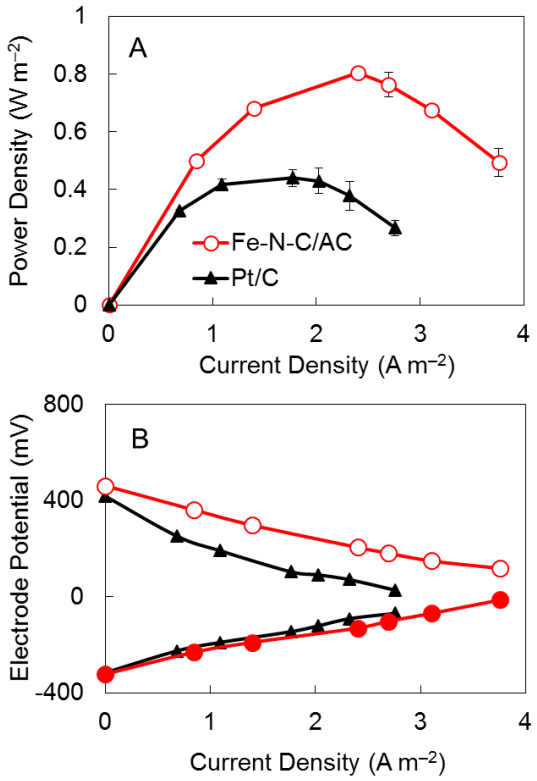

Figure 7-3. (A) Power density curves in domestic waste water for Fe-N-C/AC and Pt/C cathodes. (B) Electrode potentials (solid symbols, anode potentials; open symbols, cathode potentials).

7.3.4 Electrochemical tests of different catalysts

Cathodes using Fe-N-C/AC showed the best electrochemical performance compared to nitrogen doped AC (N-AC), iron doped AC (Fe-AC) or plain AC cathodes (50 mM PBS) in LSV tests over a wider range of potentials than those examined in MFCs (Figure 7-4A). For example, at 0 V vs. SHE, the Fe-N-C cathode had the highest current density of 21 A m^{-2}, followed by the N-AC cathode (14 A m^{-2}). Both Fe-AC and pure AC cathodes showed 25% lower current densities (10 A m^{-2}) at this potential than the Fe-N-C cathode. This showed that Fe treatment did not improve the ORR kinetics, consistent with the XPS results showing a lack of Fe addition to the carbon when used without the organic nitrogen precursor. At a more positive potential of 0.1 V (typical of that of an MFC cathode), Fe-N-C/AC cathode still exhibited a higher current density of 14 A m^{-2}, compared to 6 A m^{-2} for the Fe-AC and AC cathodes (Figure 7-4A).

Charge transfer resistance was found to be related to electron transfer for the ORR, with a lower charge transfer resistance indicating a more catalytic active catalyst. Based on the impedance spectra, the Fe-N-C/AC cathode exhibited the lowest charge transfer resistance (size of the semicircle in the Nyquist plots) of 0.5 Ω, which was 80% lower than that of the unmodified AC cathode (2.5 Ω), which could lead to improved ORR rates (Figure 7-4B). The Fe-AC cathode showed essentially no change in the impedance spectra compared to AC cathode, consistent with XPS results showing a lack of Fe with this Fe-only treatment. The N-AC cathode also showed a decreased charge transfer resistance of 1 Ω, but was still 50% higher than Fe-N-C/AC catalyst (Figure 7-4B).

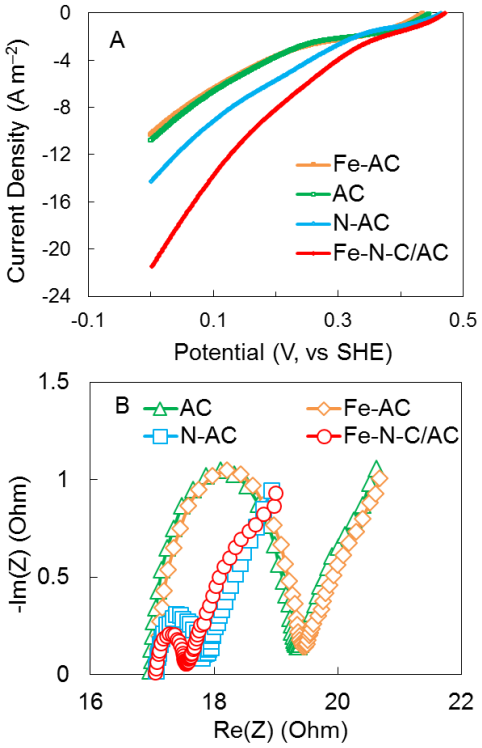

Figure 7-4. (A) LSV curves for the AC cathodes using AC, Fe-AC, N-AC and Fe-N-C/AC catalysts in an electrochemical cell (B) EIS spectra for the AC cathodes using AC, Fe-AC, N-AC and Fe-N-C/AC catalysts.

7.3.5 Oxygen reduction reaction characterization

The ORR activities of Fe-N-C/AC and other doped AC catalysts were characterized using a rotating disk electrode, so that kinetic reaction rates could be obtained under minimal mass transfer limited conditions (Figure 7-5A; Appendix D, Figure S7-2). The Fe-N-C/AC catalyst produced the highest current densities over the potential range from 0.4 V to –0.8 V, followed by the N-AC electrode (Figure 7-5B). The Fe-AC and non-modified AC showed similar current densities, indicating no enhancement of current due to the sole addition of Fe (Figure 7-5B). The diffusion limiting current of 0.24 mA at 2100 rpm for Fe-N-C/AC catalyst was higher than 0.21 mA for N-AC catalyst, also indicating a better ORR capability for the Fe-N-C/AC electrode than the other

electrodes (Figure 7-5B). The onset potential, where oxygen reduction reaction started to occur, was 0.44 V for Fe-N-C/AC cathode, compared to 0.39 V for the N-AC (Table 7-2).

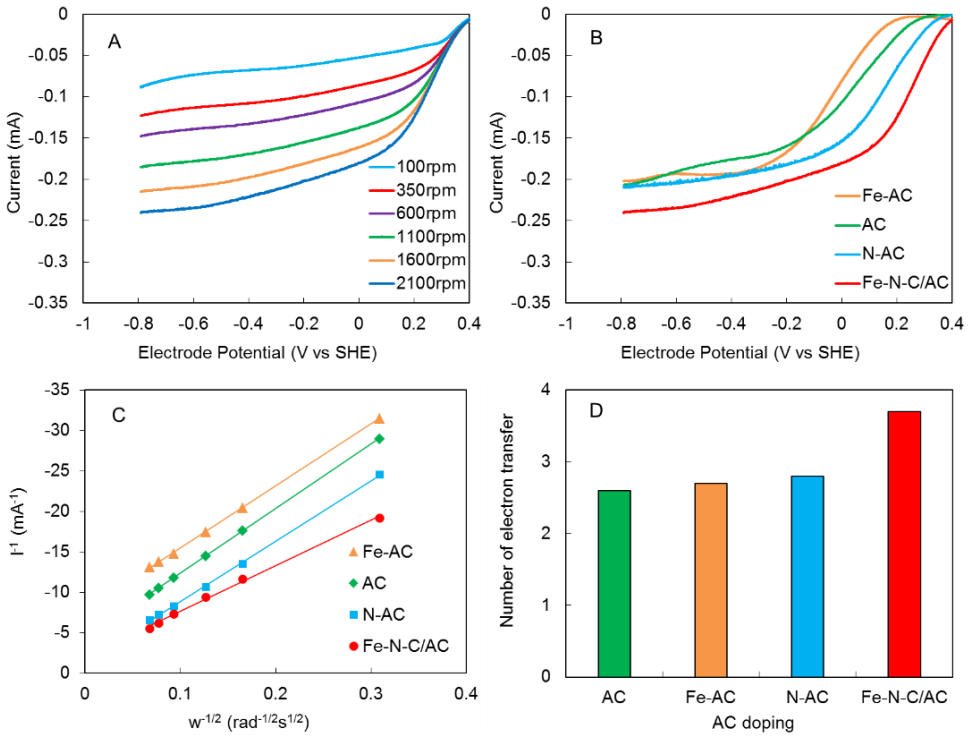

Figure 7-5. (A) LSV curves for Fe-N-C/AC catalyst in 50 mM PBS at different rotation speed. (B) LSV curves for AC, Fe-AC, N-AC and Fe-N-C/AC catalysts in 50 mM PBS at 2100 rpm. (C) K-L plots of different catalysts at 0 V vs. SHE. (D) Number of electron transfer for different catalysts at 0 V vs. SHE.

Data were fit to the Koutecky-Levich equation fitting to evaluate the reaction pathway for the ORR with the different electrodes at a potential of 0 V (Figure 7-5C). Fe-AC and AC showed a similar electron transfer numbers of 2.6 and 2.7 (Figure 7-5D), indicating a predominantly two-electron pathway *(9)*. Although the N-AC had shown a higher current production than AC and Fe-AC electrodes in MFC and LSV tests, the number of electrons transferred was quite similar at 2.8 (Figure 7-5D). A four electron pathway was not obtained using a nitrogen doped AC cathode, in contrast to previous reports *(22, 23)*, likely due to a lower amount of N loading (0.7%) on the AC here than in previous studies (Table 7-1). However, the number of electrons transferred for the Fe-N-C/AC was 3.7, supporting a quasi-four-electron reaction pathway (Figure 7-5D). Therefore,

immobilizing both the Fe and N achieved a more catalytically active surface than that due to N or Fe alone. The Fe-N-C loaded AC catalyst was also the most efficient in current generation with a mass current density of 1.97 mA mg^{-1}, and 0.92 mA cm^{-2} based on the projected area (Table 7-2). This was 19% higher than that of the N-AC catalyst (1.65 mA mg^{-1}, 0.77 mA cm^{-2}) and 74% higher than plain AC (1.13 mA mg^{-1}, 0.53 mA cm^{-2}).

Table 7-2. Summary of electrochemical results for AC and modified AC catalysts.

Catalyst	E_{onset} [V]	E_{half} [V]	I_s [mA cm^{-2}]	I_m [mA mg^{-1}]	n
AC	0.33	0.06	0.53	1.13	2.6
Fe-AC	0.24	-0.02	0.39	0.83	2.7
N-AC	0.39	0.16	0.77	1.65	2.8
Fe-N-C/AC	0.44	0.26	0.92	1.97	3.7

(E_{onset}, E_{half}, Is, I_m and n denote onset potential, half-wave potential, specific current, mass current density and electron transfer number. I_s, I_m and n correspond to values determined at 0 V and 2100 rpm.)

7.4 Conclusions

An iron-based, metal organic framework catalyst was successfully immobilized onto AC, as demonstrated by clear peaks for both Fe and N in the XPS spectra of the Fe-N-C/AC catalyst. The modified AC altered the ORR reaction from the original two-electron pathway to a nearly four-electron pathway (electron-transfer number of 3.7). A maximum power density of 4.7 ± 0.2 W m^{-2} was produced in MFCs using this cathode catalyst in 200 mM PBS, compared to 3.4 ± 0.2 W m^{-2} for the unmodified AC cathodes. The addition of the Fe-N-C onto AC also improved the maximum power density obtained with domestic wastewater to 0.8 ± 0.03 W m^{-2}, which was double that obtained using a typical Pt/C cathode. Catalyst preparation using only a $FeCl_3$ solution failed to retain Fe onto the activated carbon, and the relatively small amount of N-precursor resulted in only moderate improvement in the catalyst performance compared to AC alone. The use of this Fe-

N-C immobilized activated carbon as cathode catalyst can therefore substantially improve power production, and its used could enable practical applications of MFCs for wastewater treatment.

7.5 Acknowledgments

This research was supported by the Strategic Environmental Research and Development Program (SERDP) and a graduate scholarship from the China Scholarship Council (CSC) to W. Y.

7.6 Literature cited

1. Logan, B. E., *Microbial fuel cells*. John Wiley & Sons, Inc.: Hoboken, NJ, 2008; p 300.
2. Niessen, J.; Schröder, U.; Scholz, F., Exploiting complex carbohydrates for microbial electricity generation- a bacterial fuel cell operating on starch. *Electrochem. Commun.* **2004,** *6*, 955-958.
3. Allen, R. M.; Bennetto, H. P., Microbial fuel-cells - electricity production from carbohydrates. *Appl. Biochem. Biotechnol.* **1993,** *39*, 27-40.
4. Bond, D. R.; Holmes, D. E.; Tender, L. M.; Lovley, D. R., Electrode-reducing microorganisms that harvest energy from marine sediments. *Science* **2002,** *295*, 483-485.
5. Lovley, D. R., Bug juice: harvesting electricity with microorganisms. *Nat. Rev. Microbiol.* **2006,** *4*, 497-508.
6. Kim, K.-Y.; Yang, W.; Logan, B. E., Impact of electrode configurations on retention time and domestic wastewater treatment efficiency using microbial fuel cells. *Water Res.* **2015,** *80*, 41-46.
7. You, S.; Gong, X.; Wang, W.; Qi, D.; Wang, X.; Chen, X.; Ren, N., Enhanced cathodic oxygen reduction and power production of microbial fuel cell based on noble-metal-free electrocatalyst derived from metal-organic frameworks. *Adv. Energy Mater.* **2016,** *6*.
8. Yang, W.; Zhang, F.; He, W.; Liu, J.; Hickner, M. A.; Logan, B. E., Poly (vinylidene fluoride-co-hexafluoropropylene) phase inversion coating as a diffusion layer to enhance the cathode performance in microbial fuel cells. *J. Power Sources* **2014,** *269*, 379-384.
9. Watson, V. J.; Nieto Delgado, C.; Logan, B. E., Influence of chemical and physical properties of activated carbon powders on oxygen reduction and microbial fuel cell performance. *Environ. Sci. Technol.* **2013,** *47*, 6704-6710.

10. Zitolo, A.; Goellner, V.; Armel, V.; Sougrati, M.-T.; Mineva, T.; Stievano, L.; Fonda, E.; Jaouen, F., Identification of catalytic sites for oxygen reduction in iron-and nitrogen-doped graphene materials. *Nat. Mater.* **2015,** *14*, 937-942.
11. Gong, K.; Du, F.; Xia, Z.; Durstock, M.; Dai, L., Nitrogen-doped carbon nanotube arrays with high electrocatalytic activity for oxygen reduction. *Science* **2009,** *323*, 760-764.
12. Lin, Z.; Waller, G.; Liu, Y.; Liu, M.; Wong, C. P., Facile synthesis of nitrogen-doped graphene via pyrolysis of graphene oxide and urea, and its electrocatalytic activity toward the oxygen-reduction reaction. *Adv. Energy Mater.* **2012,** *2*, 884-888.
13. Zhang, F.; Saito, T.; Cheng, S.; Hickner, M. A.; Logan, B. E., Microbial Fuel Cell Cathodes With Poly(dimethylsiloxane) Diffusion Layers Constructed around Stainless Steel Mesh Current Collectors. *Environ. Sci. Technol.* **2010,** *44*, 1490-1495.
14. Dong, H.; Yu, H.; Wang, X.; Zhou, Q.; Feng, J., A novel structure of scalable air-cathode without Nafion and Pt by rolling activated carbon and PTFE as catalyst layer in microbial fuel cells. *Water Res.* **2012,** *46*, 5777-87.
15. Yang, W.; He, W.; Zhang, F.; Hickner, M. A.; Logan, B. E., Single step fabrication using a phase inversion method of poly (vinylidene fluoride)(PVDF) activated carbon air cathodes for microbial fuel cells. *Environ. Sci. Technol. Lett.* **2014,** *1*, 416-420.
16. Savizi, I. S. P.; Janik, M. J., Acetate and phosphate anion adsorption linear sweep voltammograms simulated using density functional theory. *Electrochim Acta* **2011,** *56*, 3996-4006.
17. Janicek, A.; Fan, Y.; Liu, H., Performance and stability of different cathode base materials for use in microbial fuel cells. *J. Power Sources* **2015,** *280*, 159-165.
18. Logan, B. E.; Wallack, M. J.; Kim, K.-Y.; He, W.; Feng, Y.; Saikaly, P. E., Assessment of microbial fuel cell configurations and power densities. *Environ. Sci. Technol. Lett.* **2015,** *2*, 206-214.

19. Dong, H.; Yu, H.; Wang, X., Catalysis kinetics and porous analysis of rolling activated carbon-PTFE air-cathode in microbial fuel cells. *Environ. Sci. Technol.* **2012,** *46*, 13009-13015.
20. Serp, P.; Figueiredo, J. L., *Carbon materials for catalysis*. John Wiley & Sons: 2009.
21. Guo, D.; Shibuya, R.; Akiba, C.; Saji, S.; Kondo, T.; Nakamura, J., Active sites of nitrogen-doped carbon materials for oxygen reduction reaction clarified using model catalysts. *Science* **2016,** *351*, 361-365.
22. Zhang, B.; Wen, Z.; Ci, S.; Mao, S.; Chen, J.; He, Z., Synthesizing nitrogen-doped activated carbon and probing its active sites for oxygen reduction reaction in microbial fuel cells. *ACS Appl. Mater. Interfaces* **2014,** *6*, 7464-7470.
23. Watson, V. J.; Nieto Delgado, C.; Logan, B. E., Improvement of activated carbons as oxygen reduction catalysts in neutral solutions by ammonia gas treatment and their performance in microbial fuel cells. *J. Power Sources* **2013,** *242*, 756-761.
24. Bezerra, C. W.; Zhang, L.; Lee, K.; Liu, H.; Marques, A. L.; Marques, E. P.; Wang, H.; Zhang, J., A review of Fe–N/C and Co–N/C catalysts for the oxygen reduction reaction. *Electrochim Acta* **2008,** *53*, 4937-4951.
25. Alt, H.; Binder, H.; Sandstede, G., Mechanism of the electrocatalytic reduction of oxygen on metal chelates. *J. Catal.* **1973,** *28*, 8-19.
26. Nguyen, M.-T.; Mecheri, B.; Iannaci, A.; D'Epifanio, A.; Licoccia, S., Iron/Polyindole-based Electrocatalysts to Enhance Oxygen Reduction in Microbial Fuel Cells. *Electrochim. Acta.* **2016,** *190*, 388-395.
27. Santoro, C.; Serov, A.; Narvaez Villarrubia, C. W.; Stariha, S.; Babanova, S.; Schuler, A. J.; Artyushkova, K.; Atanassov, P., Double-chamber microbial fuel cell with a non-platinum-group metal Fe-N-C cathode catalyst. *ChemSusChem* **2015,** *8*, 828-834.

28. Pan, Y.; Mo, X.; Li, K.; Pu, L.; Liu, D.; Yang, T., Iron–nitrogen–activated carbon as cathode catalyst to improve the power generation of single-chamber air-cathode microbial fuel cells. *Bioresour. Technol.* **2016**.

29. Cheng, S.; Liu, H.; Logan, B. E., Increased performance of single-chamber microbial fuel cells using an improved cathode structure. *Electrochem. Commun.* **2006,** *8*, 489-494.

30. Logan, B. E.; Cheng, S.; Watson, V.; Estadt, G., Graphite fiber brush anodes for increased power production in air-cathode microbial fuel cells. *Environ. Sci. Technol.* **2007,** *41*, 3341-3346.

31. Cheng, S.; Xing, D.; Call, D. F.; Logan, B. E., Direct biological conversion of electrical current into methane by electromethanogenesis. *Environ. Sci. Technol.* **2009,** *43*, 3953-3958.

32. Yang, W.; Kim, K.-Y.; Logan, B. E., Development of carbon free diffusion layer for activated carbon air cathode of microbial fuel cells. *Bioresour. Technol.* **2015,** *197*, 318-322.

33. Gojkovic, S. L.; Gupta, S.; Savinell, R. F., Heat-treated iron(III) tetramethoxyphenyl porphyrin supported on high-area carbon as an electrocatalyst for oxygen reduction - I. Characterization of the electrocatalyst. *J. Electrochem. Soc.* **1998,** *145*, 3493-3499.

34. Chen, Y.; Lv, Z.; Xu, J.; Peng, D.; Liu, Y.; Chen, J.; Sun, X.; Feng, C.; Wei, C., Stainless steel mesh coated with MnO 2/carbon nanotube and polymethylphenyl siloxane as low-cost and high-performance microbial fuel cell cathode materials. *J. Power Sources* **2012,** *201*, 136-141.

35. Cheng, S.; Liu, H.; Logan, B. E., Power densities using different cathode catalysts (Pt and CoTMPP) and polymer binders (Nafion and PTFE) in single chamber microbial fuel cells. *Environ. Sci. Technol.* **2006,** *40*, 364-369.

36. Fan, Y.; Sharbrough, E.; Liu, H., Quantification of the internal resistance distribution of microbial fuel cells. *Environ. Sci. Technol.* **2008,** *42*, 8101-8107.

37. Xia, X.; Zhang, F.; Zhang, X.; Liang, P.; Huang, X.; Logan, B. E., Use of Pyrolyzed Iron Ethylenediaminetetraacetic Acid Modified Activated Carbon as Air–Cathode Catalyst in Microbial Fuel Cells. *ACS Appl. Mater. Interfaces* **2013,** *5*, 7862-7866.

38. Ren, L.; Ahn, Y.; Logan, B. E., A two-stage microbial fuel cell and anaerobic fluidized bed membrane bioreactor (MFC-AFMBR) system for effective domestic wastewater treatment. *Environ. Sci. Technol.* **2014,** *48*, 4199-4206.

39. Logan, B. E.; Elimelech, M., Membrane-based processes for sustainable power generation using water and wastewater *Nature* **2012,** *288*, 313-319.

40. Hays, S.; Zhang, F.; Logan, B. E., Performance of two different types of anodes in membrane electrode assembly microbial fuel cells for power generation from domestic wastewater. *J. Power Sources* **2011,** *196*, 8293-8300.

Chapter 8

Substantial Humic Acid Adsorption to Activated Carbon Air Cathode Produces a Small Reduction in Catalytic Activity

Abstract

Long-term operation of microbial fuel cells (MFCs) can result in substantial degradation of activated carbon air-cathode performance. In order to examine a possible role in fouling from natural organic matter in water, cathodes were exposed to high concentrations of humic acids. Cathodes treated with 100 mg L^{-1} of humic acids did not exhibit any significant change in performance. Exposure to 1000 mg L^{-1} of humic acids, which increased the mass of the cathodes by ~5% (14 ± 2 mg of organic matter per cathode), decreased the maximum power density of the MFCs by 14% (from 1310 ± 30 mW m^{-2} to 1130 ± 30 mW m^{-2}). Total cathode resistance increased by 30% (from 57 Ω to 74 Ω) for cathodes treated with 1000 mg L^{-1} of humic acids, primarily due to an increase in the diffusion resistance (from 32 Ω to 50 Ω), based on resistance components measured using electrochemical impendance spectroscopy. The adsorption of the humic acids decreased the total surface area by 12% (from 520 m^2 g^{-1} to 460 m^2 g^{-1}), suggesting that the main impact of the adsorption of organic matter was due to pore blockage. Minimization of external mass transfer resistances using a rotating disk electrode reduced the impact of organic matter adsorption to only a 5% reduction in current, indicating about half the impact of the humics was associated with external mass transfer resistance and the remainder was due to internal resistances. Rinsing the cathodes with deionized water did not restore cathode performance. These results demonstrated that humic acids could contribute to cathode fouling, but the extent of power reduction was relatively small in comparison to large mass of humics adsorbed. Other factors, such as microbially

produced biopolymers, or precipitation of inorganic chemicals in the water, are therefore likely more important contributors to long term fouling of MFC cathodes.

8.1 Introduction

Microbial fuel cells (MFCs) can harvest energy during wastewater treatment by extracting electricity from organics using exoelectrogenic bacteria *(1-5)*. Electrons are released by the exoelectrogenic bacteria via oxidation of organics and transferred through an external circuit to the cathode, where oxygen reduction typically takes place. Air cathodes are used in MFCs to reduce energy for treatment by avoiding the need for aerating water *(6-8)*. Activated carbon (AC) is an effective oxygen reduction reaction (ORR) catalyst for air cathodes in MFCs due to its high catalytic activity and low cost ($1.4 kg^{-1}) *(9-11)*. However, operation of MFCs with AC cathodes has shown decreased power generation over time *(12, 13)*. A 40% drop in power was observed after one year of MFC operation using acetate in a phosphate buffer solution *(12)*. Cleaning the cathodes by physically removing the biofilm restored only 12% of the performance, compared to a complete recovery to the initial power performance by using a new cathode, indicating cathode fouling and not the anode was the main reason for decreased power *(12)*. The cathode biofilm has been indicated to be a major cause of cathode fouling due to hindered proton diffusion *(14, 15)*. However, AC cathode performance cannot be completely restored by removing the biofilm as described *(12)*, indicating internal fouling behavior of AC cathode.

The cost of the cathode materials is about half that of all of the MFC materials *(16)* and therefore a long lifetime of the cathodes is critical for economical applications of MFCs. In order to maintain the cathode performance over time, it is essential to understand internal fouling mechanisms. AC is routinely used to adsorb organics in water and wastewater treatment systems due to its large internal surface area, which ranges from 800 to 1500 m^2 g^{-1} *(17)*. Previous studies

have shown that AC is a strong adsorbent for organic matter in water such as humic acid (HA) *(18, 19)*. Humic acids are the major components of natural organic matter (NOM) in aquatic systems and at high concentrations they have been used as mediators in various bio-electrochemical systems (BES) *(20-22)*. Enhanced current generation was observed in the presence of humic acids and bacteria *(21)*. indicating enhanced charge transfer by adding HA. Studies have also indicated improved MFC performance using cathodes doped with the mediator 9,10-anthraquinone-2-sulfonic acid (AQS), which is an analog to HA in terms of electron shuttling *(23)*. The cathodic oxygen reduction reaction is a three phase reaction that involves both a solid AC phase and a solution phase *(24)*. which provides potential sites for organic adsorption within the AC catalyst. The adsorbed organic molecules could potentially increase the diffusion resistance and thus impair cathode performance. It is therefore unclear whether the addition of HAs would improve MFC performance due to the mediator effect of adsorbed HAs, or whether such adsorption might block catalyst sites and hinder cathode performance over time.

To identify the effect of HA adsorption on AC cathode performance, two different concentrations of HA were loaded onto AC. The catalytic performance of the AC in cathodes was then compared to controls lacking HAs in both electrochemical and MFC tests. Changes in carbon properties were also evaluated in terms of total surface area, pore volume, and cathode mass.

8.2 Materials and methods

8.2.1 Cathode Fabrication and Operation

Activated carbon cathodes with AC loading of 26.5 mg cm^{-2} were fabricated using a phase inversion method as previously described *(11)*. Briefly, AC powder (Norit SX plus, Norit Americas Inc.) was mixed with 10% Poly(vinylidene fluoride) solution (Mw ~534,000, Sigma Aldrich) and

carbon black (Vulcan XC-72, Cabot Corporation, USA) at the mass ratio of 3:1:0.3. The mixture was then spread onto an 11.3 cm^2 circular section of stainless steel mesh (50 × 50, type 304, McMaster-Carr, USA) with a spatula. The cathodes were immersed into a distilled water bath for 15 min to induce phase inversion at room temperature. Cathodes were then air dried in a fume hood for over 6 h prior to tests.

Single-chamber, cubic MFCs used for all MFC tests were constructed from a Lexan block 4 cm in length, with an inside chamber diameter of 3 cm *(25)*. The anodes were graphite fiber brushes (2.5 cm in both diameter and length) that were heat treated at 450 °C in air for 30 min, and placed horizontally in the middle of MFC chambers *(25)*. Anodes were fully pre-acclimated by MFC operation at a constant temperature (30 °C) and fixed external resistance (1000 Ω). The medium contained 1 g L^{-1} sodium acetate dissolved in 50 mM phosphate buffer solution (PBS) (Na_2HPO_4, 4.58 g L^{-1}; $NaH_2PO_4 \cdot H_2O$, 2.45 g L^{-1}; NH_4Cl, 0.31 g L^{-1}; KCl, 0.31 g L^{-1}; pH = 6.9; κ = 6.94 mS cm^{-1}) amended with 12.5 mL L^{-1} minerals and 5 mL L^{-1} vitamins *(26)*.

Single cycle polarization tests using AC cathodes were conducted in the cubic, single-chamber MFCs by varying the external resistance from 1000 Ω to 20 Ω at 20 min intervals *(24)*. The voltage drop (U) across an external resistor was recorded by a computer based data acquisition system (2700, Keithley Instrument, OH). Current densities (i) and power densities (P) were normalized to the exposed projected cathode area (A = 7 cm^2), and calculated as $i = U/RA$ and $P = iU/A$, where R is the external resistance.

8.2.2 Humic Acid Adsorption

HA solutions with 100 and 1000 mg L^{-1} were prepared by dissolving a commercial humic acid sodium salt (Sigma Aldrich, USA) in deionized (DI) water. The solutions were then filtered

through 1.2 and 0.22 μm membrane filters (Polyvinylidenedifluoride, PVDF, 47 mm diameter, Millipore, USA) to remove any solids, and stored at 4 °C prior to tests.

HA adsorption onto the carbon was examined by dispersing 1 g of AC powder into 100 mL containing 0, 100 and 1000 mg L^{-1} HA solutions in sealed flasks, with continuous stirring for 24 h at 30°C. The AC/HA slurries were then filtered through a 1.2 μm PVDF membrane and the filtered solutions were collected for analysis. The AC powders were further dried in a vacumm oven at 100 °C for 24 h. HA was adsorbed onto the cathodes by filtering solutions containing 0, 100, and 1000 mg L^{-1} of humic acids directly through the AC cathodes to shorten the time of HA adsorption into AC cathodes. Prior to the filtration process, AC cathodes were sequentially wetted by ethanol and DI water each for 10 min. HA solutions (30 mL) were then pressure filtrated through the cathodes and filtrated HA solutions were collected for analysis. The cathodes were dried in the fume hood for 12 h prior to testing.

The extent of humic acid desorption from the AC was examined by filtering 30 mL of DI water through AC cathodes following previous procedures, and collecting the effluent for further analysis.

8.2.3 Electrochemical Characterization

A rotating disk electrode (RDE) was used to examine the catalytic activity of the AC in the absence of appreciable external mass transfer limitations. An AC catalyst ink was prepared by adding 30 mg of powdered AC into 3 mL of dimethylformamide with sonification (Model 450, Branson, USA) pulsed at 20% for 8 min in an ice bath. Nafion (5 wt %, 270 μL) was then added into the solution and mixed for another 8 min. A drop of 10 μL ink solution was coated onto a glassy carbon disk (Pine Instruments, USA) 5 mm in diameter, and dried overnight as previously described *(27)*. All RDE tests were conducted in 50 mM PBS sparged with nitrogen and then air.

Solutions were sparged with a gas for 30 min before conducting linear sweep voltammetry (LSV) tests and the gas was constantly streamed into the headspace during LSV runs. The potential of the disk electrode was scanned from 0.2 V to –1 V (vs. Ag/AgCl) at 10 mV s^{-1}, at rotation rates of 100 rpm to 2100 rpm. The current generated under nitrogen sparging was subtracted from that obtained under air sparging to evaluate current generation due only to oxygen reduction *(28)*.

The electrochemical performance of AC cathodes were evaluated by LSV in an electrochemical cell (2 cm length, 3 cm diameter) containing two chambers separated by an anion exchange membrane (AEM; AMI-7001, Membrane International Inc., USA). The electrolyte was 50 mM PBS prepared as described above. The counter electrode was a 7 cm^2 round platinum plate. An Ag/AgCl reference electrode (RE-5B, BASi, West Lafayette, IN; + 0.209 V vs a standard hydrogen electrode) was placed close to cathode and kept in the same position for all tests. All potentials reported here were corrected to that of a standard hydrogen electrode (SHE). A potentiostat (VMP3 Multichannel Workstation, Biologic Science Instruments, USA) was used for all measurements in a constant temperature room (30 °C). The potentials on the cathodes were scanned from + 0.509 V to – 0.209 V versus SHE for 7 times to reach steady state.

Impedance measurements of AC cathodes were conducted at 0.1 V vs SHE over a frequency range of 100 kHz to 2 mHz with a sinusoidal perturbation of 14.2 mV amplitude. The spectra were then fitted into an equavalent circuit (Appendix E, Figure S8-1) to identify the solution resistance (R_s), charge transfer resistnace (R_{ct}) and diffusion resistance (R_d).

8.2.4 Physical and Chemical Analysis

The concentrations of HA solutions were determined by a total organic carbon (TOC) analyzer (TOC-V CSN, Shimadzu, Japan) with a carrier gas pressure of 200 kPa and gas flow rate of 130 mL/min.

The incremetnal surface area and pore volume distribution of ACs were determined from nitrogen adsorption isotherms (at 77.3 K) by progressively increasing relative pressures of 5×10^{-6} to 0.99 atm atm^{-1} (ASAP 2420, Micromeritics Instrument Corp., GA). All samples were degassed at 100 °C for 16 h prior to measurements. The Brunauer-Emmet-Teller (BET) specific surface area was evaluated using adsorption data in a relative pressure range between 5×10^{-6} to 0.2 atm atm^{-1}. Pore size distribution data was collected in the relative pressure range of 5×10^{-6} to 0.99 atm atm^{-1} and calculated on the basis of the desorption branches using density functional theory (DFT) modeling software. Three pore sizes of micropores (< 2 nm), mesopores (2 ~ 50 nm) and macropores (> 50 nm) were reported here based on the International Union of Pure and Applied Chemistry (IUPAC) definitions *(29)*.

8.3 Results and discussion

8.3.1 HA Adsorption

Treatment of the cathodes with HA solution resulted in substantial and measurable adsorption of organic matter onto the activated carbon. Analysis of the HA concentrations on the basis of TOC before and after cathode treatment indicated 14.2 mg-C had been adsorbed with 1000 mg L^{-1} HA solution. Only 1.4 ± 0.1 mg-C were adsorbed onto the cathode with 100 mg L^{-1} HA solution (Appendix E, Table S8-1). In batch adsorption tests, the surface area and pore volume of ACs decreased inversely with the HA concentrations. The total BET surface area for AC in 0 mg L^{-1} HA was 520 m^2 g^{-1} and decreased to 460 m^2 g^{-1} for AC in 1000 mg L^{-1} HA, which is a 12% decrease and among which the micropore surface area has decreased most from 430 to 380 m^2 g^{-1} for AC in 1000 mg L^{-1} HA (Figure 8-1A). The AC in 100 mg L^{-1} HA had a BET surface area of 490 m^2 g^{-1} and only showed a 6% decrease (Figure 8-1A), suggesting much less surface coverage at the lower

HA concentration. The pore volume of ACs also decreased from 0.49 $cm^3\ g^{-1}$ at 0 mg L^{-1} to 0.47 $cm^3\ g^{-1}$ at 100 mg L^{-1} and 0.45 $cm^3\ g^{-1}$ at 1000 mg L^{-1} (Figure 8-1B). Studies have indicated that the inner pore surface of AC is critical for catalyzing ORR *(27, 30)* and therefore, the the extent of this decrease in surface area and pore volume could potentially block the reactive surface area, and lower ORR activity.

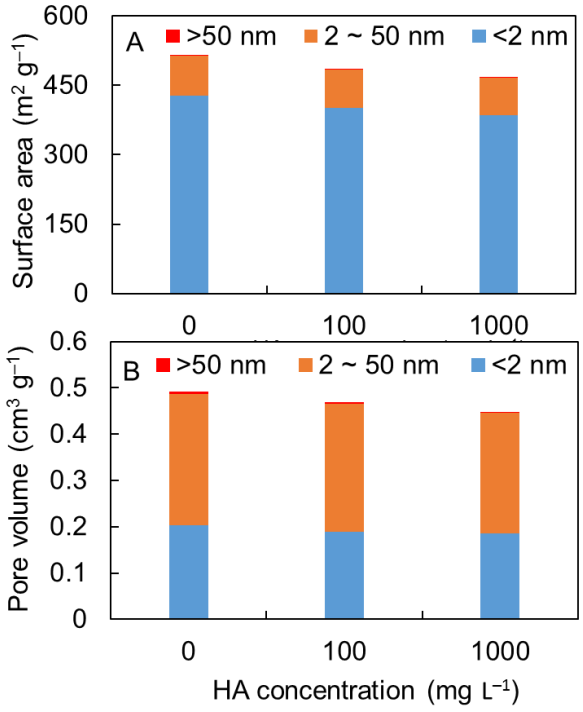

Figure 8-1. (A) Surface area of AC adsorbed in 0, 100 and 1000 mg L^{-1} HA solutions at pore sizes of < 2 nm, 2 ~ 50 nm and > 50 nm. (B) Pore volume of AC adsorbed in 0, 100 and 1000 mg L^{-1} HA solutions at pore sizes of < 2 nm, 2 ~ 50 nm and > 50 nm.

8.3.2 Cathode Performance in Electrochemical and MFC tests

Analysis of the cathodes using linear sweep voltammetry showed little change in performance between the cathode treated with the 100 mg/L HA solution compared to the control. However, the cathode treated with the 1000 mg/L HA solution showed appreciably reduced cathode performance. For example, an oxygen reduction potential of 0.09 V was obtained with the 1000 mg L^{-1} HA

treated AC cathode, compared to a higher voltage of 0.14 V for AC cathodes treated with 0 and 100 mg L^{-1} HA solutions at the current density of 5 A m^{-2} (Figure 8-2). These are potentials that are typically measured in these types of MFCs at their maximum power density *(24)*. The maximum current density of the AC cathode treated with 1000 mg L^{-1} HA solution only reached 8 A m^{-2} compared to 11 A m^{-2} for the control (0 mg L^{-1} HA) (Figure 8-2), which is a 27% decrease. However, no significant change in current density was observed for this AC cathode at the lower HA concentration over the potential window of 0.5 to 0 V vs. SHE (Figure 8-2). This shows that some HA adsorption onto the AC does not impair cathode performance.

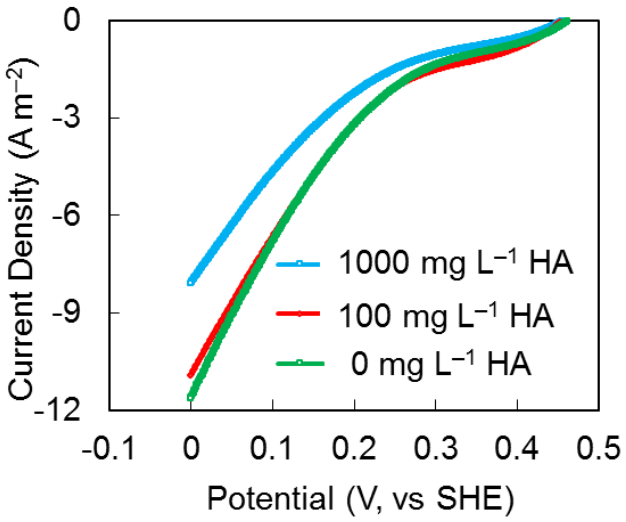

Figure 8-2. Current-voltage (polarization) curves for the AC cathodes treated with 0, 100 and 1000 mg L^{-1} HA solutions in an abiotic electrochemical cell.

Reduced AC cathode performance was observed in MFC tests for the high HA concentration solutions. MFCs with AC cathodes treated by 1000 mg L^{-1} HA produced a maximum power density of 1130 ± 30 mW m^{-2}, which was 14% lower than that obtained with the control (1310 ± 30 mW m^{-2}, 0 mg L^{-1} HA) (Figure 8-3A). AC cathodes treated with the lower HA concentration of 100 mg L^{-1} HA had a maximum power density of 1360 ± 10 mW m^{-2}, similar to that of the control (1310 ± 30 mW m^{-2}) (Figure 8-3A). These MFC results at both HA concentrations were consistent

with the LSV results (Figure 8-2), and indicated that only a very high amount of HA adsorbed onto the carbon would reduce the cathode performance.

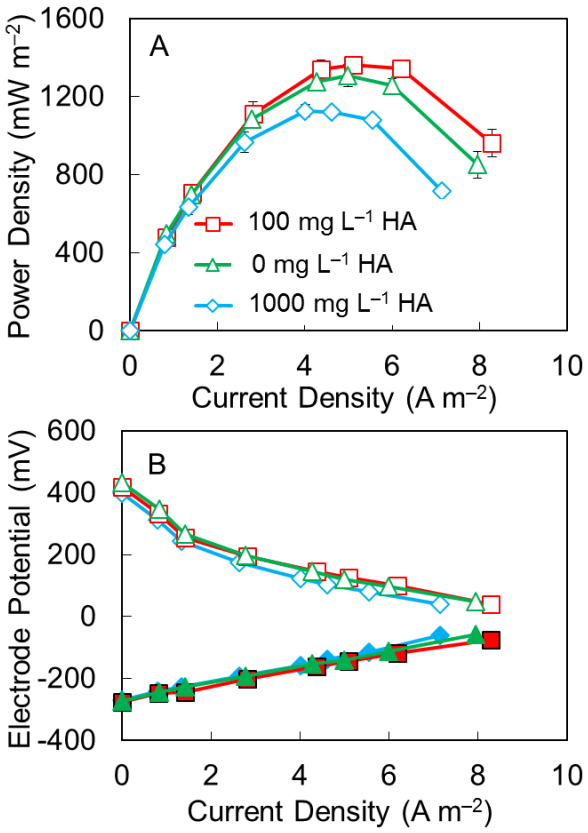

Figure 8-3. (A) Power density curves for AC cathodes treated with 0, 100 and 1000 mg L^{-1} HA solutions. (B) Electrode potentials (solid symbols, anode potentials; open symbols, cathode potentials).

8.3.3 Impact of HA adsorption on the Oxygen Reduction Reaction

The ORR activities of AC treated with and without HAs were characterized using rotating disk electrode technique, so that kinetic reaction rates could be obtained under minimal mass transfer limited conditions. The changes in ORR generally showed the same trend in results as the LSV and MFC tests, although the reaction rate was inhibited to a lesser extent after adsorption at 1000 mg L^{-1} HA (Figure 8-4). Mass transfer resistances were greatly minmized with oxygen gas sparging

by using a rotation rate of 2100 rpm, (Figure 8-4; Appendix E, Figure S8-2). AC treated with 1000 mg L^{-1} HA showed a 5% decrease in the kinetic limiting current of 0.19 mA, compared to control lacking HA exposure (0.20 mA) at a potential of –1 V vs. Ag/AgCl (Figure 8-4B). Current production was not appreciably changed for the catalyst exposed to the lower HA concentrations (Figure 8-4B). No redox peaks were observed with exposure to either HA concentration in LSV scans (Figure S8-3), showing that HA adsorption did not function as a mediator and only acted to block catalytic sites at high concentrations.

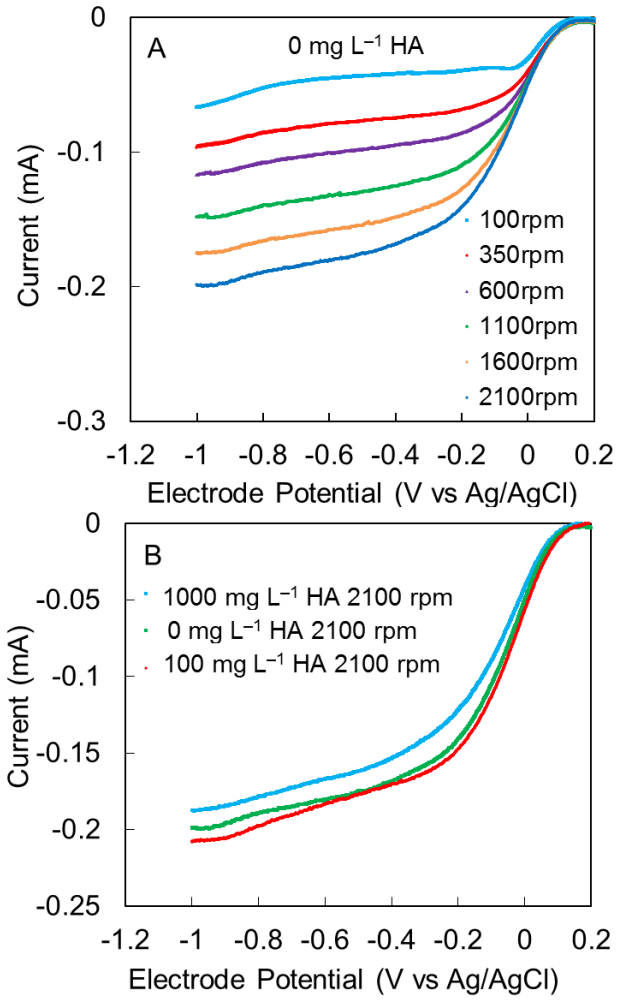

Figure 8-4. (A) Current-potential curves at different rotation rates for AC adsorbed with 0 mg L^{-1} HA solutions. (B) Current-potential curves at 2100 rpm for AC adsorbed with 0, 100 and 1000 mg L^{-1} HA solutions.

8.3.4 Cathode Impedance Analysis

The impact of HA adsorption on the total cathode resistance, and the individual components of the resistance, was examined using EIS. The main impact of treatment with 1000 mg/L of HA was an increase in the diffusion resistance, as solution resistance and charge transfer resistance remained essentially constant (Figure 8-5B). The overall cathode resistance increased to 74 Ω for AC cathode treated with 1000 mg L^{-1} HA, compared to 57 Ω for the control (no HA addition), primarily due to a 32% increase in the diffusion resistance (50 Ω compared to 32 Ω) (Figure 8-5B). This 18 Ω increase in diffusion resistance was a 56% increase compared to an overall diffusion resistance of 32 Ω, which likely resulted from hindered proton diffusion to the catalyst site *(12)*. AC cathodes treated with 100 mg L^{-1} HA only showed 2 Ω increase in diffusion resistance and overall cathode resistance (Figure 8-5B).

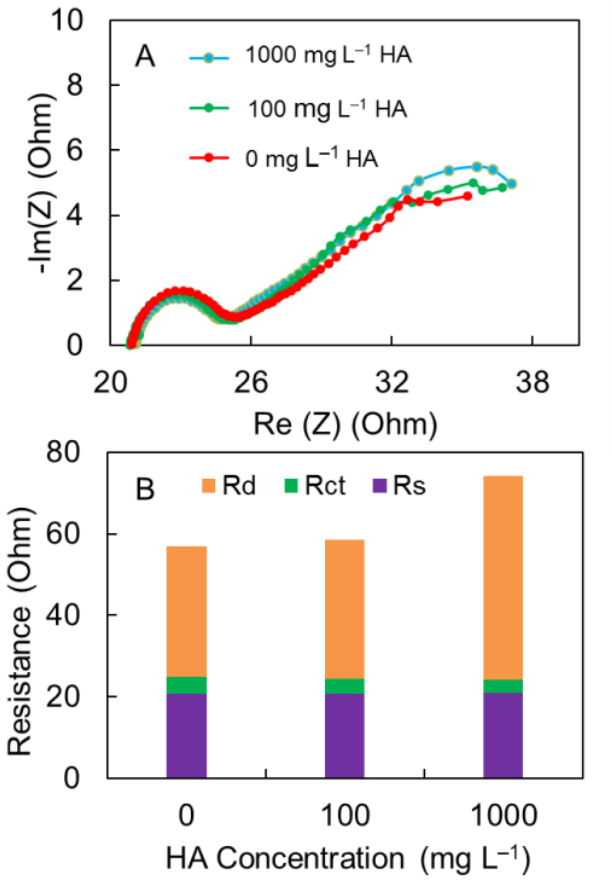

Figure 8-5. (A) Nyquist plots of EIS spectra of AC cathodes treated with 0, 100 and 1000 mg L^{-1} HA solutions at polarized conditions of 0.1 V vs. SHE. (B) Component analysis of internal resistance of the AC cathodes.

8.3.5 Cathode Rinsing

Cathodes were rinsed with deionized water to determine if organic matter on the AC could be easily removed. However, little organic matter was recovered following rinsing, indicating that only slow desorption of HA would occur. The maximum power density of the rinsed AC cathode was 1170 ± 40 mW m^{-2}, which was very similar to 1130 ± 40 mW m^{-2} of the non-rinsed AC cathode treated with 1000 mg L^{-1} HA solution (Figure 8-6A). The cathode potentials of the rinsed and non-rinsed cathodes were almost identical over the current density range of 0 to 8 A m^{-2} (Figure 8-6B), similarly showing no cathode performance change by rinsing with DI water. The HA concentration of rinsing effluent was measured to be 12 ± 1 mg-C L^{-1} (Appendix E, Table S8-2), which was much lower compared to the 190 ± 1 mg-C L^{-1} of 1000 mg L^{-1} HA concentration after adsorption in bach adosrption tests (Appendix E, Table S8-1), suggesting rinsing with DI water might not have washed out all the adsorbed HA substance. It is well known that HAs strongly bind to AC and that special methods, such as thermal treatment, are required to regerate AC adsorption capacity *(31-33)*. Thus, the HA adsoroption observed here was likely irreversible with respect to its impact on cathod performance even if using solutions with much lower HA concentrations.

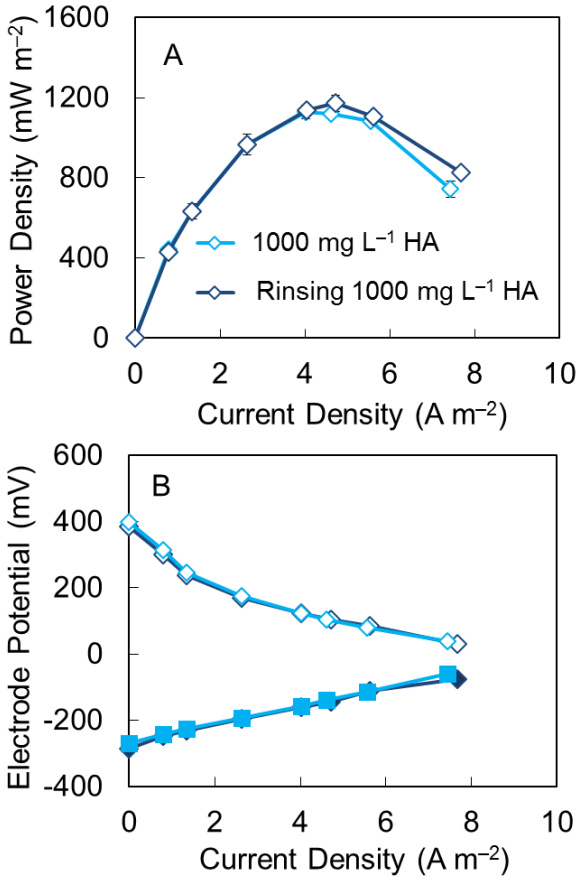

Figure 8-6. (A) Power density curves for AC cathodes treated with 1000 mg L^{-1} HA solution with and without rinsing. (B) Electrode potentials (solid symbols, anode potentials; open symbols, cathode potentials).

8.4 Conclusions

Extensive cathode fouling following a year of MFC operation has previously been shown to reduce power by almost 40%, with about 12% of this attributed to biofilm growth on the cathode surface *(12)*. Thus, most of the reducion in power production is due to internal catalyst fouling. It was shown here that substantial adsorption of HAs on the AC reduced power, but only by as much as 14%. This suggests that other reasons for a reduction in power over long periods of time are more likely due to foulants such as microbially produced biopolymers or irreversibly precipitated

salts. Better understanding of the mechanisms of AC catalyst fouling is critical and essential for developing methods to ensure stable and long term operation of MFC cathodes.

8.5 Acknowledgments

This research was supported by the Strategic Environmental Research and Development Program (SERDP) and a graduate scholarship from the China Scholarship Council (CSC) to W. Y.

8.6 Literature cited

1. Lowy, D. A.; Tender, L. M.; Zeikus, J. G.; Park, D. H.; Lovley, D. R., Harvesting energy from the marine sediment-water interface II - Kinetic activity of anode materials. *Biosens. Bioelectron.* **2006,** *21*, 2058-2063.
2. Logan, B. E., *Microbial fuel cells*. John Wiley & Sons, Inc.: Hoboken, NJ, 2008; p 300.
3. Niessen, J.; Schröder, U.; Scholz, F., Exploiting complex carbohydrates for microbial electricity generation: a bacterial fuel cell operating on starch. *Electrochem. Commun.* **2004,** *6*, 955-958.
4. Allen, R. M.; Bennetto, H. P., Microbial fuel-cells - electricity production from carbohydrates. *Appl. Biochem. Biotechnol.* **1993,** *39*, 27-40.
5. Bond, D. R.; Holmes, D. E.; Tender, L. M.; Lovley, D. R., Electrode-reducing microorganisms that harvest energy from marine sediments. *Science* **2002,** *295*, 483-485.
6. Yang, W.; Zhang, F.; He, W.; Liu, J.; Hickner, M. A.; Logan, B. E., Poly (vinylidene fluoride-co-hexafluoropropylene) phase inversion coating as a diffusion layer to enhance the cathode performance in microbial fuel cells. *J. Power Sources* **2014,** *269*, 379-384.
7. Cheng, S. A.; Wu, J. C., Air-cathode preparation with activated carbon as catalyst, PTFE as binder and nickel foam as current collector for microbial fuel cells. *Bioelectrochemistry* **2013,** *92*, 22-26.
8. Wang, X.; Feng, C. J.; Ding, N.; Zhang, Q. R.; Li, N.; Li, X. J.; Zhang, Y. Y.; Zhou, Q. X., Accelerated OH- transport in activated carbon air cathode by modification of quaternary ammonium for microbial fuel cells. *Environ. Sci. Technol.* **2014,** *48*, 4191-4198.
9. Dong, H.; Yu, H.; Wang, X.; Zhou, Q.; Feng, J., A novel structure of scalable air-cathode without Nafion and Pt by rolling activated carbon and PTFE as catalyst layer in microbial fuel cells. *Water Res.* **2012,** *46*, 5777-87.

10. Zhang, F.; Cheng, S.; Pant, D.; Bogaert, G. V.; Logan, B. E., Power generation using an activated carbon and metal mesh cathode in a microbial fuel cell. *Electrochem. Commun.* **2009,** *11*, 2177-2179.
11. Yang, W.; He, W.; Zhang, F.; Hickner, M. A.; Logan, B. E., Single step fabrication using a phase inversion method of poly (vinylidene fluoride)(PVDF) activated carbon air cathodes for microbial fuel cells. *Environ. Sci. Technol. Lett.* **2014,** *1*, 416-420.
12. Zhang, F.; Pant, D.; Logan, B. E., Long-term performance of activated carbon air cathodes with different diffusion layer porosities in microbial fuel cells. *Biosens. Bioelectron* **2011,** *30*, 49-55.
13. Zhang, F.; Ge, Z.; Grimaud, J.; Hurst, J.; He, Z., Long-Term Performance of Liter-Scale Microbial Fuel Cells Treating Primary Effluent Installed in a Municipal Wastewater Treatment Facility. *Environ. Sci. Technol.* **2013,** *47*, 4941-4948.
14. Cheng, S.; Liu, H.; Logan, B. E., Power densities using different cathode catalysts (Pt and CoTMPP) and polymer binders (Nafion and PTFE) in single chamber microbial fuel cells. *Environ. Sci. Technol.* **2006,** *40*, 364-369.
15. Yang, S.; Jia, B.; Liu, H., Effects of the Pt loading side and cathode-biofilm on the performance of a membrane-less and single chamber microbial fuel cell. *Bioresour. Technol.* **2009,** *100*, 1197-1202.
16. Rozendal, R. A.; Hamelers, H. V. M.; Rabaey, K.; Keller, J.; Buisman, C. J. N., Towards practical implementation of bioelectrochemical wastewater treatment. *Trends Biotechnol.* **2008,** *26*, 450-459.
17. Serp, P.; Figueiredo, J. L., *Carbon materials for catalysis*. John Wiley & Sons: 2009.
18. Kilduff, J. E.; Karanfil, T.; Weber, W. J., Competitive interactions among components of humic acids in granular activated carbon adsorption systems: Effects of solution chemistry. *Environ. Sci. Technol.* **1996,** *30*, 1344-1351.

19. Lee, M. C.; Snoeyink, V. L.; Crittenden, J. C., Activated carbon adsorption of humic substances. *J. Am. Water. Works. Assoc.* **1981**, 440-446.

20. Radjenović, J.; Farré, M. J.; Mu, Y.; Gernjak, W.; Keller, J., Reductive electrochemical remediation of emerging and regulated disinfection byproducts. *Water Res.* **2012,** *46*, 1705-1714.

21. Lovley, D. R.; Coates, J. D.; Blunt-Harris, E. L.; Phillips, E. J. P.; Woodward, J. C., Humic substances as electron acceptors for microbial respiration. *Nature* **1996,** *382*, 445-448.

22. Sund, C. J.; McMasters, S.; Crittenden, S. R.; Harrell, L. E.; Sumner, J. J., Effect of electron mediators on current generation and fermentation in a microbial fuel cell. *Appl. Microbiol. Biotechnol.* **2007,** *76*, 561-568.

23. Li, Y.; Liu, L.; Liu, J.; Yang, F.; Ren, N., PPy/AQS (9, 10-anthraquinone-2-sulfonic acid) and PPy/ARS (Alizarin Red's) modified stainless steel mesh as cathode membrane in an integrated MBR/MFC system. *Desalination* **2014,** *349*, 94-101.

24. Yang, W.; Kim, K.-Y.; Logan, B. E., Development of carbon free diffusion layer for activated carbon air cathode of microbial fuel cells. *Bioresour. Technol.* **2015,** *197*, 318-322.

25. Logan, B. E.; Cheng, S.; Watson, V.; Estadt, G., Graphite fiber brush anodes for increased power production in air-cathode microbial fuel cells. *Environ. Sci. Technol.* **2007,** *41*, 3341-3346.

26. Cheng, S.; Xing, D.; Call, D. F.; Logan, B. E., Direct biological conversion of electrical current into methane by electromethanogenesis. *Environ. Sci. Technol.* **2009,** *43*, 3953-3958.

27. Watson, V. J.; Nieto Delgado, C.; Logan, B. E., Influence of chemical and physical properties of activated carbon powders on oxygen reduction and microbial fuel cell performance. *Environ. Sci. Technol.* **2013,** *47*, 6704-6710.

28. Gojkovic, S. L.; Gupta, S.; Savinell, R. F., Heat-treated iron(III) tetramethoxyphenyl porphyrin supported on high-area carbon as an electrocatalyst for oxygen reduction - I. Characterization of the electrocatalyst. *J. Electrochem. Soc.* **1998,** *145*, 3493-3499.

29. Rouquerol, J.; Avnir, D.; Fairbridge, C.; Everett, D.; Haynes, J.; Pernicone, N.; Ramsay, J.; Sing, K.; Unger, K., Recommendations for the characterization of porous solids (Technical Report). *Pure Appl. Chem.* **1994,** *66*, 1739-1758.

30. Dong, H.; Yu, H.; Wang, X., Catalysis kinetics and porous analysis of rolling activated carbon-PTFE air-cathode in microbial fuel cells. *Environ. Sci. Technol.* **2012,** *46*, 13009-13015.

31. Moreno-Castilla, C.; Rivera-Utrilla, J.; Joly, J. P.; López-Ramón, M. V.; Ferro-García, M. A.; Carrasco-Marín, F., Thermal regeneration of an activated carbon exhausted with different substituted phenols. *Carbon* **1995,** *33*, 1417-1423.

32. Dąbrowski, A.; Podkościelny, P.; Hubicki, Z.; Barczak, M., Adsorption of phenolic compounds by activated carbon—a critical review. *Chemosphere* **2005,** *58*, 1049-1070.

33. Namasivayam, C.; Kavitha, D., Removal of Congo Red from water by adsorption onto activated carbon prepared from coir pith, an agricultural solid waste. *Dyes and Pigments* **2002,** *54*, 47-58.

Chapter 9

Future work

In this dissertation, I optimized the activated carbon (AC) cathode performance by using a phase inversion coating as the diffusion layer to improve the cathode oxygen permeability, developed a single-step fabricated AC cathode using phase inversion process, investigated the use of a hydrophobic polyvinylidene fluoride membrane as the cathode diffusion layer and proposed a new cathode structure with double catalyst layer to improve cathode performance. I also chemically modified AC with an iron-nitrogen-carbon framework to improve the oxygen reduction reactivity. Finally I probed into the effect of humic acid adsorption on the reactivity of AC, a potential fouling mechanism of cathode degradation over long term MFC operation. These studies mainly targeted on developing a scalable AC cathode with new fabrication techniques and materials. However, the feasibility of the optimized cathode still needs to be examined in scaled up MFCs. Specific questions remaining to be addressed are as follows.

1. The degradation rate of AC cathode needs to be examined with long term MFC operation. The long term stability of those optimized AC cathodes remains unclear relative to other cathodes, and therefore it should be examined whether the initially improved cathode performance can be maintained over the cathode lifetime.
2. Different fouling mechanisms need to be investigated to better help understand the reasons for the decline in power over time with activated carbon cathodes. Humic acid adsorption onto the AC cathodes only produced a small reduction in the cathode performance, which suggested that other fouling possibilities exist and contribute to the cathode fouling. Such information on the mechanisms of fouling could lead to anti-fouling strategies.

3. MFCs with larger volumes should be tested with the optimized AC cathode using domestic wastewater as the fuel. Many studies have been conducted with acetate and phosphate buffers, but few have considered fouling using actual wastewaters.

Appendix A

Supporting information for chapter 4

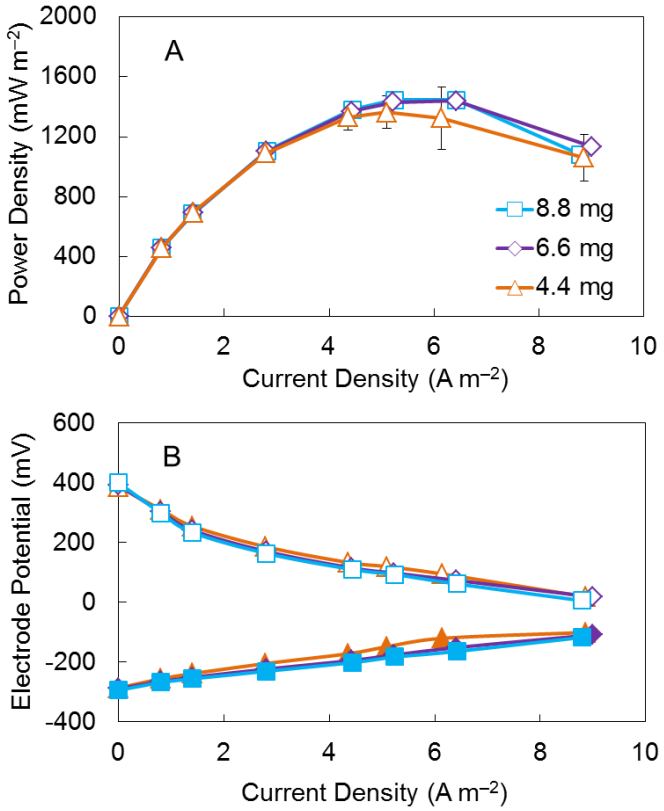

Figure S4-1. (A) Power density curve for cathodes with different PVDF loadings (8.8, 6.6 and 4.4 mg cm^{-2}) (B) Electrode potentials (solid symbols for anode potentials and open symbols for cathode potentials).

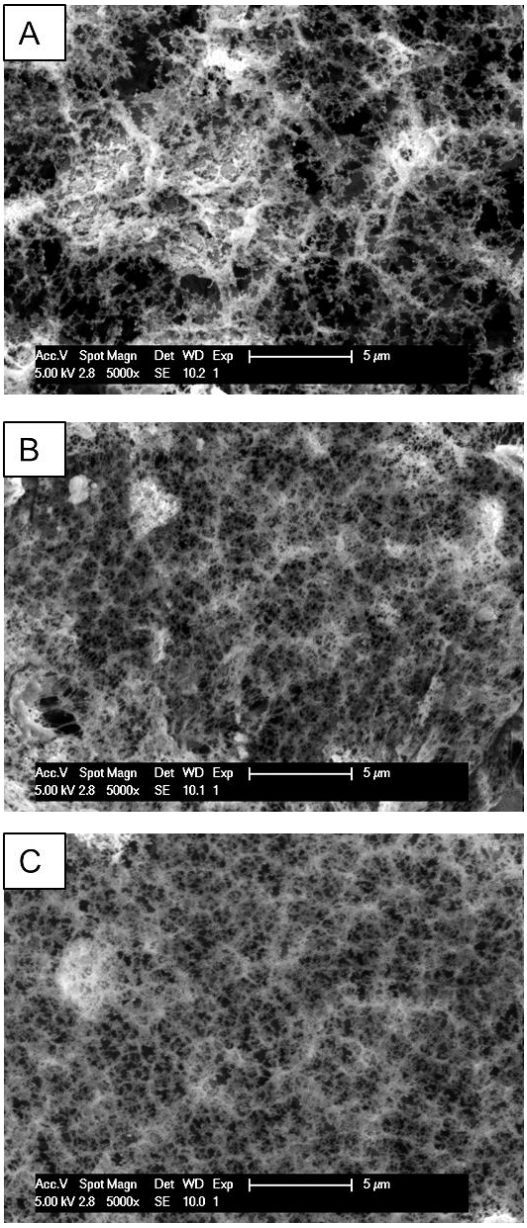

Figure S4-2. SEM images for cathode surfaces with different PVDF loadings (A) 4.4 mg cm^{-2}, (B) 6.6 mg cm^{-2} (C) 8.8 mg cm^{-2}. (Enhanced: brightness +20% and controsat +20%)

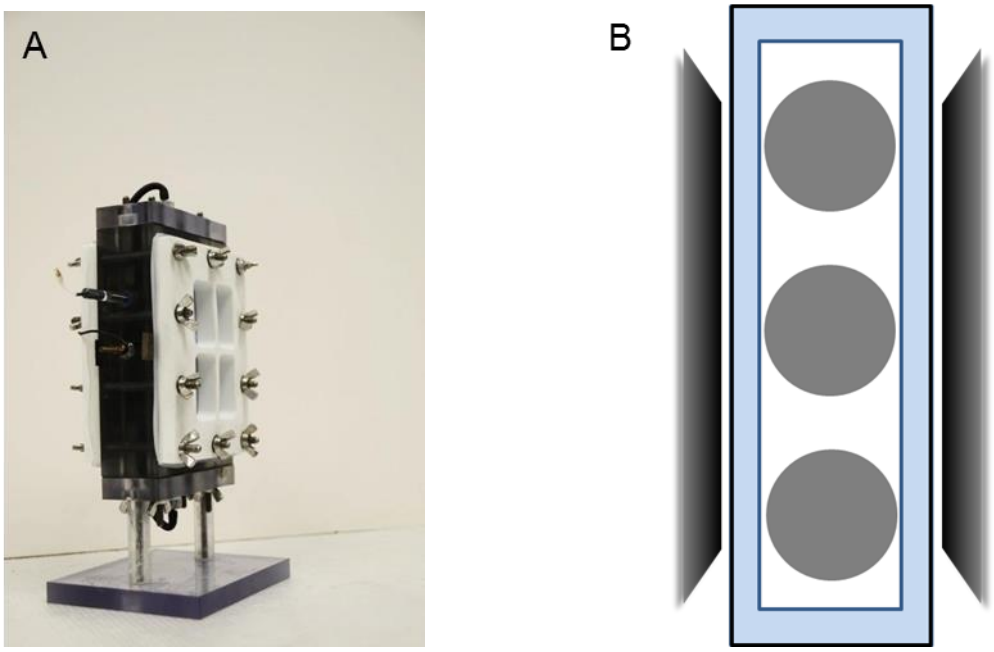

Figure S4-3. (A) Scheme of a scale up MFC (B) Configuration of reactor with three anodes in the middle and two cathodes on air sides.

Single chamber MFC (130 mL liquid volume) was constructed as previously reported *(1)*. with three brush anodes (0.25 cm in diameter and 0.35 cm in length) made from carbon fibers (PANEX 33 160K, ZOLTEK) wound into a titanium wire core *(2)*. The anodes were connected together externally by a single copper wire. Carbon cloth-based cathode with platinum catalyst (ETEK C1-10 10% Pt on Vulcan XC-72) and a PTFE diffusion layer was prepared as previously described *(3)*. and used as a control to evaluate performance relative to the AC/PVDF cathode in the MFC. Both cathodes were fabricated with 7 cm in width and 10 cm in length (projected area 35 cm^2, 5 cm × 7 cm) and operated without a separator. Domestic waste water, collected from the primary clarifier of the Pennsylvania State University Waste Water Treatment Plant, was used as the inoculum. The waste water was collected and then stored in 4 °C room to minimize COD changes. The concentration of COD in the waste water was 500 ± 20 mg-COD L^{-1}.

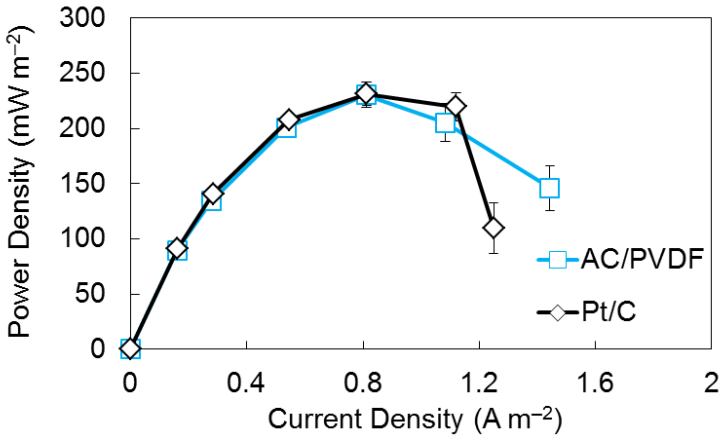

Figure S4-4. Power density curve for scaled up AC/PVDF cathode and carbon cloth based Pt/C cathode (5 cm ×7 cm projected area).

Table S4-3. Unit prices of different materials in cathode fabrication

Material	Calculating price	Supplier price	Sources
Stainless steel 50 × 50 mesh, type 304	\$12 m^{-2}	\$6-17 m^{-2}	http://www.alibaba.com/product-detail/50-micron-stainless-steel-wire-mesh_509492050.html
Nickel foam	\$20 m^{-2}	\$10-30 m^{-2}	http://www.alibaba.com/product-detail/Continuous-Metal-Nickel-Foam-for-NiMh_1548642996.html
Activated carbon (AC)	\$1.4 Kg^{-1}	\$0.9-1.8 Kg^{-1}	http://www.alibaba.com/product-detail/Bamboo-wood-based-activated-carbon-manufacturer_1459751266.html
Carbon black (CB)	\$3.3 Kg^{-1}	\$3.3 Kg^{-1}	http://www.sidrich.com/products-and-pricing/pricing/carbon-black-pricing/
PTFE powder	\$25 Kg^{-1}	\$10-40 Kg^{-1}	http://www.alibaba.com/product-detail/Virgin-Molding-PTFE-Powder_797829147.html
PVDF powder	\$24 Kg^{-1}	\$22.5-25.5 Kg^{-1}	http://www.alibaba.com/product-detail/Factory-directly-pvdf-powder-with-competitive_1033781222.html
PDMS	\$2.6 Kg^{-1}	\$2.2-3 Kg^{-1}	http://www.alibaba.com/product-detail/PDMS-Polydimethylsiloxane-Dimethicone-Simethicone-Silicon-silicon_591079545.html?s=p
Nafion	\$3.6 g^{-1}	\$3.6 g^{-1}	http://detail.1688.com/offer/1259522935.html
Platinum (Pt/C, 10%)	\$163 g^{-1}	\$135-190 g^{-1}	http://us1007331355.fm.alibaba.com/product/131142716-103514002/60_Platinum_on_Vulcan.html
Carbon cloth (30% wet proofed)	\$625 m^{-2}	\$625 m^{-2}	http://fuelcellearth.com/shop/

(The prices were all reported based on specific suppliers and median price was adopted if a range was given in the supplier price)

Literature cited

1. Ahn, Y.; Logan, B., Domestic wastewater treatment using multi-electrode continuous flow MFCs with a separator electrode assembly design. *Appl. Microbiol. Biotechnol.*, 1-8.
2. Logan, B. E.; Cheng, S.; Watson, V.; Estadt, G., Graphite fiber brush anodes for increased power production in air-cathode microbial fuel cells. *Environ. Sci. Technol.* **2007,** *41*, 3341-3346.
3. Cheng, S.; Liu, H.; Logan, B. E., Increased performance of single-chamber microbial fuel cells using an improved cathode structure. *Electrochem. Commun.* **2006,** *8*, 489-494.

Appendix B

Supporting information for chapter 5

Figure S5-1. Synthesis of PVDF membrane via phase inversion method and solvent exchange process.

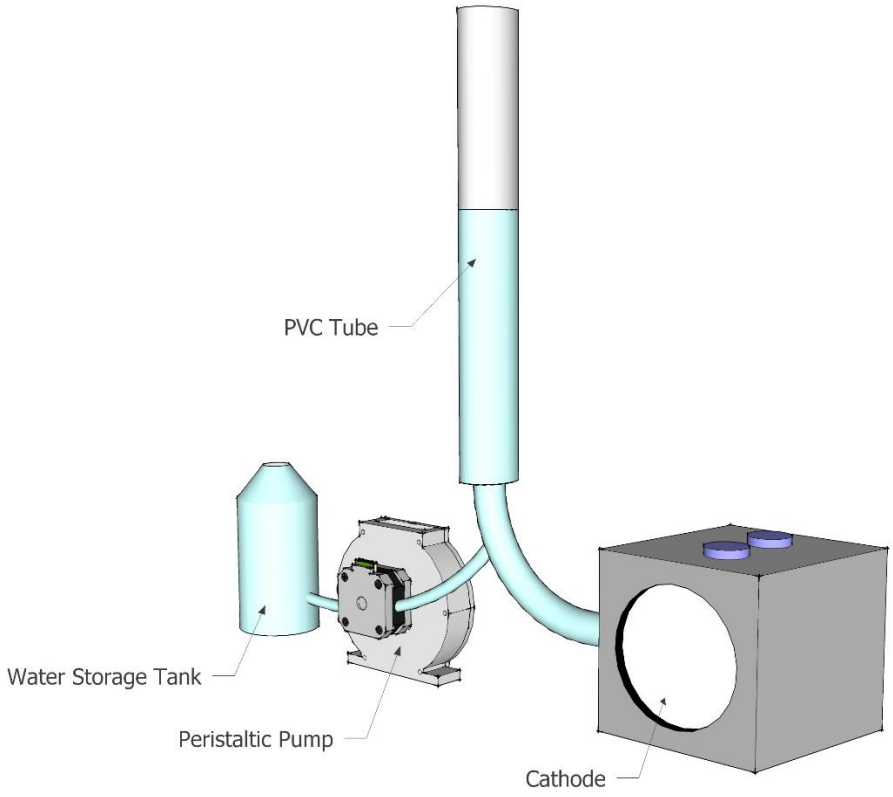

Figure S5-2. Configuration of cathode pressure test system.

Table S5-1. Oxygen mass transfer coefficient for different DLs

DL type	Oxygen mass transfer coefficient $k \times 10^{-3}$ (cm/s)
15% PVDF	2.4 ± 0.5
20% PVDF	2.9 ± 0.3
25% PVDF	2.5 ± 0.4
PDMS wipe	3.1 ± 0.5

Single chamber MFC (130 mL liquid volume) was constructed as previously reported *(1)*, with three brush anodes (0.25 cm in diameter and 0.35 cm in length) made from carbon fibers (PANEX 33 160K, ZOLTEK) wound into a titanium wire core *(2)*. The anodes were connected together externally by a single copper wire. Cathodes were fabricated with 7 cm in width and 10 cm in length (projected area 35 cm^2, 5 cm × 7 cm) and operated without a separator. Domestic waste water, collected from the primary clarifier of the Pennsylvania State University Waste Water Treatment Plant, was used as the inoculum. The waste water was collected and then stored in 4 °C room to minimize COD changes. The concentration of COD in the waste water was 500 ± 20 mg-COD/L.

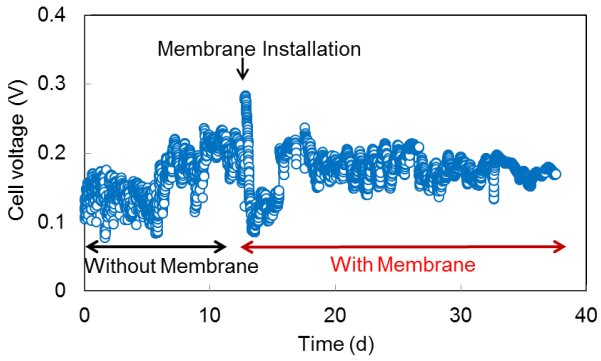

Figure S5-3. Cell voltage produced by AC/PVDF cathode (5 cm ×7 cm) with and without 20% (w/v) PVDF membrane in a single chamber MFC (130 mL liquid volume).

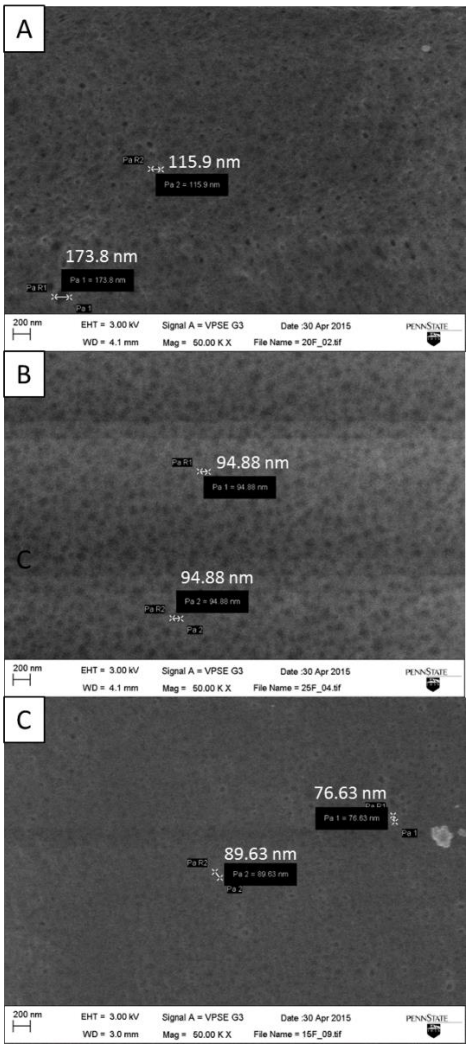

Fig S5-4. SEM images of membrane surfaces for (A) 15% (w/v) (B) 20% (w/v) (C) 25% (w/v) PVDF membranes.

Literature cited

1. Ahn, Y.; Logan, B. E., Domestic wastewater treatment using multi-electrode continuous flow MFCs with a separator electrode assembly design. *Appl. Microbiol. Biotechnol.* **2013,** *97*, 409-416.
2. Logan, B. E.; Cheng, S.; Watson, V.; Estadt, G., Graphite fiber brush anodes for increased power production in air-cathode microbial fuel cells. *Environ. Sci. Technol.* **2007,** *41*, 3341-3346.

Appendix C

Supporting information for chapter 6

Figure S6-1. Pressing machine with temperature control unit.

Table S6-1. Oxygen mass transfer coefficient for AC cathodes pressed at 25, 60 and 120 °C

Temperature (°C)	Oxygen mass transfer coefficient $k \times 10^{-3}$ (cm s^{-1})
25	2.6 ± 0.2
60	2.5 ± 0.1
120	3.0 ± 0.3

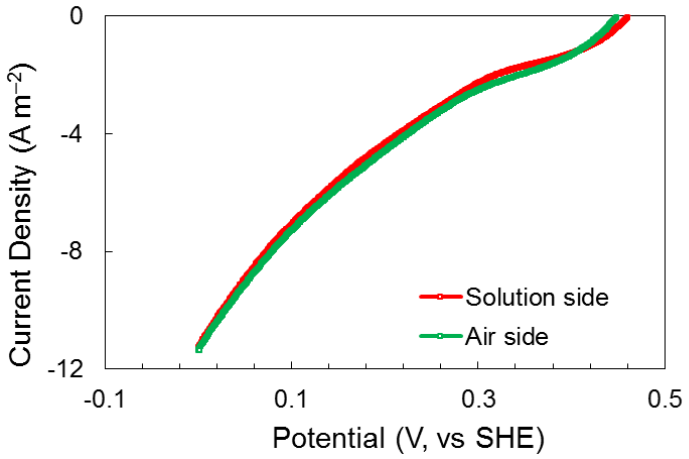

Figure S6-2. Current-voltage (polarization) curves for the AC cathodes (no diffusion layer) with CL facing solution side and air side in an abiotic electrochemical cell.

Appendix D

Supporting information for chapter 7

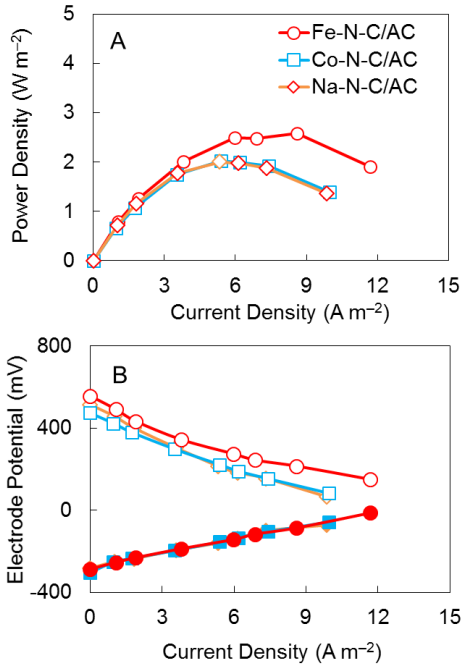

Figure S7-1. (A) Power density curves in 50 mM PBS for Fe-N-C/AC, Co-N-C/AC and Na-N-C/AC cathodes. (B) Electrode potentials (solid symbols, anode potentials; open symbols, cathode potentials).

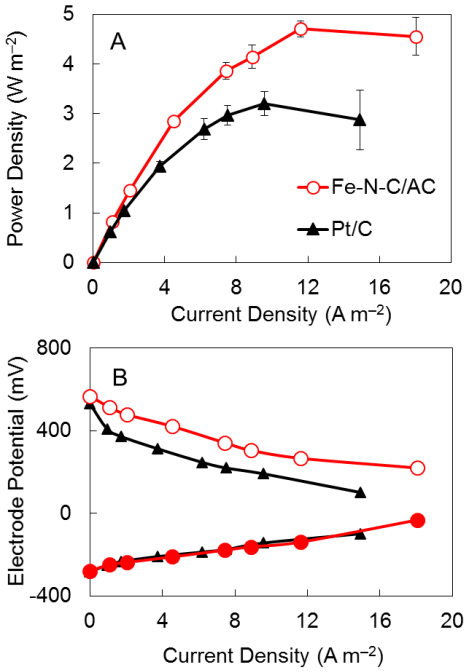

Figure S7-2. (A) Power density curves in 200 mM PBS for Fe-N-C/AC and Pt/C cathodes. (B) Electrode potentials (solid symbols, anode potentials; open symbols, cathode potentials).

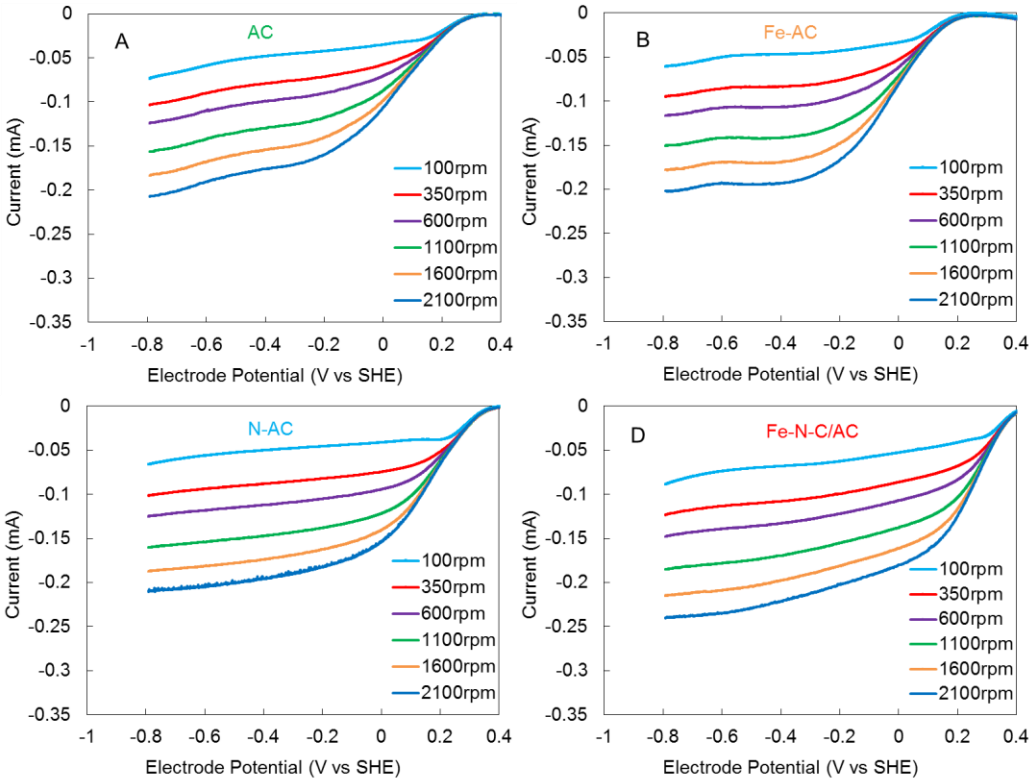

Figure S7-3. LSV curves for (A) AC (B) Fe-AC (C) N-AC (D) Fe-N-C/AC catalysts in 50 mM PBS at different rotation speed.

Appendix E

Supporting information for chapter 8

Table S8-1. HA concentrations before and after AC adsorption

Sample	Before (mg-C L^{-1})	After (mg-C L^{-1})	Adsorption mass (mg-C)
100 mg L^{-1}	33 ± 2	20 ± 1	1.4 ± 0.1
1000 mg L^{-1}	330 ± 20	190 ± 1	14 ± 2

Table S8-2. HA concentration and loading of back wash effluent

Effluent volume (mL)	Concentration (mg-C L^{-1})	Mass (mg-C)
30	12 ± 1	0.36 ± 0.04

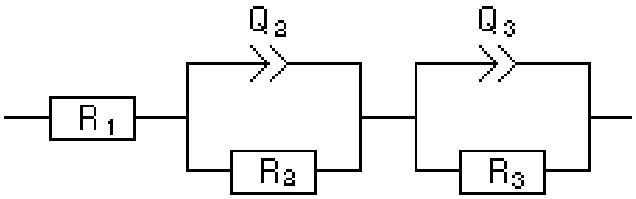

Figure S8-1. Equivalent circuit for EIS spectra (R_1: solution resistance; R_2: charge transfer resistance; R_3: diffusion resistance; Q_2, Q_3: constant phase elements).

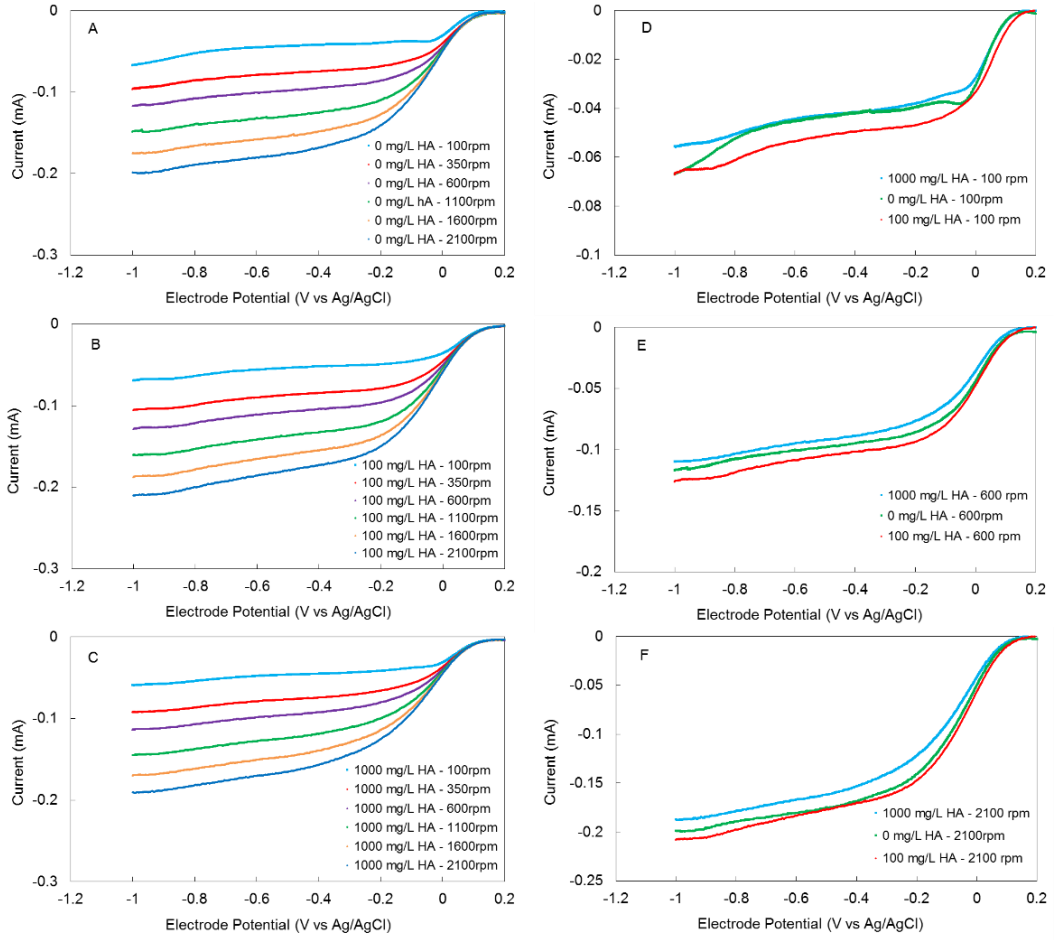

Figure S8-2. (A-C) Current-potential curves at different rotation rates for AC adsorbed with 0, 100 and 1000 mg L^{-1} HA solutions. (D-E) Current-potential curves at100, 600 and 2100 rpm for AC adsorbed with 0, 100 and 1000 mg L^{-1} HA solutions.

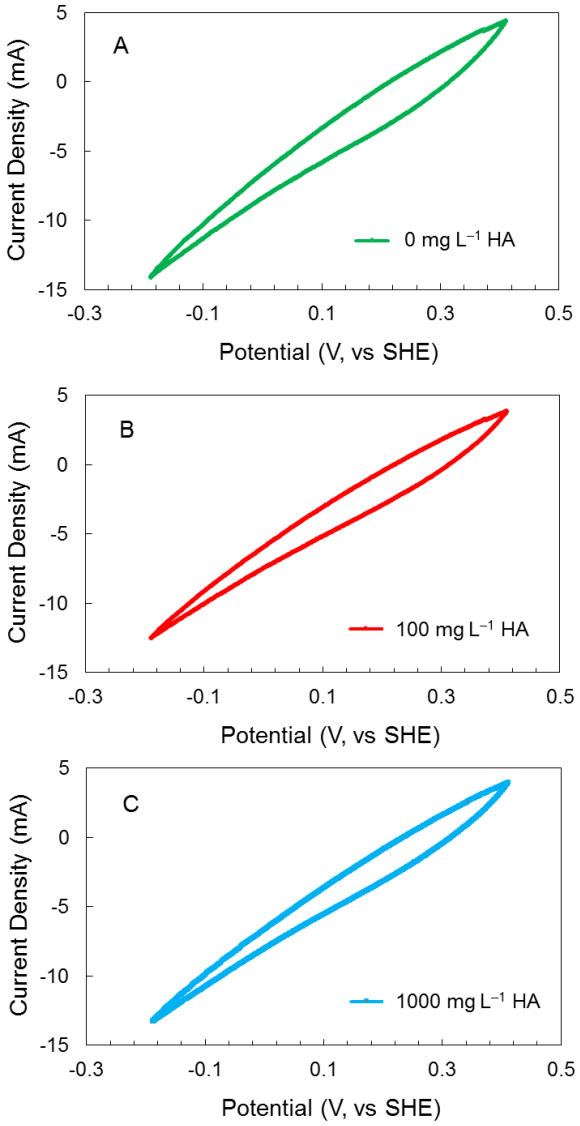

Figure S8-3. (A-C) Cyclic voltammetry curves of activated carbon cathode in 0, 100 and 1000 mg L^{-1} HA solution buffered with 50 mM PBS.

Wulin Yang

EDUCATION

8/2012 – 8/2016	**Ph.D. in Environmental Engineering**, Penn State University, *Advisor: Prof. Bruce E. Logan*
9/2011 - 6/2012	**M.S. in Environmental Engineering**, Yale University *Advisor: Prof. Menachem Elimelech*
9/2007 - 7/2011	**B.S. in Environmental Science**, Peking University

JOURNAL PUBLICATIONS

1. Kim, K.-Y.; **Yang, W.**; Ye, Y.; LaBarge, N.; Logan, B. E., Performance of anaerobic fluidized membrane bioreactors using effluents of microbial fuel cells treating domestic wastewater. *Bioresour. Technol.* **2016,** *208*, 58-63.
2. **Yang, W.**; Kim, K.-Y.; Logan, B. E., Development of carbon free diffusion layer for activated carbon air cathode of microbial fuel cells. *Bioresour. Technol.* **2015,** *197*, 318-322.
3. Kim, K.-Y.; **Yang, W.**; Logan, B. E., Impact of electrode configurations on retention time and domestic wastewater treatment efficiency using microbial fuel cells. *Water Res.* **2015,** *80*, 41-46.
4. **Yang, W.**; Zhang, F.; He, W.; Liu, J.; Hickner, M. A.; Logan, B. E., Poly (vinylidene fluoride-co-hexafluoropropylene) phase inversion coating as a diffusion layer to enhance the cathode performance in microbial fuel cells. *J. Power Sources* **2014,** *269*, 379-384.
5. **Yang, W.**; He, W.; Zhang, F.; Hickner, M. A.; Logan, B. E., Single step fabrication using a phase inversion method of poly (vinylidene fluoride)(PVDF) activated carbon air cathodes for microbial fuel cells. *Environ. Sci. Technol. Lett.* **2014,** *1*, 416-420.
6. Zhu, X.; **Yang, W.**; Hatzell, M.; Logan, B. E., Energy recovery from solutions with different salinities based on swelling and shrinking of hydrogels. *Environ. Sci. Technol.* **2014,** *48*, 7175-7163.
7. Ziemba, C.; **Yang, W.**; Peccia, J., Modeling human off-site aerosol exposures to polybrominated flame retardants emitted during the land application of sewage sludge. *Environ Int* **2013,** *60*, 232-241.

CONFERENCE PRESENTATIONS

1. **Yang, W.**; Logan, B. E., 2015. Consideration of cathode specific surface area and hydrodynamics in scaling up microbial fuel cells. Invited presentation at bio-electrochemical system workshop, Ruhr-Universität Bochum, Germany, Nov 25.
2. **Yang, W.**; Kim, K.-Y.; Logan, B. E., 2015. Development of carbon free diffusion layer for activated carbon air cathode of microbial fuel cells. Oral presentation at North American Meeting of the International Society for Microbial Electrochemistry and Technology (NA-ISMET), Arizona State University, USA, Oct 1-4.

HONORS and REWARDS

2015 Podium Award at 87th Pennsylvania Water Environment Association Conference
2012 China Scholarship Council (CSC) Fellowship

PROFESSIONAL MEMBERSHIPS

Association of Environmental Engineering & Science Professors (AEESP) (since 2015)
International Society for Microbial Electrochemistry and Technology (ISMET) (since 2012)

JOURNAL REVIEWER

Langmuir
ChemElectroChem
ACSSusChemEng
Journal of Power Sources
Energy & Fuels